NREL/TP-441-7229 • UC Category: 1213 • DE96000492

Advanced Wind Turbine Near-Term Product Development

Final Technical Report

R. Lynette & Associates
Seattle, Washington

NREL Technical Monitor:
Brian Smith

National Renewable Energy Laboratory
1617 Cole Boulevard
Golden, Colorado 80401-3393
A national laboratory of the U.S. Department of Energy
Managed by Midwest Research Institute
for the U.S. Department of Energy
under contract No. DE-AC36-83CH10093

Prepared under Subcontract No. ZG-0-19090-3

January 1996

NOTICE

Available to DOE and DOE contractors from:
Office of Scientific and Technical Information (OSTI)
P.O. Box 62
Oak Ridge, TN 37831
Prices available by calling (615) 576-8401

Available to the public from:
National Technical Information Service (NTIS)
U.S. Department of Commerce
5285 Port Royal Road
Springfield, VA 22161
(703) 487-4650

Printed on paper containing at least 50% wastepaper, including 10% postconsumer waste

Foreword

The U.S. Department of Energy (DOE) sponsors a multifaceted program to help develop competitive, high-performance wind turbine technology for global energy markets. As part of these efforts, the National Renewable Energy Laboratory (NREL), on behalf of DOE, awarded four subcontracts under the Near-Term Product Development Program in 1992. The goal of these subcontracts was to develop improved wind turbines for introduction to the market by 1995.

The first of these subcontracts was awarded to R. Lynette and Associates of Seattle, Washington, to develop the AWT-26. The AWT-26 is a 275-kW, downwind, stall-regulated machine incorporating a 26-m, two-bladed, teetered rotor. The turbine is based on the ESI-80, a turbine developed in the 1980s. Two prototypes have been successfully operated in Tehachapi, California, and a third prototype is installed at NREL's National Wind Technology Center in Golden, Colorado. The AWT-26 is produced by Advanced Wind Turbines, Incorporated (formerly R. Lynette and Associates), and is marketed in the U.S. and abroad by FloWind Corporation. The AWT-26 was recently selected for a 25-MW wind power plant in Washington and a 50-MW wind power plant in India.

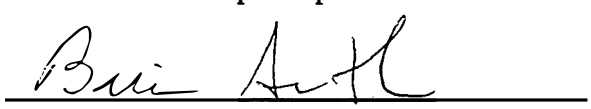

Brian Smith, Technical Monitor
National Renewable Energy Laboratory

Notice

Preface

The following employees of R. Lynette & Associates have written and contributed to this Conceptual Study Report:

Robert Lynette	Principal Investigator
David Malcolm	Senior Scientist
Robert Poore	Systems Operation Manager
Timothy McCoy	Project Engineer/Testing & Analysis
Shawn Lawlor	Project Engineer/Aerodynamics
Bruce Babcock	Project Engineer/Mechanical
Richard Beckett	Project Engineer
Rana Vilhauer	Technician

TABLE OF CONTENTS

TABLE OF CONTENTS, Cont.

TABLE OF CONTENTS, Cont.

LIST OF FIGURES

LIST OF FIGURES, Cont.

LIST OF TABLES

EXECUTIVE SUMMARY

In 1990 the U.S. Department of Energy initiated the Advanced Wind Turbine (AWT) Program to assist the growth of a viable wind energy industry in the United States. This program, which has been managed through the National Renewable Energy Laboratory (NREL) in Golden, Colorado, has been divided into three phases: 1) conceptual design studies, 2) near-term product development, and 3) next-generation product development.

The goals of the second phase were to bring into production wind turbines which would meet the cost goal of $0.05 kWh at a site with a mean (Rayleigh) windspeed of 5.8 m/s (13 mph) and a vertical wind shear exponent of 0.14. These machines were to allow a U.S.-based industry to compete domestically with other sources of energy and to provide internationally competitive products.

In 1992, R. Lynette & Associates (RLA) was awarded a contract under the second phase of the AWT program. This report presents the technical results of that contract. It also includes a summary of RLA's project funded under phase 1 of the DOE program. It describes the rationale behind the selection of the "baseline" wind turbine, the modifications made to that design, the fabrication and testing of two prototypes, and the plans for machine production. The major differences between the various wind turbines is summarized below.

Item	ESI-80	ESI-retrofit	AWT-26/P1	AWT-26/P2A	AWT-26/P2B
blade	80-ft diameter NASA LS-1 airfoils	86-ft diameter NREL thick airfoils	86-ft diameter NREL thick airfoils	86-ft diameter NREL thick airfoils	86-ft diameter NREL thick airfoils
tower	3-sided truss	3-sided truss 80-ft high	3-sided truss 80-ft high	tapered steel tube, 80-ft high	guyed steel tube, 140-ft high
mainframe	cast steel	cast steel	welded steel	cast iron	cast iron
main bearings	integral with gearbox	integral with gearbox	2 pillow blocks	integral with gearbox	integral with gearbox
gearbox	secured to mainframe	secured to mainframe	supported from shaft torque links to mainframe	secured to mainframe	secured to mainframe
hub	cast iron	cast iron	welded steel	cast iron	cast iron
hub adapters	cast steel	cast steel	cast steel	omitted	omitted
mechanical brake	high speed	high speed	low speed	high speed	high speed

Information is given in the report on design values of peak loads and of fatigue spectra and the results of the design process are summarized in a table. Measured response is compared with the results from mathematical modeling using the ADAMS code and is discussed.

Detailed information is presented on the estimated costs of maintenance and on spare parts requirements. A failure modes and effects analysis was carried out and resulted in approximately 50 design changes including the identification of ten previously unidentified failure modes.

The performance results of both prototypes are examined and adjusted for air density and for correlation between the anemometer site and the turbine location. The anticipated energy production at the reference site specified by NREL is used to calculate the final cost of energy using the formulas indicated in the Statement of Work. The value obtained is $0.0514/kWh in January 1994 dollars.

1.0 INTRODUCTION

1.1 Background

In 1990 the U.S. Department of Energy initiated the Advanced Wind Turbine (AWT) Program to assist the growth of a viable wind energy industry in the United States. This program, which has been managed through the National Renewable Energy Laboratory (NREL) in Golden, Colorado, has been divided into three phases: 1) conceptual design studies, 2) near-term product development, and 3) next-generation product development.

The objectives of Phase 1 were to study possible improvements to existing wind turbine designs and manufacturing methods. The goal was to identify improvements that could reduce the cost of electricity to $0.05/kWh at sites with mean wind speeds of approximately 5.8 m/s (13 mph) at a height of 10 m. These improvements were to be such that they could be incorporated into machine production in 1993 -- 1995. Phase 1 also aimed to initiate studies of advanced concepts that would further reduce the cost of electricity and possibly be incorporated into machines by 1998 -- 2000.

R. Lynette & Associates (RLA) was awarded a contract under Phase 1 of the AWT program. The findings of that project were presented to NREL in the report "Advanced Wind Turbine Conceptual Study Final Report" subcontract ZG-0-19090-3, March 13, 1992. That project studied ways in which the ESI-80 wind turbine might be modified to increase energy capture and reliability, and decrease the cost of energy.

In 1992 RLA acted as subcontractor to the Smith Wind Corporation (SWEC) in a project entitled "ESI-80 Rotor Performance and Reliability Enhancement Program" (REP). This program was conducted under the auspices of NREL's Government/Industry Wind Technology Applications Project. The project involved the retrofit of a 26.2-m (86-ft) diameter rotor using the NREL "thick airfoil" family of newly designed airfoils. A report was submitted by RLA to NREL in December 1992 (Reference 4).

The goals of the second phase were to bring into production wind turbines which would meet the cost goal identified above. These machines were to allow a U.S.-based industry to compete domestically with other sources of energy and to provide internationally competitive products.

1.2 Project Schedule

The project was divided into eight major tasks, from assessment of the baseline turbine to preparation of a final report. These tasks and subtasks and the initial schedule are presented in Figure 1-1.

The important milestones in the project were:

- June 17, 1992 kickoff meeting
- July 21, 1992 preliminary design review (PDR)
- March 1993 conceptual study report (tasks 1, 2 and 3)
- May 13, 1993 final design review

ADVANCED WIND TURBINE NEAR-TERM PRODUCT DEVELOPMENT
R. LYNETTE and ASSOCIATES

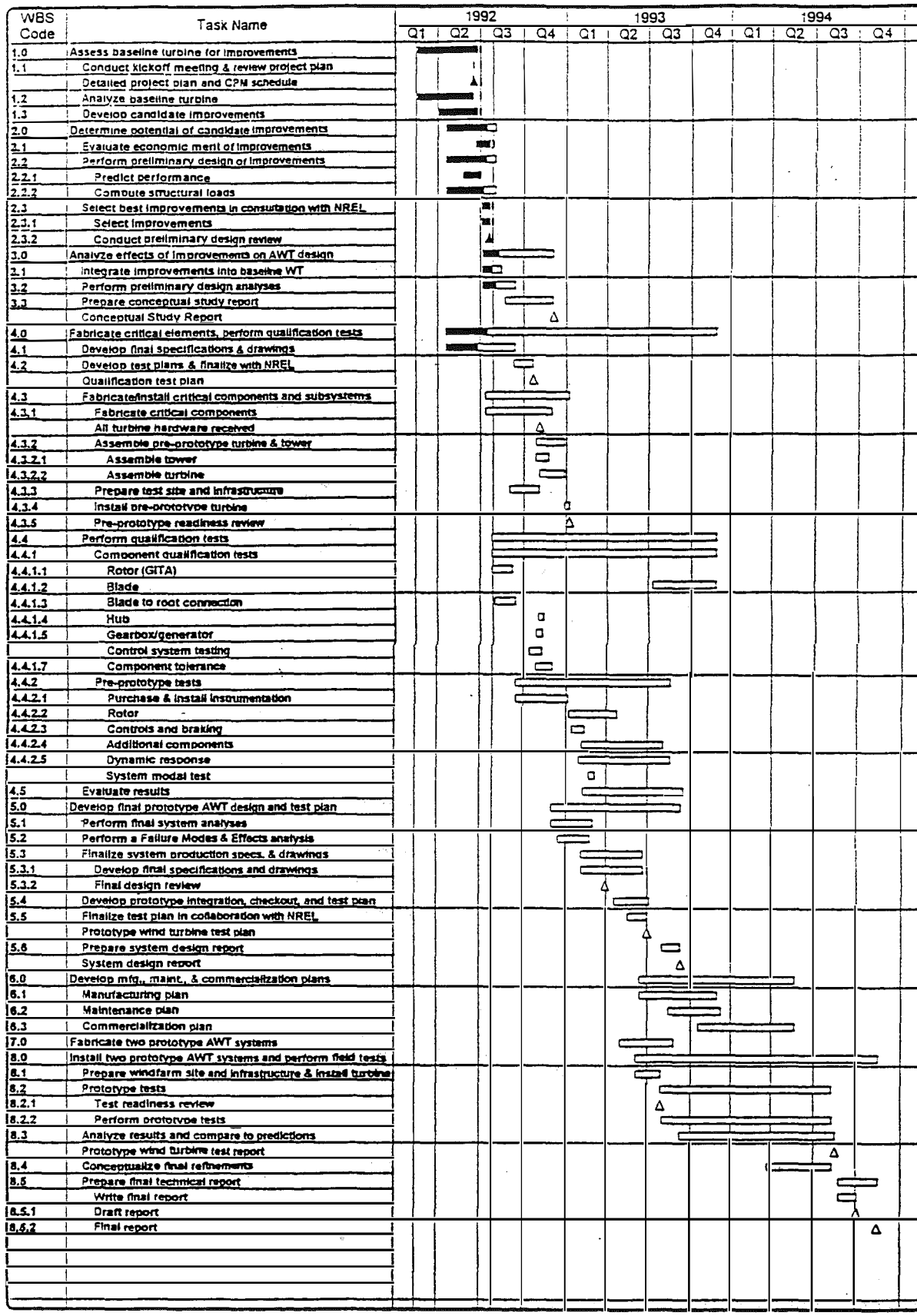

Figure 1-1. Schedule of project tasks

Some significant changes were made to the scope during the course of the project. These mainly involved some configuration changes and additions to the test programs for the two prototype wind turbines. They included

- The dynamic brake was replaced by aerodynamic tip brakes.
- The tip brake design was improved.
- The bracing members on the P1 tower were altered to reduce drag.
- A tubular tower was designed for P2.
- A guyed taller tubular tower was designed and built as an alternative for P2 (designated P2B).
- Additional modeling of the dynamic system was carried out.
- An Operation and Maintenance manual was prepared.

These modifications did not have a significant effect on the overall project schedule although they did increase the total value of the program; the draft final report was submitted on schedule in late 1994. Detailed progress was described in the series of monthly progress reports from RLA to NREL.

1.3 Objectives

The primary objectives of this project were to:

1. identify the changes required to be made to the ESI-80 wind turbine to meet the cost of energy goals of the Advanced Wind Turbine Program ($0.05/kWh in a 13 mph mean wind site);
2. carry out detailed design calculations and drawings for two prototype machines;
3. fabricate, install, and test two prototype models;
4. collect data on the power production and structural response of the two prototypes and evaluate this data;
5. evaluate the performance and reliability of the prototypes and identify desired changes; and
6. prepare detailed plans for the production of the final preferred configuration.

1.4 Organization of this Report

This report does not aim to describe all of the work that has been done in the course of the project; nor does it describe all of the minor configuration changes made during the test program. Instead, it attempts to summarize the rationale for the design choices, the final configurations selected, the design loads used, and the important test results.

There are substantial differences between the designs of the first and second prototypes (designated as P1 and P2, respectively). However, to avoid unnecessary duplication, both are treated and discussed together in the following sections. This approach allows easy comparison between the two systems.

In accordance with the Department of Energy requirements, all reporting is given in S.I. (metric) units with other units in parentheses. Because the procurement was done within the U.S., all drawings were prepared using "U.S.", or customary units. In addition, many of the supporting calculations and spreadsheets were carried out in U.S. units, and it has not been considered appropriate to change all of these.

The second section of this report -- Summary of Conceptual Design Report -- reviews the findings of the Phase 1 project conducted by RLA. Phase 1 provided important background information to the current project because it investigated the suitability of the ESI-80 as a baseline machine.

The third section, System Specifications, presents the specifications that RLA adopted for the design of the prototype machines. These specifications identify the design wind regime and the load combinations to be considered.

The fourth section, System Loads, presents the loads that were used in the design of the prototypes. It also explains how and why these peak values and fatigue spectra were selected.

The fifth section, Description of Configuration, describes the final design and specifications for all components and subassemblies of both prototypes.

The sixth section, Field Test Results, summarizes the important results from the two field test programs. The power performance curves achieved are given, as well as typical results from the instrumentation on the blades, the low-speed shaft, the mainframe, and the tower.

The seventh section, Model Simulation, describes the computer models used in attempts to simulate the static and operating responses of both prototypes. It presents results from the static modal tests and shows how they were used to tune the computer models.

The eighth section, Reliability and Maintainability, addresses the reliability and maintainability issues. The improvements from the ESI-80 baseline are identified.

The ninth section, Manufacturing and Commercialization Plans, concerns the commercialization of the AWT-26. This section lists any intended modifications for commercial production and estimates the cost of energy in certain wind regimes.

The final section presents overall conclusions and achievements of this project.

Not all of the design information that led up to the final configuration is included in this report. Only that information which is most relevant is included. Additional design data is available at the subcontractor's facility. Some of the cost information is regarded as commercially sensitive; this is available for review by NREL personnel only.

2.0 Summary of Conceptual Design Report

2.1 General

Intermediate results of the present project were submitted to NREL in the report entitled "Advanced Wind Turbine Near-Term Development, Conceptual Study Report", dated March 16, 1993. That report described the findings of the first three tasks of this project:

Task 1. Assess baseline wind turbine for design improvements
Task 2. Determine the potential of candidate improvements
Task 3. Analyze effects of improvements on AWT design

It should be noted that the name given initially to the new design was the "WC-86" in earlier reports. This name was later changed to "AWT-26" to reflect a more international understanding. While both names may appear in past reports, this report will use the AWT name except where reference is made to past terminology.

2.2 The ESI-80

The baseline selected for study and development was the ESI-80 wind turbine. This machine has a two-bladed rotor with a diameter of 24.3 m (80 ft). The rotor is teetered (with zero delta-3) with a coning angle of 7° and is downwind. The nacelle is free yaw and the tower (approximate height 80 ft [24 m]) is a three-sided truss tower which can be tipped down.

Braking is done by a mechanical brake on the high-speed shaft in conjunction with deployable vanes on the tips of the blades. The main bearings are integral with the gearbox, which sits on a cast-steel mainframe.

RLA's direct involvement in the ESI-80 retrofit (REP) program, through SWEC, significantly increased understanding of the ESI-80, its operation, controls, maintenance, dynamic behavior, and structural characteristics.

The problems identified in Phase 1 were addressed in the final report for that subcontract. Solutions for the newly-identified problems (Phase 2) have been incorporated into the AWT-26 configuration.

Table 2-1 summarizes the ESI-80 problems identified by RLA.

2.2.1 Dynamics Problems

The REP test produced further insight into the potential for dynamics and loads problems with the AWT-26. Higher-than-expected loads were encountered in several components. These appeared to be associated with system dynamic responses rather than a lack of understanding of the external wind loading. A brief modal test was conducted to gather modes and frequency data, which helped explain these dynamic responses.

The two most significant dynamic problems encountered during the test were an infrequent teeter/yaw instability during start-up and a 7-per (7P) revolution blade edgewise mode which interacted with a tower bending/nacelle pitch mode.

Occasional dynamic interaction between teeter motion, yaw motion, and tower bending was excited during start-up. A severe response was excited only occasionally and appeared to be started by a rapid yaw motion at a certain point in the starting cycle.

Table 2-1. Summary of ESI-80 Problems

ESI-80 problems identified in Phase 1
Aerodynamic tip brakes -- mechanism failures
Rotor teeter bearings -- premature wear
Rotor teeter dampers -- premature failure
Rotor slip rings -- contamination and wear
Gearbox high-speed and low-speed seals -- leaks
Gearbox gears -- pitting
High-speed brake -- high maintenance
Yaw bearing -- possible premature wear
Tower -- fasteners loosen and minor cracks
ESI-80 problems identified in Phase 2
Teeter/yaw/tower dynamic instability
Controller problems
Maintenance expense
Protection
Starting procedure
Reliability
Gearbox high-speed bearing failures
Generator -- low efficiency

RLA believed that more teeter damping would substitute for the aerodynamic damping present at full operating speed and thereby solve the problem. This was demonstrated, although not conclusively, on the REP test by installing a second teeter damper configuration. The second teeter damper configuration tested contained Jarret dampers, and the problem was not encountered with those dampers installed. However, the operating time with the second set of test dampers installed was not sufficient to conclude that the problem would not reoccur. Further testing on the pre-prototype was planned.

2.2.2 Control System

The ESI-80 utilizes two different control systems, the American High Tech system and the Second Wind Alpha 7. Both are old, extremely unreliable, poorly documented, provide insufficient control, and are inflexible. For these reasons, RLA chose to design and install a new control system for the test machine. This new system was based on two Allen Bradley Programmable Logic Controllers (PLCs), and proved to be very useful for operating the machine and gathering loads during the test.

Further insight into the requirements for starting and stopping controls was provided by work on RLA's control system for the REP test machine. The need for precise timing of the on-line contactor closure, or use of a soft start system, was clearly demonstrated. Also, control of brake application timing and friction was shown to be very important in minimizing torque spikes.

High starting and braking torques during initial full-speed testing on the REP test program necessitated modifications to RLA's control system to reduce the torques to acceptable levels. This experience with RLA's programmable control system on the REP test helped set the preliminary

requirements for control of starting and stopping for the AWT-26. This test determined the best parameters for controlling the system and provided good estimates for initial settings.

2.2.3 Yaw Bearing

Analysis and inspections of the ESI-80 yaw bearings indicated that the yaw bearings are reliable if properly maintained. The inspections indicated that wear was occurring, but no galling was present. In addition, the measured loads were within the vendor's stated capacity. RLA and SWEC concluded that proper lubrication and sufficient grease distribution around the entire perimeter would ensure adequate life.

2.2.4 Gearbox

The ESI-80's PZ-140 gearboxes have suffered failures due to the upwind output shaft bearing, which is a ball bearing with limited radial capacity. Failure of this bearing can cause loss of all of the high-speed gears, requiring a very expensive repair. RLA located a roller bearing that matched the bore and shaft sizes of the original bearing with approximately five times the radial capacity. This is easy to replace if the gearbox is being serviced.

RLA believes that failures of this bearing are related to a combination of shaft misalignment and lateral loads caused by twisting of the frame under torque load from the gearbox. The need for good shaft alignment across the high-speed coupler was apparent and considered in the design of the AWT-26 drivetrain and mainframe.

2.2.5 Generator

REP test data and further discussions with vendors indicated that the generator on the ESI-80 test machine was inefficient, especially at low power levels. Near rated power, the generator was 95% efficient, but this dropped significantly at lower output to only 45% efficiency at 30 kW. This explained the poor 81% overall efficiency at a representative wind site.

2.2.6 Evaluation of Candidate Improvements

The list of candidate improvements studied and discussed in the Advanced Wind Turbine Conceptual Study Final Report (Phase 1) remained essentially unchanged after report submittal. This list, shown in Table 2-2, was discussed with NREL during the Phase 2 PDR, July 21, 1992.

During the PDR meeting, use of ailerons as an alternative to the tip brakes was discussed and incorporated into the list of items to be investigated. Also discussed at this meeting was a recommendation by RLA that the dynamic brake originally proposed by RLA be replaced with tip brakes for the recommended configuration. This, together with other improvements, is discussed in the subsections below.

2.2.7 Braking Systems

A trade-off study of the proposed generator dynamic brake, tip brakes on the blades, and the capacity of the low-speed braking system was conducted. More detailed preliminary design of the dynamic brake indicated that the components required to gently control stopping under all conditions would be larger and more expensive than anticipated. Several reports on the dynamic brake were included in Appendix A of the Advanced Wind Turbine Near-Term Product Development Conceptual Study report (Reference 9).

Table 2-2. Candidate Improvements for the AWT-26

No aerodynamic tips
Low-speed brake
Dynamic brake
Improved aerodynamic tips plus low-speed brake
New airfoils and larger diameter
NREL thin
NREL thick
Redesigned teeter bearings
Redesigned teeter dampers
Redesigned hub to accommodate new blades without root connections
Induction device in place of slip rings
Alternate low-speed shaft, bearing, gearbox configurations
Higher rated gearbox
New controller/starting
Variable speed
Taller towers
Add maintenance platform and yaw lock
Add means of parking blades horizontally

This increase in the expected cost of the dynamic brake made the cost of this system greater than the cost of tip brakes, and the development risk was higher. Also, tip brakes have the advantage of reducing the stopping torque load in the drivetrain and providing a possible small augmentation to energy production. One negative aspect of tip brakes is their impact on blade loading and fatigue. RLA believes this effect can be reduced by decreasing the tip brake system mass.

RLA's extensive analysis of tip brake deployment dynamics, combined with the experience and data gathered during the REP test, has provided increased confidence in the use of tip brakes. RLA developed a design using gas-pressurized dampers which have been quite effective at removing any large shock when the tips deploy. This should eliminate the problems encountered on the ESI-80 tip brakes.

Once the decision to use tip brakes was established, the trade-off between tip brake size and low-speed brake system capacity was studied. The analysis recognized that the two tip brakes are mechanically independent of each other and it was unlikely that both would fail closed at the same

time. It was decided to design the control system to detect the failure of one of the tip brakes to deploy, so that a single failure could not go undetected. Icing conditions that could prevent both tips from deploying would be detected and the wind turbine would not be allowed to operate under those conditions.

Two design criteria were then established. One dealt with the ability of one tip brake and half of the low-speed brake capacity to stop the rotor in all operating conditions. The other was the ability for both tip brakes to prevent overspeed in all conditions. Both criteria were achievable with 0.63 m^2 (6.75-ft^2) tip brakes and two 20,300-N·m (15,000-ft-lb) brake calipers. This was the chosen preliminary braking configuration for the AWT-26/P1. The brakes could be operated in two modes: a partial-pressure mode providing a relatively gentle stop, and a full-pressure dump emergency mode.

2.2.8 Driveline Configuration

A study of the driveline layout and low-speed shaft bearings was also conducted. The extended gearbox housing design, as used on the ESI-80, was compared to the use of pillow blocks to support a separate shaft. It was decided that pillow blocks would allow more flexibility in the choice of gearboxes for the machine and reduce the final cost of that component.

A comparison between foot mounting and shaft mounting the gearbox was conducted. A foot-mounted gearbox could replace the upwind pillow block, but its input bearing would be subjected to higher radial loading. This would preclude the use of a standard Flender gearbox, which seemed to be the lowest production cost choice. Overall, the lowest cost configuration, using the components available at the time, appeared to be a two-pillow-block arrangement with the gearbox supported by the rotating low-speed shaft. The gearbox torque would then be reacted by vertical torque links into the frame. Figure 2-1 shows the chosen drivetrain configuration.

Alternative mounting arrangements for the hub on the main shaft were studied to eliminate the expensive shrink disc and the tendency for the trunnion to spin on the shaft and gall the shaft. This problem was encountered during the REP test.

2.2.9 Generators

The experience with the generator on the ESI-80 led RLA to choose a much more efficient (low slip) generator for the AWT-26. The overall efficiency was 94% compared to 81% for the ESI-80 generator. These figures utilized the design wind speed distribution to calculate hours at various torque levels. Peak efficiency was 97% and good efficiency was expected even at low output levels (90% at 30 kW).

The increase in "stiffness" of the generator resulting from this change was analyzed for its effect on driveline torque loads. The small increase in higher frequency loads calculated had no significant effect on the fatigue life of the shaft or gearbox.

The specifications for the generator configuration have changed since the Phase 1 report. RLA believed that a totally enclosed, fan-cooled (TEFC) generator was not needed. Experience showed that use of the best recently available potting epoxy material and potting techniques could provide the required resistance to moisture and dirt penetration into the windings. This in turn provided the required life, even with an open, drip-proof (ODP) configuration. Use of an ODP generator was estimated to save approximately 320 kg (700 lbs) and $1,000 per machine.

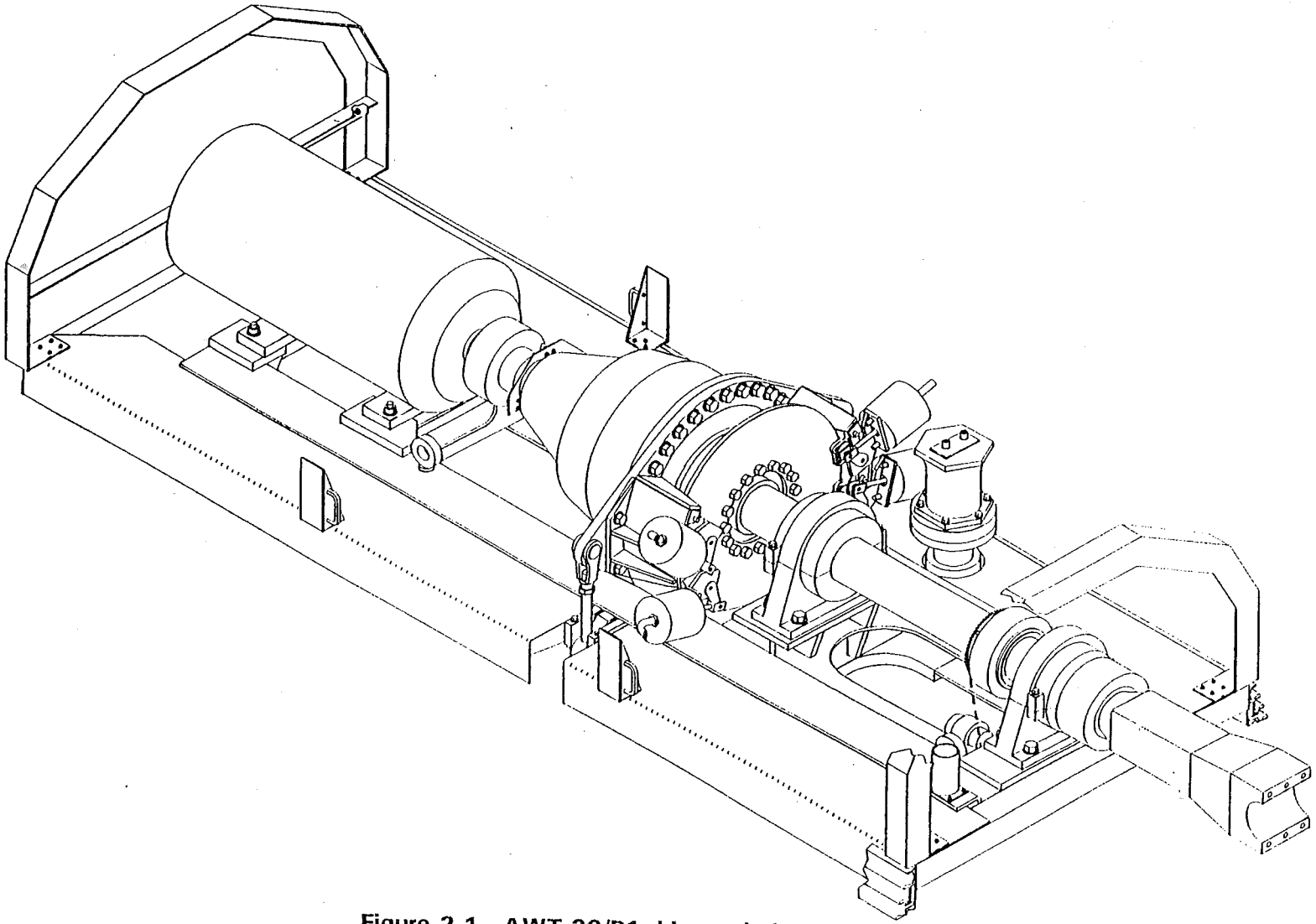

Figure 2-1. AWT-26/P1 drive train layout

2.2.10 Ailerons

As discussed at the PDR meeting, use of ailerons for peak power control and aerodynamic braking was evaluated for the AWT-26/P1. The investigation concluded that ailerons could be best applied to a larger rotor for a future model to be used for lower wind speed sites. This would allow a larger swept area to be used without exceeding the peak power of the AWT-26. However, development of this concept would be a major undertaking and was considered to be outside the scope of the current contract.

2.2.11 Towers

In addition to the 24.4-m (80-ft) and 36.6-m (120-ft) towers discussed in the Phase 1 report, a 45.7-m (150-ft) tower was planned for the AWT-26. This would allow the turbine to take maximum advantage of high wind shear sites and to meet the $0.05/kWh goal for 5.8-m/s (13 mph) wind sites. The height chosen is limited by FAA requirements for special visibility provisions for structures above 200 feet. These provisions apply to the maximum blade tip height.

The optimum configuration for taller towers was evaluated. The study showed that free-standing lattice towers are practical up to about 36.6 m (120 ft). Towers above that height may require guy cables to achieve the required strength and stiffness. Preliminary design of the selected 45.7-m (150-ft) tower would be a straight, four-leg truss tower, with one set of four guy cables attached to the tower below the rotor swept area.

2.3 Selected Improvements

The selected improvements and a description of the proposed configuration were included in a letter sent to NREL on October 1, 1992. These improvements and the entire AWT/P1 configuration were reviewed by NREL at informal design review meetings on September 1, 1992, and October 16, 1992. A complete description of the selected configuration was attached as Appendix B of Reference 9. The major differences between the "baseline" ESI-80 Retrofit and the AWT-26/P1 are summarized in Table 5-1 on pages 34 and 35.

3.0 System Specifications

This section presents extracts from the final system specifications. They define the wind turbine operating environment, the control and safety system requirements, the machine operation modes, and the circumstances for which these must be designed.

The full specifications may be found in the following RLA/AWT documents.

- SS263008 AWT-26 wind turbine system specification
- SS263007 AWT-26 wind turbine system design criteria

Some of the general specifications for the AWT-26/P2 are given below.

Item	Specification
number of blades	2
diameter	86 ft (26.2 m)
airfoil	NREL thick airfoils S815, S810, S809
blade construction	wood epoxy
orientation	downwind
power regulation	fixed pitch, stall regulated
coning angle	7 degrees
rotational speed (synchronous)	57.1 rpm
hub configuration	teetered, zero delta-3
maximum teeter angle	7 degrees
yaw bearing	free
transmission	3-stage planetary
gear ratio	31.5
nominal electrical power rating	275 kW
voltage	480 V, 3 phase
primary brake	high speed mechanical
secondary brakes	aerodynamic tip vanes

3.1 Wind Regime

The wind regime for which the wind turbine shall be designed is specified below. This wind regime meets or exceeds the requirements of a Class 2 site as described in the IEC safety code (reference 10). Unless stated otherwise, all conditions refer to the turbine hub height.

- mean annual wind speed for optimal performance: 17 mph (7.6 m/s)
- mean annual wind speed for structural design: 19.0 mph (8.5 m/s)
- Weibull distribution shape factor: 2.0 (Rayleigh distribution)
- air density: 0.0766 lb/ft^3 -- 0.06253 lb/ft^3 (1.225 kg/m^3 -- 1.0 kg/m^3)
- vertical wind shear exponent: 0.20
- turbulence intensity (including wake): 20% (as defined in IEC draft)

- extreme operating gust amplitude for hub height wind speeds in excess of 18.2 m/s (40.7 mph) (all conditions) is given by: Vgust = 0.16 Vmean + 0.75 Vhub where Vmean = 19.0 mph (8.5 m/s) and Vhub is the 10 minute average wind speed at hub height. For hub height wind speeds below 18.2 m/s (40.7 mph), the extreme gust amplitude shall be 15 m/s (33.6 mph). The gust magnitude shall be considered a cosine curve, with a rise of six seconds and a fall of six seconds.

- extreme direction changes are given by $\theta(Vhub) = 210 - 4.4\ Vhub$; $50^\circ < \theta(Vhub) < 180^\circ$ where Vhub is in m/s and q is in degrees. The change shall be assumed to follow a cosine curve and to occur over eight seconds. The corresponding maximum rates of direction change are given by

  $R(Vhub) = 31.7 - 0.69\ Vhub$; $10^\circ/s < R(Vhub) < 30^\circ/s$ where Vhub is in m/s and R(Vhub) is in °/s.

- extreme horizontal wind shear (linear gradient in m/s/m) = 0.76 Vhub/D where D is the rotor diameter in meters.

- extreme vertical wind shear exponent: 1.0 (cosine curve, 6-sec rise, 6-sec fall)

- extreme 3-sec gust (stationary rotor): 133-mph (59.5-m/s) peak (associated vertical wind shear exp. = 0.1)

3.2 Physical Environment

The wind turbine shall be designed to withstand the following environment:

- maximum operating temperature: +50°C (122°F);

- minimum operating temperature: -30°C (-22°F) design to include provision for equipment required to operate to -40°C (-40°F) at customer's option;

- maximum ice covering: 2.0 in. (50 mm) on all external surfaces (60 lb/ft^3 [900 kg/m^3]);

- design hail stone: 0.06 lb @ 45 mph (0.027 kg @ 20m/s);

- solar radiation intensity: 1,100 watts/m^2;

- humidity: 0 to 100%;

- precipitation: up to 2 in./hr (50 mm/hr);

- salt: not applicable to standard model; and

- seismic: per 1991 Uniform Building Code, Chapter 23, (Reference 11). Zone 4 using an RW factor from Table 23-Q of 3.

In addition, the design shall assume the possibility of lightning strikes to the turbine and minimize the effect of lightning on turbine operability. Lightning protection within the blade has not been installed but possible methods are currently under development.

3.3 Control and Protection System

The purposes of the control and protective systems are to control the operation of the wind turbine, minimize component damage in the event of failures, and maintain the wind turbine in a non hazardous condition at all times. The control and protective systems shall detect all unsafe conditions and cause the machine to cease operation and/or return to a safe or non hazardous condition.

The control and protective systems shall satisfy the following minimum requirements.

3.3.1 Redundant Brakes

The turbine shall be designed with redundant braking, such that, in the event of failure of any one component, the braking system(s) will stop rotation or maintain a safe rotational speed in any design wind condition. An example of a single component failure would be failure of a single tip or single caliper. One braking system will act on the rotor or the low-speed shaft.

3.3.2 Safe Operation

A safe turbine condition will be assured despite the failure of any one component, part, or power source which is not designed for "safe-life".

The probability of multiple failures resulting in an unsafe condition will be reduced by automatic detection of component failures to the extent practical.

The control and protection system shall, at all times during operation, be able to detect and ensure safe shutdown for the following conditions:

- excessive wind velocity;
- a rotor overspeed of 10% above the normal operating speed;
- excessive vibration;
- loss of grid connection;
- generator overload; and
- excessive cable twisting.

The control and protection system shall provide redundant means of detecting and reacting to rotor overspeed.

The control system shall provide for horizontal parking of the rotor to $\pm 20^{\circ}$ from the horizontal during normal operation and for selective position parking at the option of maintenance personnel during maintenance activities.

Operation of the turbine shall be prevented if the turbine is locked in yaw.

3.4 Design Life

The wind turbine shall be designed for a minimum life of 30 years. Overhaul, replacement and/or reconditioning of any components may be allowed for during the 30-year life, if cost effective.

3.5 Performance and Operational Criteria

In addition to the performance characteristics specified in the System Specification (SS263008A), the design shall assume the following performance and operational characteristics. All wind speeds refer to turbine hub height unless otherwise specified.

cut-in wind speed	11 mph (4.9 m/s)
cut-out wind speed	50 mph (22.3 m/s)
rotor operating (synchronous) speed	5.98 rad/sec (57.14 rpm)
gearbox ratio (see SS263002)	31.5:1
max (nominal) aerodynamic power	325 kW
max (nominal) aerodynamic torque	39,925 ft-lbs (54,153 N·m)
maximum electrical transient torque (high-speed shaft)	3,100 ft-lbs (4,204 N·m) for 0.04 seconds
maximum (nominal) mechanical brake torque (high-speed shaft) (see SS263006)	2,200 ft-lbs (2,983 N·m)
design overspeed	63 rpm
tower shadow deficit (wind speed at blade)	30%
electrical voltage	480 V ±10%
electrical frequency	60 Hz ±4%
maximum 3-phase fault current	35,000 A
maximum single-phase fault current	35,000 A

The wind turbine shall be designed in accordance with the following criteria.

- number of low wind stops per operating hour: 0.3; maximum = 3.0/hr
- number of high wind stops per operating hour: 0.01; maximum = 3.0/hr
- number of emergency stops per operating hour: 0.01; maximum = 3.0/hr

3.6 Modes of Operation

The operation of the wind turbine shall be divided into the following possible modes.

1. normal operation;
2. operation with a fault occurrence (until shutdown initiated);
3. starting sequence;
4. normal shutdown;
5. emergency shutdown;

6. parked/stationary; and
7. transportation, installation.

These modes or conditions are distinct from the various loads which may occur, although some modes automatically, or through the control system, will preclude certain loads or load combinations.

3.7 Basic Load Cases

The list below gives the types of loads that must be considered. Some of these are "internal" (defined by the machine design and system) and others are "external" (defined by outside influences).

1. Gravity

2. Inertia (centrifugal, Coriolis forces, mass imbalance, dynamic amplification, etc.)

3. Normal aerodynamic loads on the machine. This will include the effects of wind shear, tower shadow, turbulence, yaw errors, and aerodynamic imbalance and will be associated with fatigue design. They will be considered for both operating and non operating conditions.

4. Extreme aerodynamic loads (return period = 50 years) on the operating machine. These will be infrequent loads associated with gusts, direction changes, and extreme wind shear (which may occur simultaneously).

5. Extreme aerodynamic loads (return period = 50 years) on the stationary machine. This is the "survival wind" or hurricane loading (which occurs with a reduced vertical wind shear).

6. Normal braking loads

7. Emergency braking loads

8. Fault/accident loading. This could be loads due to internal faults such as electrical short circuit, control system failure, or other single-point failures. External faults include grid failure.

9. Ice loading

10. Seismic loads. These will depend on the site, but are not usually critical for a wind turbine.

11. Lightning

12. Impact loads due to hail or bird impact

13. Locked yaw loads

3.8 Load Combinations

The wind turbine shall be designed for the following load combinations.

mode	load combination	criterion
normal operation	gravity + inertia + normal aero	fatigue
	gravity + inertia + extreme aero	single peak
	gravity + inertia + extreme aero + lightning	single peak
	gravity + inertia + normal aero + seismic	single peak
	gravity + inertia + normal aero + impact	single peak
	gravity + inertia + normal aero + ice	single peak
operation + fault	gravity + inertia + normal aero + internal fault	single peak
	gravity + inertia + extreme aero + external fault	single peak
	gravity + inertia + extreme aero + overspeed	single peak
starting	gravity + inertia + normal aero	fatigue
	gravity + inertia + extreme aero	single peak
	gravity + inertia + normal aero + ice	single peak
normal stop	gravity + inertia + normal aero	fatigue
	gravity + inertia + extreme aero	single peak
	gravity + inertia + normal aero + seismic	single peak
	gravity + inertia + normal aero + ice	single peak
emergency stop	gravity + inertia + normal aero	single peak
	gravity + inertia + extreme aero + internal fault	single peak
	gravity + inertia + extreme aero + seismic + external fault	single peak
	gravity + inertia + ice	single peak
	gravity + inertia + extreme aero + external fault	single peak
parked/stationary	gravity + ice	single peak
	gravity + extreme aero	single peak
	gravity + ice + .5 extreme aero load	single peak
	gravity + lightning	single peak
	gravity + seismic	single peak
	gravity + normal aero	fatigue
	gravity + normal aero + locked yaw	single peak
transportation/ installation	gravity + inertia	single peak

3.9 Safety Factors

The safety factors for the design of structural components of the wind turbine shall be as follows.

A. General safety factors:

Material yield	1.5
Material ultimate failure	2.0
Component buckling	2.0

B.	Hydraulic components:	
	Material yield	2.0
	Rupture	3.0
C.	Pneumatic components:	
	Material yield	2.0
	Burst	5.0
D.	Bolted connections:	
	Loss of bolt tension preload	1.5
	Transverse slip	1.5
E.	Hoisting and handling equipment:	
	Material yield	3.0
	Ultimate failure	5.0
F.	Foundations:	
	Pullout	2.0
	Bearing ultimate failure	2.0

These safety factors are required for all analyses utilizing the "characteristic" values of loads and material properties. Characteristic material properties are defined as the properties exceeded by 95% of all samples with 95% confidence. Characteristic loads shall be the best estimate of the maximum loads the wind turbine will actually experience.

These safety factors meet or exceed the requirements of the IEC draft standard as illustrated in Table 3-1.

For purchased components (gearbox, bearings, generator, teeter dampers, etc.) the safety margins used shall be consistent with common practice for each component and with the operations, maintenance and design life requirements of the system specification.

Table 3-1. Comparison of RLA and IEC Analysis Requirements

Load Type	Component Class	Limiting Mode	IEC Load Factor	Resistance Factor (steel)	IEC Total Factor	AWT-26 Safety Factor	Difference AWT-26 less IEC
Aerodynamic	Any	Yield	1.30	1.1	1.43	1.50	0.03
(w/gravity loads)	Any	Ult.	1.30	1.33*	1.73	2.00	0.27
	Fail-safe	Fatigue	1.00	1.00	1.00	1.25	0.25
	non Fail-safe	Fatigue	1.00	1.25	1.25	1.25	0.00
Braking	Any	Yield	1.40	1.1	1.54	1.50	-0.04
(w/gravity &	Any	Ult.	1.40	1.33*	1.86	2.00	0.14
aero. loads)	Fail-safe	Fatigue	1.00	1.00	1.00	1.25	1.25
	non Fail-safe	Fatigue	1.00	1.25	1.25	1.25	0.00
Hydraulic							
Components	Any	Yield		NA		2.00	
		Rupture		NA		3.00	
Pneumatic							
components	Any	Yield		NA		2.00	
		Burst		NA		5.00	
Hoisting &							
Handling Equip.	Any	Yield		NA		3.00	
		Ult.		NA		5.00	
Bolted Connection	Any	Slip	NA	NA	NA	1.50	
		Preload	NA	NA	NA	1.50	

* Partial safety factor for material strengths defined by AISC in compliance with IEC requirements.

4.0 System Loads

4.1 Background

4.1.1 Types of Loads

Design driving loads can be regarded as falling into one of two categories: peak loads and fatigue loads. Peak loads are the maximum loads that a component is expected to experience in the 30-year life of the wind turbine, based on the design wind environment specified in the previous section. The peak loads are typically associated with extreme environmental conditions.

Fatigue loads are defined as the complete spectrum of loads (on an annual basis) expected to be applied to the component during the operational life of the wind turbine. This is affected by the system dynamics, wind environment, and control system logic.

4.1.2 AWT-26 Historical Loads Development

Loads development for the AWT-26 wind turbine occurred in several phases. The first phase involved the use of analytical codes to predict mean load and power levels. The next stage incorporated wind turbulence models to estimate stochastic loads for use in fatigue calculations. This work was done using the FLAP computer code (Reference 12) and results are presented in the RLA report titled "Advanced Wind Turbine Conceptual Study Final Report" (March 1992).

These results were used to design the retrofitted ESI-80 turbine (REP) in San Gorgonio Pass, California. The results of testing the REP rotor were presented in the RLA report "ESI-80 Rotor Performance and Reliability Enhancement Program" (March 26, 1993).

The REP test data were evaluated and used to improve the loads estimates for the first prototype AWT-26/P1. The inputs, equations, formats and other relevant information for producing, presenting, and using this loads data are given below. The same REP test data were also used to define the load spectra for the second prototype, P2. Both of these machines are currently being tested in Tehachapi, California. The data collected from P2 has been evaluated and used to validate the design load spectra for P1 and P2, and will help to define spectra of loads for subsequent models. The results appear in the Field Test Results section.

The loads obtained in this manner are considered to meet or exceed those that would be experienced in an IEC class 2 site (see Reference 10). The wind regime corresponding to the data collected exceeded the required 8.5 m/s (see Figure 4-1) and the transient conditions also appeared to exceed the IEC requirements.

Further information on the measured loads is given in the section entitled "Field Test Results, Structural Response".

4.2 Current Loads Development and Fatigue Analysis Methodology

4.2.1 Testing and Experimental Results

Testing of the turbine produced data for loads at certain locations which were selected by the need for design load information, and by the feasibility of installing instrumentation. This information is of great value; however, it may not produce an entirely clear picture of the behavior of the complete system because tests cannot be conducted during all conditions that may be expected over the operational life of the turbine. The measurements taken on all three machines (REP, P1, and P2) included:

- blade root flap bending;
- blade root edge bending;
- shaft torque;
- shaft bending;
- tower leg loads/thrust;
- teeter angle;
- yaw angle; and
- nacelle/tower accelerations.

Data were normally taken in 10-minute records across a range of operating wind speeds. Sample rates were either 50 Hz (REP and P1) or 40 Hz (P2). Additional data were taken during start-ups, normal and emergency shutdowns, non operating conditions, and during fault conditions.

The data from the REP test were reduced primarily by means of a rainflow counting algorithm (Downing and Socie 1982, Reference 22). This methodology provided fatigue cycle data as well as a means of estimating peak loads.

4.2.2 Peak Loads

Using the rainflow results, test data can be extrapolated to give approximate peak loads for the 30-year life of the machine. The statistical process being used was recently developed by researchers at NREL and their subcontractors (Reference 24). With enough available data, the rainflow counts can be fitted to a statistical distribution. The equations that have been used are:

Gaussian distribution: $N(x) = a \cdot \exp\{-0.5 \cdot ((x-b)/e)^2\}$

Log normal distribution: $N(x) = a \cdot \exp\{-0.5 \cdot (\ln(x/b)/e)^2\}$

Exponential distribution: $N(x) = a \cdot \exp\{-b \cdot x\}$

Where N is the number of counts in the bin centered on the value x, and a, b, and e are parameters varied to fit the data set. Typically, a combination of three of the above distributions is used to fit the collected data, each distribution representing a loading process present in the data (gravity, turbulence, resonance, teeter hits, etc.). In many cases, only the tail fit is of any importance since the high cycle count, low load range is below the fatigue endurance limit.

These statistical distributions of measured loads are used to extrapolate the data sets to provide extreme operating loads. The extrapolated curves are considered to include the transient environmental conditions specified in the wind environment (such as peak operating gust and maximum operating wind direction change).

Unfortunately, the extrapolation is usually based on the low cycle count region of the distribution, where by definition there is little data. This leads to some uncertainty in the results, which should be checked against what is considered rational for each load for the wind turbine.

The cycle counts are defined in terms of number of cycles per second. For our design site with 6,625 operating hours per year and a design life of 30 years, the most extreme cycle occurs once every 715,500,000 seconds.

4.2.3 Fatigue Stress Distributions

The second use of the REP cycle distributions was to develop fatigue loads. In most cases, the cycle distributions were regarded as encompassing all normal operating states and transient conditions (including starts and stops) which might contribute to the fatigue damage.

The procedure was to first determine the maximum principal stress at the point of interest due to a "unit load" (such as 1,000 lb, or 1,000 in.lb) at one location (such as a root flap bending or thrust on the hub). This principal stress was then used to scale the known spectrum of loads at that location. This spectrum of stress cycles was then applied to an S-N curve selected as appropriate for the material, the mean stress, and the particular finish and detail. Miner's cumulative damage rule was used to determine the fatigue damage that would accumulate in one year: hence, the number of years to failure was calculated.

The S-N curves used were corrected for the presence of variable rather than constant amplitude loads. This implied that in place of an endurance limit at between 10^6 and 10^7 cycles, the log-log straight line was extrapolated to $2x10^8$ cycles and held constant thereafter. This approach, adopted from Det Norske Veritas offshore codes (Reference 13), generally gave answers that were more conservative than modifying the log-log gradient beyond 10^7 cycles (as suggested by other codes).

An alternative approach to the definition of fatigue stresses was the use of the standard deviation versus windspeed curves developed from the REP data. Standard deviation is a common way of describing the fatigue cycles and was the basis of the LIFE code (Reference 25) developed at Sandia National Laboratories. If the signal is a truly narrow-band Gaussian one, then the distribution of stress excursions at any one wind speed can be shown to be a Rayleigh curve. However, this is not always the case, and a Weibull distribution with a shape factor of between 2.0 and 3.5 is often more appropriate. The LIFE7 code at RLA, based on Sandia's LIFE code, allowed this and other parameters to be selected.

As in the first method, the maximum principal stress due to a unit load was calculated and the corresponding curve of stress standard deviations versus windspeed, together with the material S-N curve were inserted into the program. The Weibull shape factor for the distribution of stress excursions, the wind regime (8.4 m/s at hub height), and cut-in and cut-out windspeeds were all specified.

A comparison of these two methods showed that the results were in close agreement if a Weibull shape factor of 3.5 was used in the LIFE7 code. This indicates that the high-value stress excursions are not as frequent as the Rayleigh distribution implies.

4.2.4 Load Combinations

The identification of the maximum expected value of each load has been described above. However, the designer must know with what other loads that peak value should be combined. The approach used was to apply "Turkstra's principle" (Reference 23), which states that, unless loads are statistically correlated, the maximum value of one load should be combined with "normal" values of other loads.

Therefore, it is necessary to decide if the circumstances producing the maximum root flap bending, for example, are likely to be the same as those producing maximum edge bending, thrust, or other quantities.

It was decided there was no condition in which the maximum values were fully correlated, and recommended that the precise value of the lesser quantities to be combined with each maximum be decided on a case-by-case basis. However, it was suggested that those lesser values should not be less than those expected to occur 0.0001 times per revolution, or once in 2.7 operating hours.

In terms of fatigue stresses, the excursions at any point within the wind turbine are typically dependent on more than one rotor load. The principal stresses due to the various loads may be aligned with each other or at some angle to each other.

If the stresses are aligned, they may be regarded as being randomly associated and combined as the root of the sum of squares. It would require that both loads be at the same frequency in phase with each other for the stresses to be combined algebraically.

If the stresses are not aligned, and there is a general 2- or 3-dimensional stress field, then the determination of the fatigue strength is more complex.

In all cases of AWT-26 fatigue design, it was discovered that one particular load dominated the stresses at any one point. It was, therefore, not necessary to consider the combination of stresses from more than one load. The fatigue life due to each individual load was calculated and the lowest life identified was taken as the fatigue life of that part or component.

4.2.5 Fatigue Load Spectra

The distribution of wind speeds for the (approximately) five hours of data used to define the REP loads is presented in Figure 4-1. The mean wind speed was 9.8 m/s (22.0 mph) with an average turbulence intensity of 22%. Hence, the wind regime from which the fatigue loads were extracted exceeds the design wind regime of a Rayleigh distribution with a mean of 8.5 m/s (19 mph). This represents some conservatism.

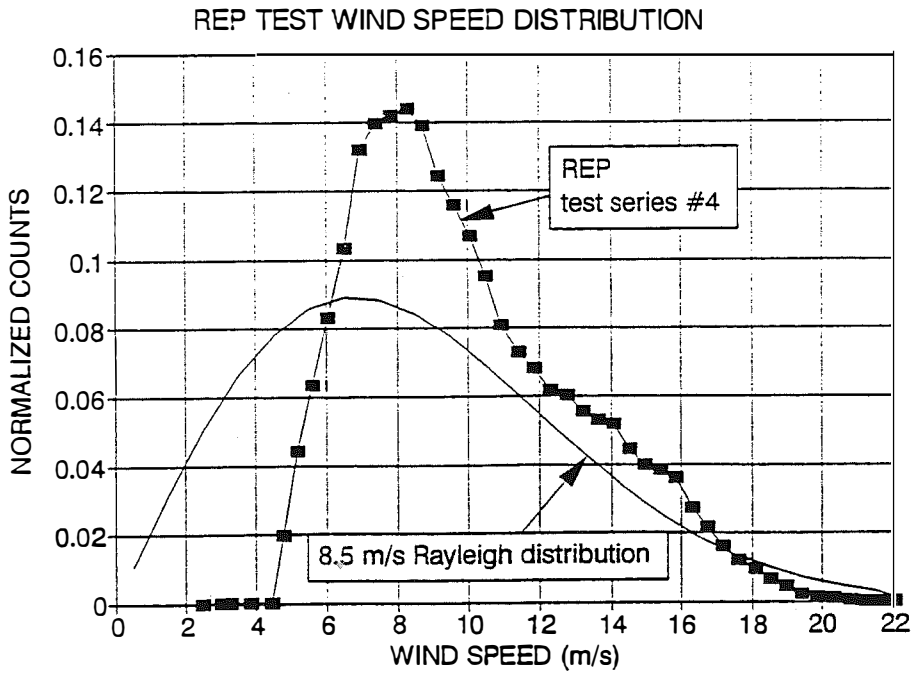

Figure 4-1. Wind speed distribution for REP data collection

4.2.6 Rotor

The primary loads governing the design of the rotor system (including blades, hub, and teeter components) are the blade flapwise and edgewise bending moments, the torque, and the teeter moment. The fatigue load spectra for each of these loads appear in Figures 4-2 through 4-5.

4.2.7 Drivetrain

The drivetrain loads are the main shaft moments: torque, horizontal and vertical bending. Horizontal bending is in the same direction as a yaw moment, and vertical bending is a pitching moment. The spectra for these two loads appear in Figures 4-6 and 4-7.

4.2.8 Mainframe

The mainframe loading includes the shaft moments, the rotor thrust, and the pitching moment at the yaw bearing. The spectra of thrust and pitching moment appear in Figures 4-8 and 4-9.

The thrust was calculated from the measurement of the bending moment at the base of the tower. It was assumed that this bending moment was produced by a single static thrust load from the rotor. The pitching moment was calculated as the rotational acceleration (from vertical accelerometer measurements) multiplied by the rotational inertia of the nacelle and rotor about the yaw axis.

4.2.9 Tower

The tower loads include the torque, thrust, and pitching moment as described previously.

4.3 Peak Loads

The peak design loads and associated safety margins are summarized in Table 4-1.

4.3.1 Rotor

The peak rotor loads are presented graphically and in tabular form in Figure 4-10. The points of load application are at the blade flanges, and the teeter damper and hard stop. The input loads are reacted at the teeter pin.

4.3.2 Drivetrain

The teeter pin carries all of the rotor loads into the drivetrain with the exception of the teeter damper/stop contact points. These loads are depicted in Figure 4-11.

4.3.3 Mainframe

The mainframe carries the loads between the teeter pin and the yaw bearing. These are depicted in Figure 4-12.

4.3.4 Tower

The tower carries the thrust loads and tower top moments to the ground. These are depicted in Figure 4-13.

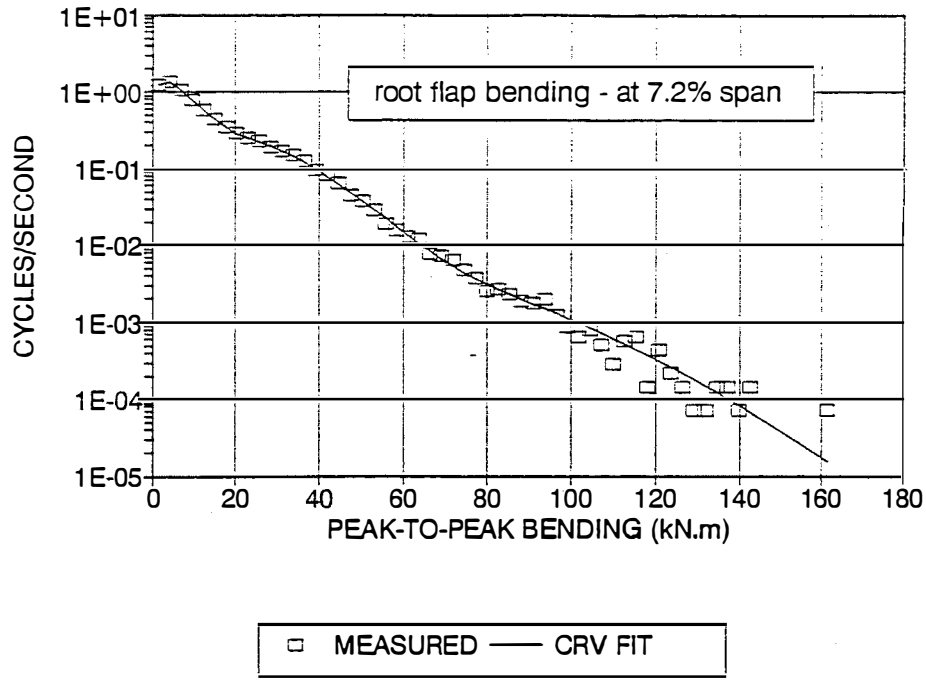

Figure 4-2. Measured cyclic loads from REP test: root flap bending

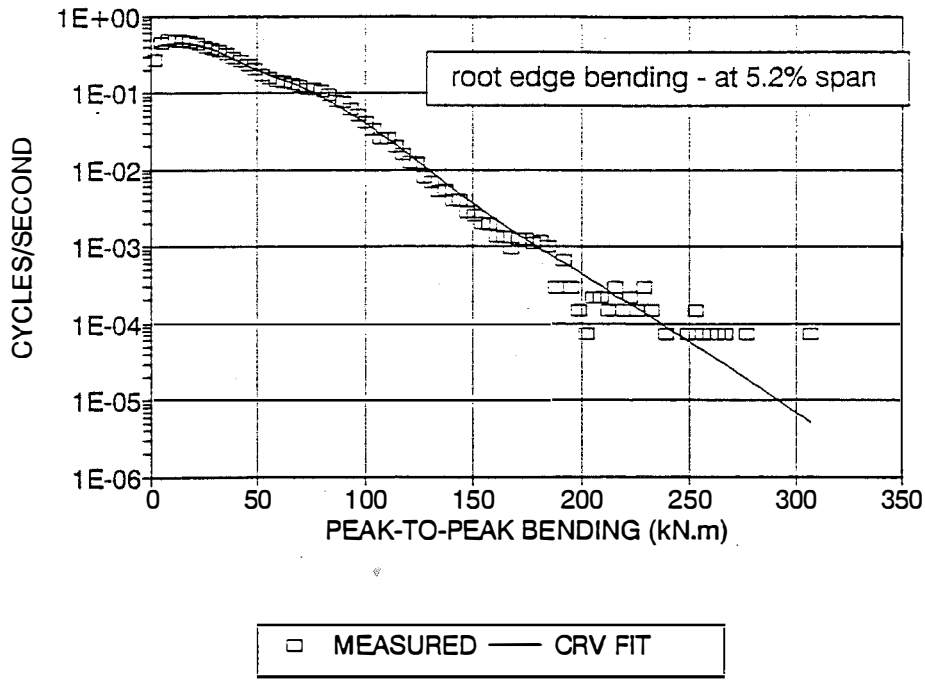

Figure 4-3. Measured cyclic loads from REP test: root edge bending

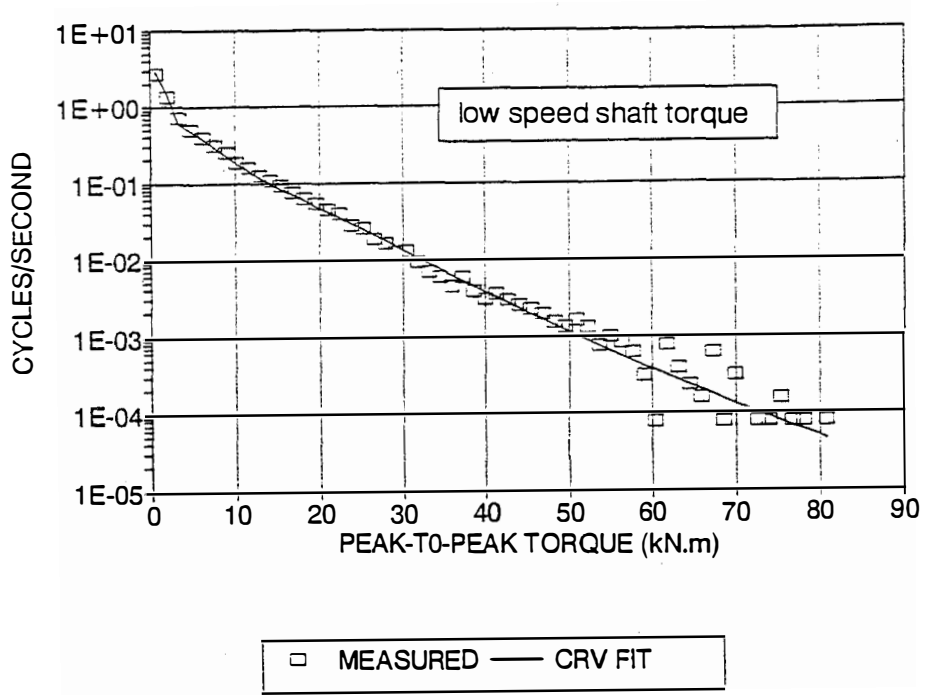

Figure 4-4. Measured cyclic loads from REP test: low-speed shaft torque

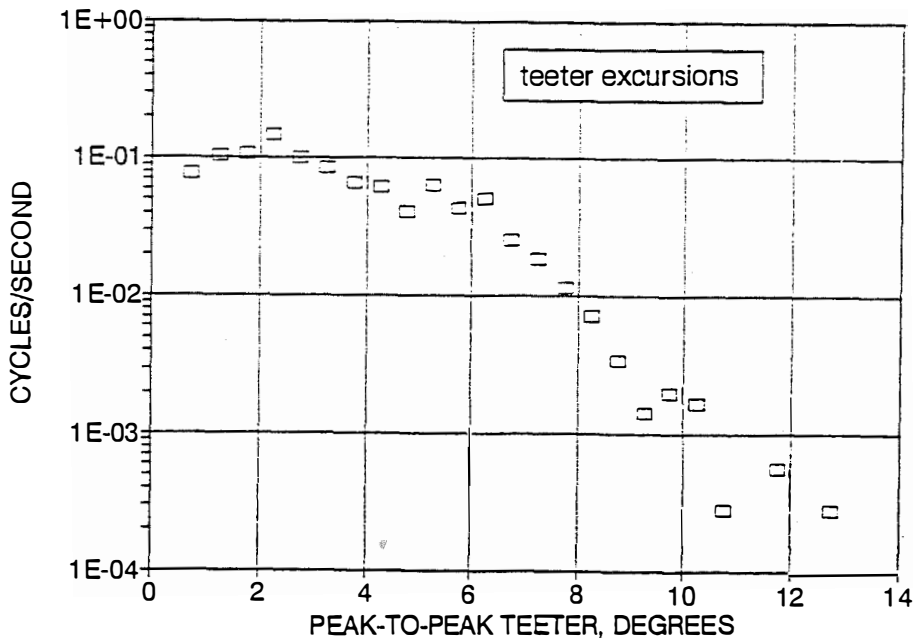

Figure 4-5. Measured cyclic loads from REP test: teeter excursions

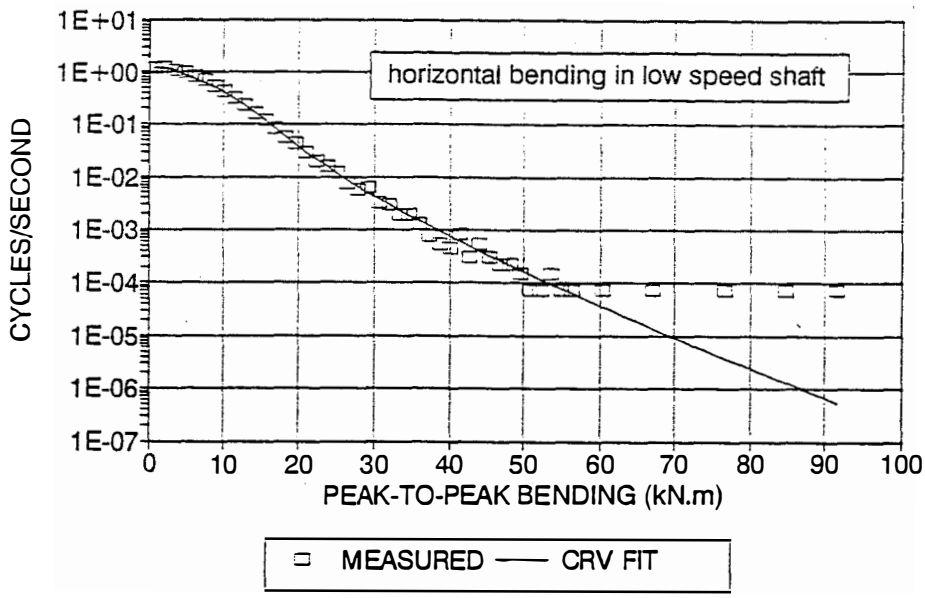

Figure 4-6. Measured cyclic loads from REP test: low-speed shaft horizontal bending

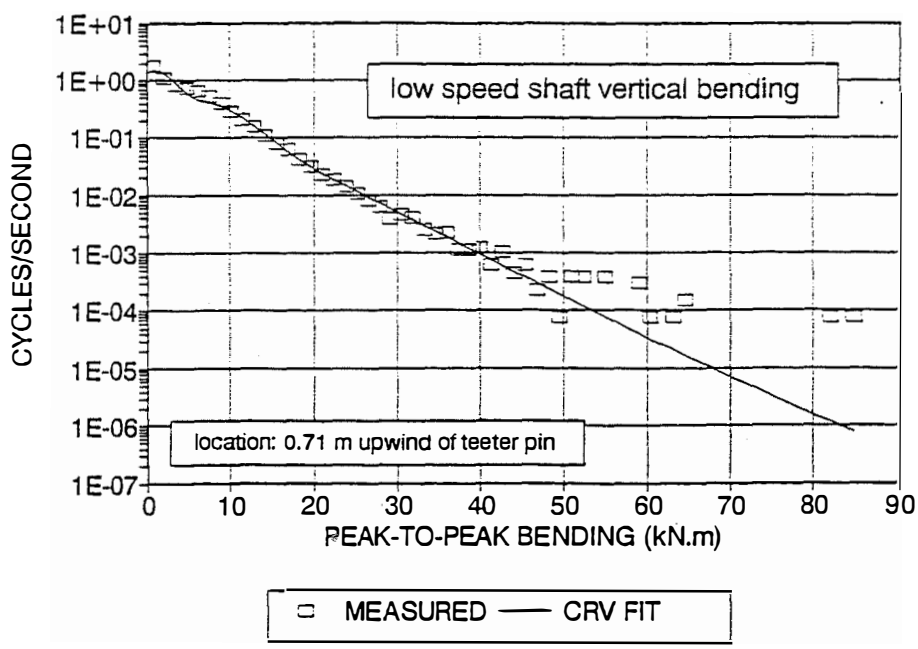

Figure 4-7. Measured cyclic loads from REP test: low-speed shaft vertical bending

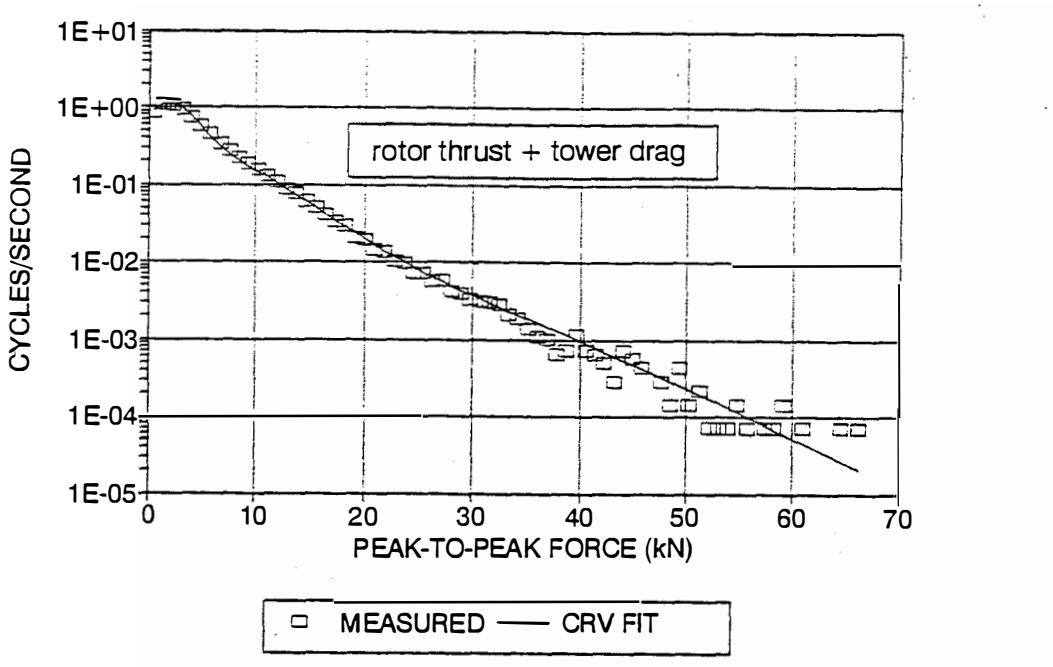

Figure 4-8. Measured cyclic loads from REP test: rotor thrust

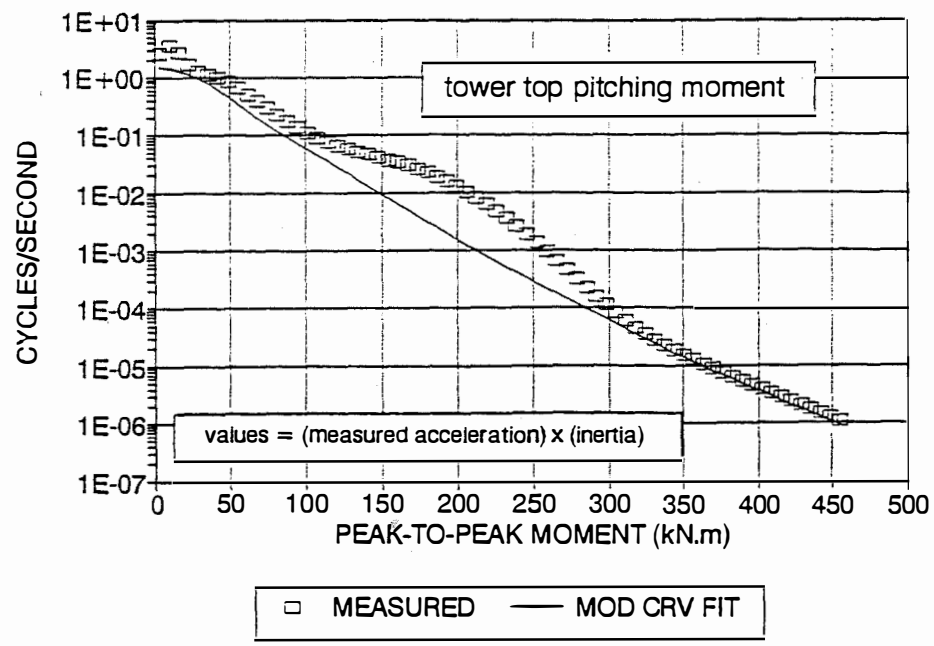

Figure 4-9. Measured cyclic loads from REP test: tower top pitching moment

AWT-26
BLADE ROOT/HUB LOADS

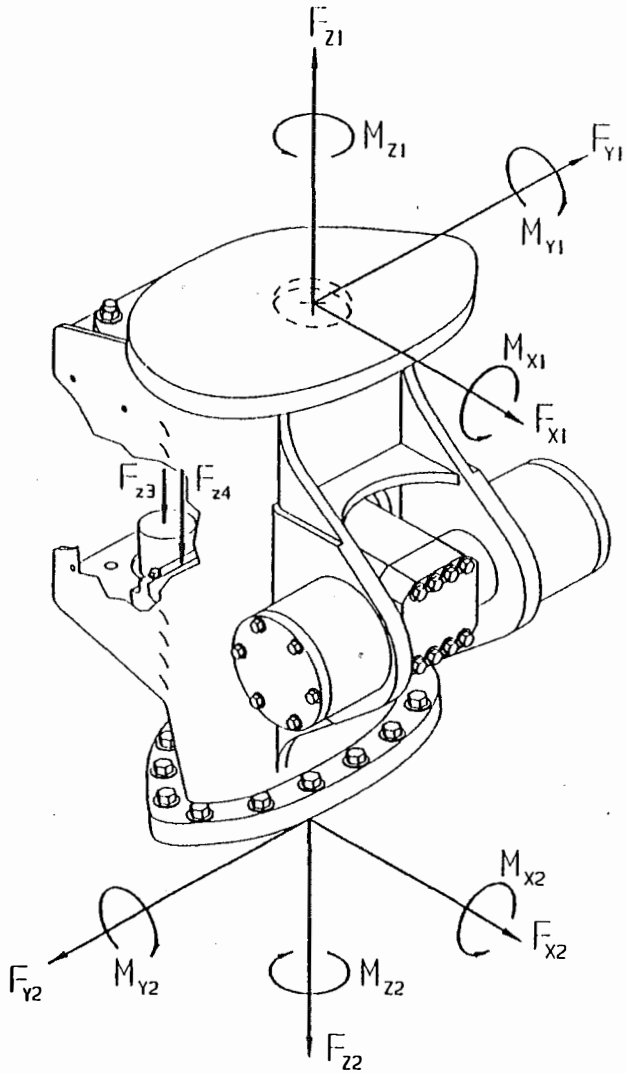

	OPERATING 30 YEAR PEAK LOAD	NON-OPERATING PEAK LOAD
F_{X1} (N)	45,288	33,375
F_{Y1} (N)	28,925	13,350
F_{Z1} (N)	107,200	13,350
M_{X1} (N · m)	99,309	27,120
M_{Y1} (N · m)	283,096	216,960
M_{Z1} (N · m)	61,698	---
F_{X2} (N)	45,288	33,375
F_{Y2} (N)	28,925	13,350
F_{Z2} (N)	107,200	13,350
M_{X2} (N · m)	45,765	27,120
M_{Y2} (N · m)	122,040	216,960
M_{Z2} (N · m)	1,581	---
F_{Z3} (N)	222,500	222,500
F_{Z4} (N)	222,500	222,500

Figure 4-10. Peak hub and blade root loads

AWT-26
SHAFT/TEETER PIN LOADS

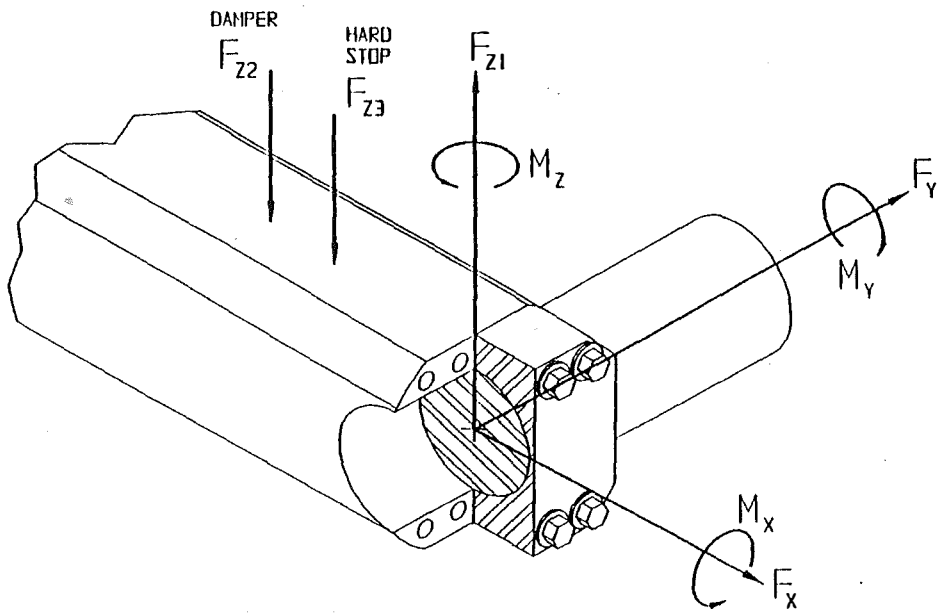

	OPERATING 30 YEAR PEAK LOAD	NON-OPERATING PEAK LOAD
F_X (N)	68,009	66,750
F_Y (N)	57,850	53,400
F_{Z1} (N)	217,213	53,400
M_X (N · m)	145,092	13,560
M_Y (N · m)	0	0
M_Z (N · m)	61,698	---
F_{Z2} (N)	222,500	222,500
F_{Z3} (N)	222,500	222,500

Figure 4-11. Peak drive shaft loads

AWT-26
MAINFRAME LOADS

	OPERATING 30 YEAR PEAK LOAD	NON-OPERATING PEAK LOAD
F_{X1} (N)	68,009	66,750
F_{Y1} (N)	57,850	53,400
F_{Z1} (N)	217,213	53,400
M_{X1} (N · m)	145,092	13,560
M_{Y1} (N · m)	0	0
M_{Z1} (N · m)	61,698	---
F_{X2} (N)	68,009	66,750
F_{Y2} (N)	68,009	66,750
F_{Z2} (N)	80,100	80,100
M_{X2} (N · m)	145,092	13,560
M_{Y2} (N · m)	216,960	67,800
M_{Z2} (N · m)	27,120	27,120

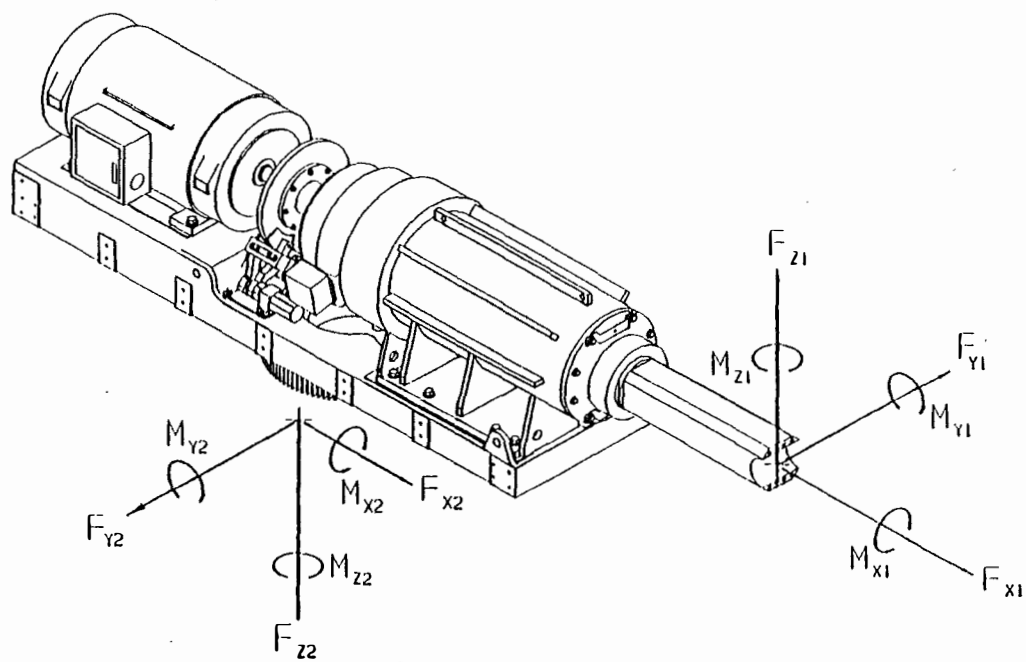

Figure 4-12. Peak mainframe loads

AWT-26
TOWER TOP LOADS

	OPERATING 30 YEAR PEAK LOAD	NON-OPERATING PEAK LOAD
F_X (N)	68,009	66,750
F_Y (N)	68,009	66,750
F_Z (N)	80,100	80,100
M_X (N · m)	145,092	13,560
M_Y (N · m)	216,960	67,800
M_Z (N · m)	27,120	27,120

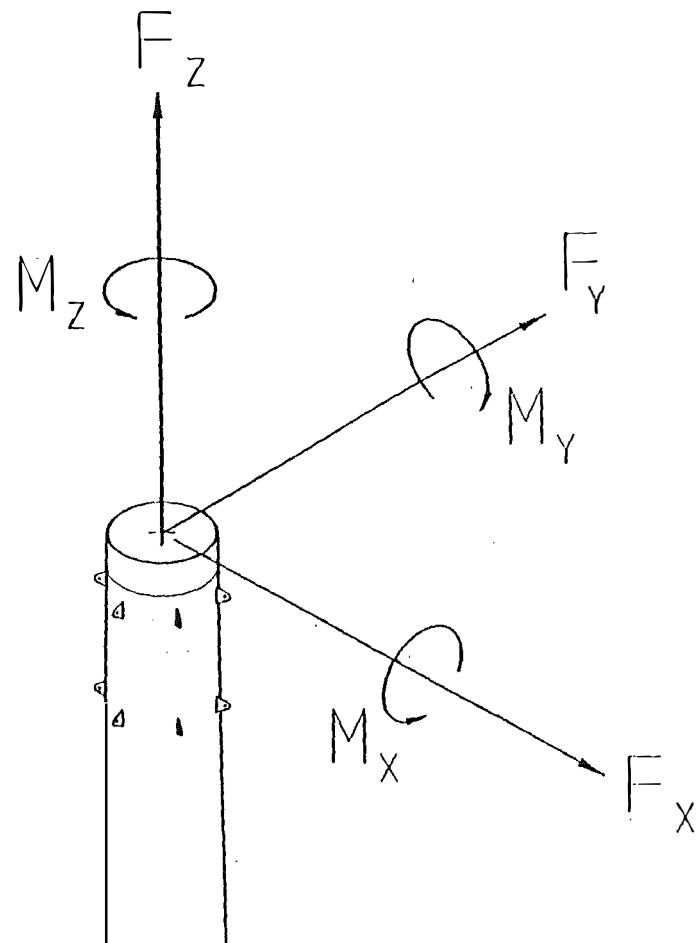

Figure 4-13. Peak tower top loads

Table 4-1. Summary of Peak Design Loads and Associated Safety Margins for the AWT 26/P2A

	component/ material	predicted peak load	calculated serviceability limit (1)	safety margin (service)	calculated ultimate capacity (2)	safety margin (ultimate)	calculated fatigue life (3)	critical location
1	**HUB**	283 kN.m flap	Fy	0.09	Fu	0.19		wall near
	ductile iron A536	57.8 kN teeter axis						blade flange
	Fy=55,000 psi	106.8 kN tension						
	Fu=80,000 psi	227 kN.m edge					30	25mm below
		50 kN teeter hit						blade flange
2	**TEETER PIN**	68 kN flap		1.15		1.09	100	12mm inside
	AISI 4140	217.2 kN						housing
	Fy=108,000 psi	145 kN.m braking						
	Fu=120,000 psi							
3	**MAIN SHAFT**	176.3 kN.m bending	317 kN.m	0.20	367 kN.m	0.07	>100	shoulder at
	ASTM A668-91/M							d'nwind bearing
	Fy=104,000 psi							
	Fu=120,000 psi							
4	**GEARBOX**							
5	**MAINFRAME**	144 kN.m shaft bend	374 kN.m	0.73	545 kN.m	0.89	68	top corner
	ductile A536	145 kN.m torque	308 kN.m	0.41	449 kN.m	0.55	1088	bottom corner
	Fy=55,000 psi	216.9 kN.m yaw pitch	494 kN.m	0.52	717 kN.m	0.65	34	bottom corner
	Fu=80,000 psi							
6	**COUPLING**	4900 N.m				0.09		
7	**BRAKE DISC (1018)**	33,700 psi			69,000 psi	0.05		
8	**BRAKE CALIPER**	1490 N.m				0.48		
9	**BRAKE BRACKET**	10,000 psi			30,000 psi	1.0		
	AL 356-T6							
10	**GENERATOR**						15	
	bearing life=100,000 h							
11	**YAW BEARING**	217 kN.m					30	
12	**TOP PLATE, TOWER**	217 kN.m						
13	**TOWER, 80 FT**	0.711ksi/1000 lb thrust					30	
	(24.4m) A36	0.024ksi/1000 in.lb pitch						
14	**NACELLE COVERS**	13,400 N, side	40 ksi	1.5	45 ksi	1.1	30	front roller bolt
	E-glass							
15	**NACELLE TRACKS**	13,400 N	40 ksi	15.7	45 ksi	13.1	30	mid track
	AL 6061-T6							
16	**BLADES**	283 kN.m flap			538 kN.m	0.37	367	blade root
17	**TIP VANE, E-glass**	117 MPa			528 MPa	3.0		
18	**TIP BASE PLATE**	96 MPa	503 MPa	2.5	572 MPa	1.89	30	first stud
	AL 7075-T6							
19	**TIP HINGE PIN, 15-5 SS**	96 MPa			470 MPa		30	hinge sides
20	**TIP HINGE BRACKET**	147 MPa	503 MPa	1.28	572 MPa	0.95	30	damper pin
	AL 7075-T6							
21	**HYDRAULIC SYSTEM**							

NOTES:

(1) Based on material yield or other deformation which limits serviceability. Safety factor = 1.5

(2) Based on material ultimate strength, stability, or other failure including possible stress redistribution and plastic deformation. Safety factor = 2.0

(3) Based on anticipated fatigue load spectrum with all loads increased by 1.25. Criterion: 30 year life

5.0 Description Of Configuration

5.1 Overview

This section presents detailed information on the AWT-26/P2 wind turbine, since that design is close to the intended production configuration. The same detail of the P1 machine is not presented since that design was superseded by P2. Where it is relevant to the choice of material or configuration, the differences between P1 and P2 are described. The major differences between P1 and P2 are given in Table 5-1.

One additional configuration was tested. This involved the transfer of the P2 rotor and drivetrain onto a guyed 140-ft (42.6-m) tower. The objective was to confirm that this combination was a possible commercial configuration and to confirm the expected increase in energy capture. This configuration was labeled the AWT-26/P2B and, where necessary for clarity, the original is termed the P2A version.

The original ESI-80 drive train was an "integrated" one in that the mainframe was a single iron casting and the main shaft bearings were appended to the gearbox. The design of P1 was more modular and aimed to reduce costs by using more standard components. This goal was not confirmed by manufacture or by testing and, therefore, the P2 design reverted to the integrated approach.

The tower of P1 was a steel truss similar to those used by ESI. However, much of the undesirable structural response of P1 was attributed to the tower shadow from this truss. In addition it became apparent that birds were attracted to truss structures, so that a tube tower was the choice for P2A and P2B.

Table 5-1. Major Differences Between the ESI-80, ESI-Retrofit, AWT-26/P1, P2 and P2B

Item	ESI-80	ESI-retrofit	AWT-26/P1	AWT-26/P2A	AWT-26/P2B
blade	80-ft diameter NASA LS-1 airfoils	86-ft diameter NREL thick airfoils	86-ft diameter NREL thick airfoils	86-ft diameter NREL thick airfoils	86-ft diameter NREL thick airfoils
tower	3-sided truss	3-sided truss 80-ft high	3-sided truss 80-ft high	tapered steel tube, 80-ft high	guyed steel tube, 140-ft high
mainframe	cast steel	cast steel	welded steel	cast iron	cast iron
main bearings	integral with gearbox	integral with gearbox	2 pillow blocks	integral with gearbox	integral with gearbox
gearbox	secured to mainframe	secured to mainframe	supported from shaft torque links to mainframe	secured to mainframe	secured to mainframe

Table 5-1. Major Differences Between the ESI-80, ESI-retrofit, AWT-26/P1, P2 and P2B (Continued)

Item	ESI-80	ESI-retrofit	AWT-26/P1	AWT-26/P2A	AWT-26/P2B
hub	cast iron	cast iron	welded steel	cast iron	cast iron
hub adapters	cast steel	cast steel	cast steel	omitted	omitted
mechanical brake	high speed	high speed	low speed	high speed	high speed

5.2 Rotor

5.2.1 Blades

5.2.1.1 Geometry

The AWT-26 blade is 12.57 m (495 in.) in length and is lofted based on three basic NREL advanced airfoil sections: S815 on the inboard region, S809 on the midspan region, and S810 on the tip region of the blade. A smooth lofting process based on cubic splines was used to generate the intermediate airfoil shapes. The root region of the blade is governed by structural considerations peculiar to the wood/epoxy laminate system used to fabricate the blade shell. The anisotropic nature of the veneer limits the rate at which surface geometry can transition from an airfoil shape to a desirable shape for attachment to the hub. As a result the first basic airfoil station (S815 airfoil) is located 4.597 m (181 in.) from the center of rotation.

Table 5-2 summarizes key features of the blade geometry, while Table 5-3 shows the spanwise variation in chord twist and thickness.

Table 5-2. AWT-26 Blade Geometry

	AWT-26/P1	AWT-26/P2
Blade length	12,115 mm (477 in)	12,570 mm (495 in)
Hub station	990 mm (39 in)	533.4 mm (21 in)
Tip station	13,106 mm (516 in)	13,106 mm (516 in)
Total blade twist	5.85 deg	6.10 deg
Root (inboard) airfoil	S815	S815
Midspan airfoil	S809	S809
Tip (outboard) airfoil	S810	S810
Furnished blade mass	447 kg (950 lb)	447 kg (950 lb)
Maximum chord	1,143 mm (45 in)	1143 mm (45 in)
Maximum chord station	3,932 mm (154.8 in)	3,932 mm (154.8 in)
Tip chord	369 mm (14.5 in)	368 mm (14.5 in)
Root chord	838 mm (33 in)	774 mm (30.5 in)

Table 5-3. Mechanical Properties of Blade at Spanwise Locations

r/R	Station (in)	Chord (in)	C/R	Section Thickness (in)	Chord Twist (deg)	Principal Axis Twist (deg)
0.041	21.00	30.46	0.0590	17.76	6.10	10.50
0.076	39.00	33.17	0.0643	17.05	5.85	10.44
0.100	51.60	35.10	0.0680	16.57	5.69	10.40
0.150	77.40	38.86	0.0753	15.56	5.39	10.21
0.200	103.20	42.09	0.0816	14.60	5.12	9.80
0.250	129.00	44.42	0.0861	13.64	4.93	9.46
0.300	154.80	45.50	0.0882	12.73	4.47	9.00
0.350	180.60	44.97	0.0871	11.70	4.01	8.41
0.400	206.40	43.56	0.0844	11.09	3.45	7.40
0.450	232.20	42.13	0.0816	10.32	2.88	6.23
0.500	258.00	40.63	0.0787	9.58	2.31	5.25
0.550	283.80	39.02	0.0756	8.92	1.76	4.09
0.600	309.60	37.29	0.0723	8.27	1.26	3.15
0.650	335.40	35.38	0.0686	7.62	0.82	2.33
0.700	361.20	33.26	0.0645	5.99	0.48	1.60
0.750	387.00	30.92	0.0599	5.57	0.25	1.17
0.800	412.80	28.41	0.0551	5.11	0.13	0.76
0.850	438.60	25.79	0.0500	4.65	0.08	0.48
0.900	464.40	23.00	0.0446	4.14	0.05	0.20
0.950	490.20	19.13	0.0371	3.44	0.03	-0.08
1.000	516.00	14.55	0.0282	2.62	0.00	-0.22

The AWT-26 blade geometry was developed in an iterative design process which considered blade mass and cost along with performance, annual energy production, and system loads. The blade was optimized for use on a site with a relatively high annual average wind speed. Based on subsequent analysis, however, it has been determined that the basic configuration and operating speed result in excellent performance characteristics on sites with a wide range of annual average wind speeds.

The design of the AWT-26 blade was assisted considerably by MDZ Consulting of Kemah, Texas, and by Gougeon Brothers Inc. of Bay City, Michigan

5.2.1.2 Structure

The blades for the AWT-26 are constructed using a wood epoxy laminate system. High-grade, 2.5-mm (0.1 in.) thick Douglas fir veneer sheets are laminated in a female mold using West System epoxy to form the high- and low-pressure half-shells. These two parts are then trimmed and bonded together including a vertical shear web as indicated in Figure 5-1, to form the basic blade shell.

The blade half-shells are laminated as follows:

1) outer gelcoat skin sprayed into molds (pigmented polyester gelcoat);
2) thickened epoxy spread into mold;
3) one layer of 12 oz/sq. yd double-biaxial E glass;

4) laminating epoxy;
5) veneer layer;
6) carbon augmentation;

Repeat 5) & 6) as per local layup schedule

7) one layer of 12 oz/yd^2 double-biaxial E glass; and
8) two coats of resin/hardener to seal interior of blade shell.

Once the blade half-shells are complete and cured, they are removed from the molds, trimmed slightly and are ready for assembly with no further painting or sanding. After the shells and the shear web are bonded together, the epoxy lines at the leading and trailing edge seams are removed and the blade shells are complete with the exception of the installation of root and tip studs.

The blades are attached to the hub by steel inserts epoxied into holes bored into the end of the blade shell as indicated in Figure 5-2. The inserts are tapered and contoured to effectively transfer the load from the wood/epoxy laminate blade shell through the thickened epoxy bond to the body of the steel insert without overloading any one of these three media. The inserts contain pre-tapped holes accommodating bolts through the flange in the hub.

A plate is attached in a similar manner to the tip of the blade, except that the threaded studs are epoxied into the holes bored into the blade top. These threaded rods have stop nuts to provide a positive surface for the hardware to be bolted down against without pre-loading the epoxy /blade shell interface.

Carbon fiber reinforcement is used to augment the blade shells in certain locations. Only the high-pressure half of the blade shell is reinforced with carbon fiber tape along the longitudinal axis of the blade. By balancing the cross-sectional area of carbon with the cross-sectional area of wood and epoxy to ensure good load sharing, significant structural augmentation can be achieved with relatively small amounts of carbon.

The blade shell wall thickness is decreased along the span of the blade by using successively fewer veneers along the span of the blade. At the root, the shell wall is rapidly built up to a thickness of 89 mm (3.5 in.) to accommodate the load concentrations associated with the root stud inserts. The shell wall thickness at the tip of the blade is similarly built up to accommodate increased loads from the tip studs and the tip vanes.

5.2.1.3 Mechanical Properties

The blade shell mechanical properties are summarized in Table 5-4. Calculated locations for the shear center (center of twist), neutral axis location and orientation, and center of mass are all summarized. Also included are mass per unit length, flapwise and edgewise flexural stiffnesses, and the torsional stiffness, all of which are estimated properties. The final "as-built" blade mass compared very well to the analytically predicted value.

5.2.2 Tip Brakes

Aerodynamic tip brakes, of a similar configuration to those used on the ESI-80, were considered the most economic and technically lowest risk form of fail-safe aerodynamic braking available. Field experience and testing of a set of Smith Wind ESI-80 tip brakes (University of Washington Aerodynamics Laboratory report #1500, 1993) were used to experimentally verify a FORTRAN code (TB5F.FOR) written to solve the governing equations of motion. Wind tunnel testing of a geometrically similar vane was used to further refine the input to the code. Field testing on the pre-prototype turbine of a set of light-weight tip vanes similar to the ESI-80 vanes identified a dynamic

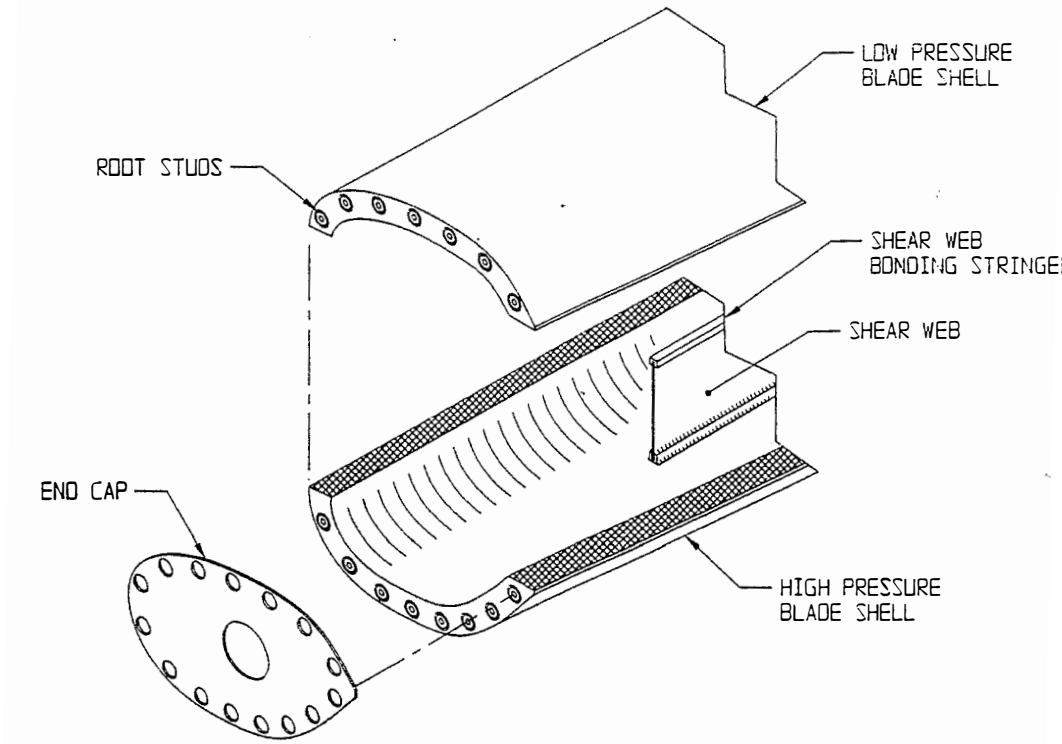

Figure 5-1. Blade shell assembly

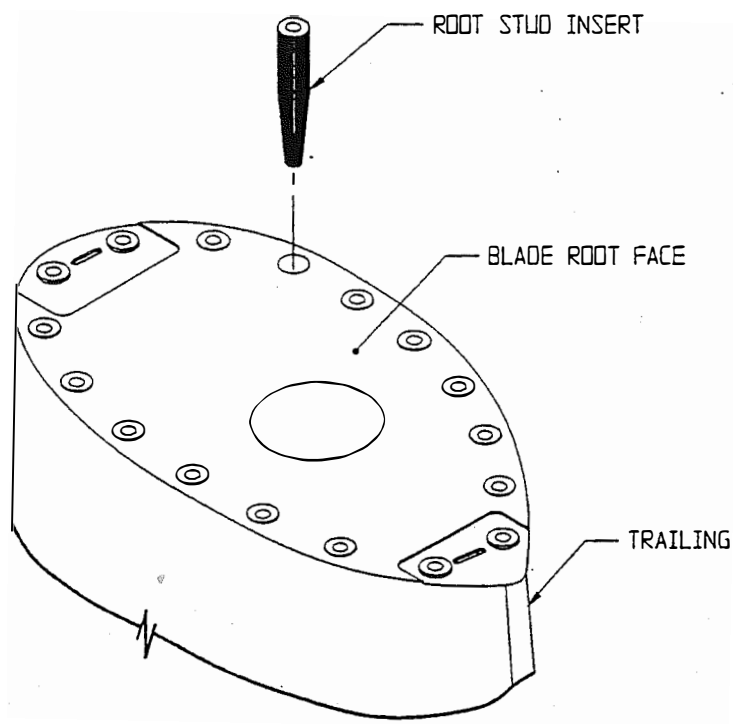

Figure 5-2. Root stud insert configuration

Table 5-4. Blade Shell Mechanical Properties

		Shear Center Location		Neutral Axis Location		CG Location		
Spanwise Location (r/R)	Spanwise Location (in)	Edgewise Location (in)	Flatwise Location (in)	Edgewise Location (in)	Flatwise Location (in)	Edgewise Location (in)	Flatwise Location (in)	Weight/ft (lb/ft)
0.076	39.00	14.99	-0.25	15.57	-0.94	15.66	-0.46	65.58
0.099	51.00	15.30	-0.31	16.41	-0.93	16.60	-0.47	68.26
0.132	68.00	15373	-0.33	17.56	-0.73	17.64	-0.48	32.84
0.150	77.40	15.78	-0.26	18.23	-0.62	18.27	-0.40	33.79
0.250	129.00	15.75	0.03	20.57	-0.16	20.51	-0.05	35.51
0.350	180.60	15.23	0.16	20.68	0.03	20.23	-0.13	31.22
0.450	232.20	14.70	0.15	19.60	0.03	19.50	0.00	26.07
0.550	283.80	14.18	0.14	18.26	0.01	18.32	0.07	21.76
0.650	335.40	13.36	0.12	16.07	-0.02	16.70	0.07	17.69
0.750	387.00	12.22	0.15	14.45	0.03	14.61	0.08	14.68
0.850	438.60	10.78	0.19	12.04	0.13	12.15	0.15	11.30
0.950	490.20	8.42	0.16	9.16	0.16	9.21	0.16	6.52

		Aerodynamic Center Location					
Spanwise Location (r/R)	Spanwise Location (in)	Chord Length (in)	Edgewise Location (in)	GJ (lb-in^2)	J (in^4)	Edgewise E1 (lb-in^2)	Flatwise E1 (lb-in^2)
0.076	39.00	33.17	8.29	2.951×10^9	7815.7	4.580×10^{10}	1.510×10^{10}
0.099	51.00	34.21	8.80	2.784×10^9	8633.1	5.301×10^{10}	1.454×10^{10}
0.132	68.00	37.78	9.44	1.637×10^9	4885.5	2.767×10^{10}	7.031×10^9
0.150	77.40	38.86	9.72	1.514×10^9	5241.8	3.158×10^{10}	6.253×10^9
0.250	129.00	44.42	11.11	9.638×10^8	6147.6	3.868×10^{10}	4.079×10^9
0.350	180.60	44.97	11.24	6.189×10^8	5276.8	3.357×10^{10}	2.621×10^9
0.450	232.20	42.13	10.53	4.122×10^8	3872.3	2.492×10^{10}	1.696×10^9
0.550	283.80	39.02	9.76	2.615×10^8	2719.8	1.695×10^{10}	1.064×10^9
0.650	335.40	35.38	8.84	1.502×10^8	1672.7	1.005×10^{10}	6.262×10^8
0.750	387.00	30.92	7.73	8.287×10^7	1098.5	6.652×10^9	3.267×10^8
0.850	438.60	25.79	6.45	3.734×10^7	586.4	3.526×10^9	1.392×10^8
0.950	490.20	19.13	4.78	1.134×10^7	176.6	9.671×10^8	3.580×10^7

Notes:

a) All edgewise locations measured from blade section leading edge
b) All flatwise locations measured from the chord line (+ = > LPS, - = > HPS)
c) Spanwise station measured from rotor apex (center of rotation)
d) Hub diameter = 39.00 in

stall transient load which was previously undefined. TB5F.FOR was refined to include this dynamic stall transient and was used to design a tip brake mechanism based on the following parameters:

- ease of manufacture, low cost;
- light-weight, robust structure;
- fail-safe deployment mechanism;
- single tip deployed free wheeling speed less than 60 rpm. (defines minimum area and maximum deployment angle); and
- minimum tower clearance of 0.609 m (24 in.) for three-leg truss tower (defines maximum vane width).

The following load cases determined the structure of the tip brake assembly:

- 75 rpm deployment + 30 g flapwise acceleration (ultimate load, overspeed condition)
- 60 rpm operating load + turbulent site flapwise accelerations, based on REP test loads data

The following paragraphs provide a summary of the design and loads for the various tip mechanism components. Details can be found in the RLA Design Handbooks (Reference 8).

Vane (part #6063101)

A composite sandwich structure of carbon fiber and PVC structural foam was chosen to provide economic production and ease of field repair. Because composite structures usually fail catastrophically, ultimate material properties were used in all strength calculations. Load distributions were assumed constant across the width and extra reinforcement was added in the bolt region to provide a sufficient factor of safety.

The ultimate load case results in a maximum aerodynamic normal force of 7340 N (1650 lb.), longitudinally distributed to simulate a leading edge suction peak created by a dynamic stall during deployment. The maximum predicted stresses and the factors of safety against ultimate strength are shown in Table 5-5.

The fatigue load adopted was the centripetal load acting on the vane during 60 rpm operation for 108 cycles. Due to its width, the vane is robust in the flapwise direction and loads due to flapwise accelerations were neglected for the vane. Table 5-6 shows the maximum stresses, the minimum endurance limits of the materials used, and the resulting factors of safety.

Fairing (part#6063110)

Because the most economic vane design was essentially a flat plate, a fairing was required to cover the hinge / damper / magnet mechanism which could not be covered inside the blade or the vane. A carbon fiber laminate of the same material used for the vane skin was chosen. A low drag shape, based on a NACA 664-021 airfoil section was employed.

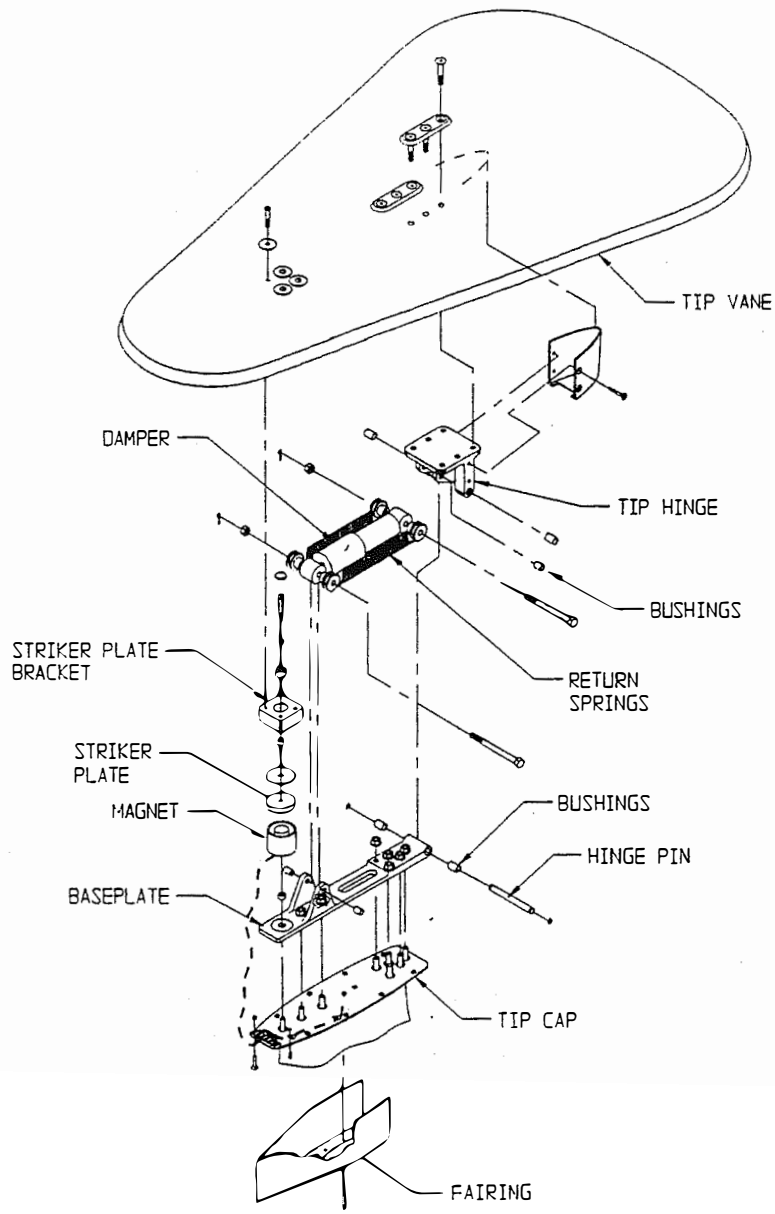

Figure 5-3. Assembly of tip brakes

Table 5-5. Peak Stresses in Tip Vane

Loading: deployment at 75 rpm

Mode	Stress (MPa)	Critical Area	Strength (MPa)	Factor of Safety
maximum upper surface tension	101	hinge	723	4.4
maximum lower surface compr.	-117	hinge	528	4.5
lower surface wrinkling	-117	hinge	175	2.6
	-66	front of balsa		
hinge loc. primary shear	3.86	front of hinge bracket	4.94	1.2
core shear	0.628	hinge location	4.94	7.8
core shear	0.477	front of balsa	1.00	2.0
core tension	0.230	hinge location	1.94	8.4
core tension	0.130	front of balsa	0.689	5.2
core compression	-0.084	hinge location	1.00	11.7

[Stress concentrations assumed: hinge holes: 2.0 front of plywood: 2.0]

Table 5-6. Cyclic Stresses in Tip Vane

Loading: tip vane stowed at 60 rpm

Item	Mean Load (MPa)	Critical Area	Strength @ 108 Cycles (MPa)	Safety Factor
upper surface compression	-44.8 @ x=482 mm (19 in)	laminate transition	200	4.4
lower surface tension	44.8	laminate transition	200	4.4
shear @ hinge	0.206	front if hinge bracket	4.94	23
core shear	-0.186	@ hinge location	4.94	26
core shear	-0.137	@ front of balsa	0.275	2.0
core tension	0.055 @ x=482 mm (19 in)	laminate transition	0.523	9.3
core compression	-0.038	laminate transition	0.275	7.1

Note: these loads assume a 6.8-kg (15-lb) vane assembly

Table 5-7. Tip Vane Damper Performance Data

Maximum speed (mm/s)	Force (N)
38	805
70	2727
140	6145
304	7244
457	7952

Damper (part #090030)

A damper, derived from a commercially proven automotive shock absorber, was used to absorb the energy of a typical deployment. Table 5-7 gives the damper performance data as provided by Bilstein of America. The damper is designed such that a loss of damping fluid will prevent the vane from closing, forcing a mechanical inspection.

Spring (part #6063140)

A set of two springs is used to close the vane against the damper preload, allowing an energized magnet to contact the striker plate, and securing the vane during operation. During deployment the spring experiences a maximum shear stress of 710 MPa (103 ksi). Commercially available springs of similar design routinely experience stresses in excess of this for at least 10^6 cycles.

Magnet (part #6063160)

A DC electromagnet was chosen to provide a fail-safe method to secure the vane during normal machine operation. Any loss of electrical power will cause a vane deployment, safely slowing the turbine. In principle, the voltage to the magnet can be set such that the magnet force equals the centripetal force at the normal rotor speed, and any overspeed condition would then centripetally deploy the vane. In practice, transient loads during start-up and high turbulence require stronger magnets than practical for overspeed protection. The magnet voltage is presently set such that the vane cannot be centripetally deployed until a steady rotor speed of 124 rpm is achieved.

A slip ring on the low-speed shaft of the gearbox provides 120 V ac to the rotating frame of the rotor. A center tap transformer steps the voltage down to 56 V ac, where a set of diodes rectify the current. The magnets are wired in parallel such that each magnet receives 24 V dc, at 550 mA. This circuit, to provide half-bridge rectified current to the magnets, was considered the most robust and reliable circuit possible; it did, however, require custom-wound magnets.

Striker Plate and Striker Plate Bracket (part #6063170, 6063180)

The striker plate is a nickel-plated steel disk which is attracted by the energized magnet. A spherical bearing is used to provide a gimbaled connection between the striker plate and the striker plate bracket, which is bolted to the tip vane. The gimbaled connection was considered necessary to assure an efficient magnetic bond to the magnet.

Hinge (part #6063130)

The tip brake hinge mounts the vane to the hinge mechanism, providing the pivot point for the vane assembly. Six 3/8-16 UNC grade 8 bolts fasten the vane to the hinge. Self-lubricating bushings at the hinge and damper pivot points assure smooth operation and prevent fretting of the hinge pin. The aluminum parent material is sized to resist the ultimate load case of a 75-rpm deployment with a 30-g flapwise acceleration. The associated stresses are significantly less than the endurance limit of the material.

Hinge Pin (part #6063200)

A 15-5, H150 stainless-steel pin is used to provide a pivot point for the hinge mechanism. Its primary loading is in shear, at levels well below the endurance limit of the material used.

Base Plate (part #6063120)

The tip brake base plate reacts all loads from the tip brake mechanism into the blade tip via steel studs embedded in the blade structure. Maximum stresses occur at the location of the leading edge tip stud where most of the centripetal and flapwise accelerations are reacted. The LIFE7 fatigue life prediction at this point is 76.9 years. The tip studs are six-inch lengths of B-7 threaded rod potted into counter bores in the blade structure with high-density epoxy.

5.2.3 Hub and Adaptor

The hub of the AWT-26 transfers the loads from the blades to the main shaft. The hub houses the mechanisms for the teeter system and provides the 7° precone angle for the rotor. The flanges of the hub have machined slots for the blade bolts to allow blade pitch adjustment between approximately ±3°.

For the P1 machine the hub had to be fabricated due to the time constraints associated with cast parts. Hub adaptors were made of cast steel and connected the circular flange of the hub to the blade root.

The AWT-26/P2 machine incorporated a cast-iron hub. The blade was extended in towards the hub to meet the airfoil-shaped flange. The casting provided a weight and cost savings, and a significantly improved fatigue resistance relative to a fabricated hub. The P2 hub assembly drawing is shown in Figure 5-4.

5.2.4 Teeter System

The teeter system is designed to allow the rotor (the hub and blades) to pivot ±7° out of the plane of rotation. The method of attachment is illustrated in the hub assembly drawing of Figure 5-4. The stepped pin (part 2) is clamped onto the end of the main shaft. This pin is hardened, ground, and chromed to reduce wear on the bearings. The thrust and radial bearings (parts 6 and 8) allow the hub to rotate on the pin. These bearings are contained within the housings (part 3) bolted to the hub.

The motion is constrained to ±7° by the hard stops (part 9) bolted to the hub casting. At ±2° contact is made with the hydraulic dampers (part 5) also bolted into the hub. The damping curve for the dampers is shown in Figure 5-5. A quadratically increasing damping is provided for the following reasons: to minimize the loading for small teeter excursions, maximize damping for large excursions, and to provide continued force at large excursions despite the teeter velocity decreasing as the apex is approached.

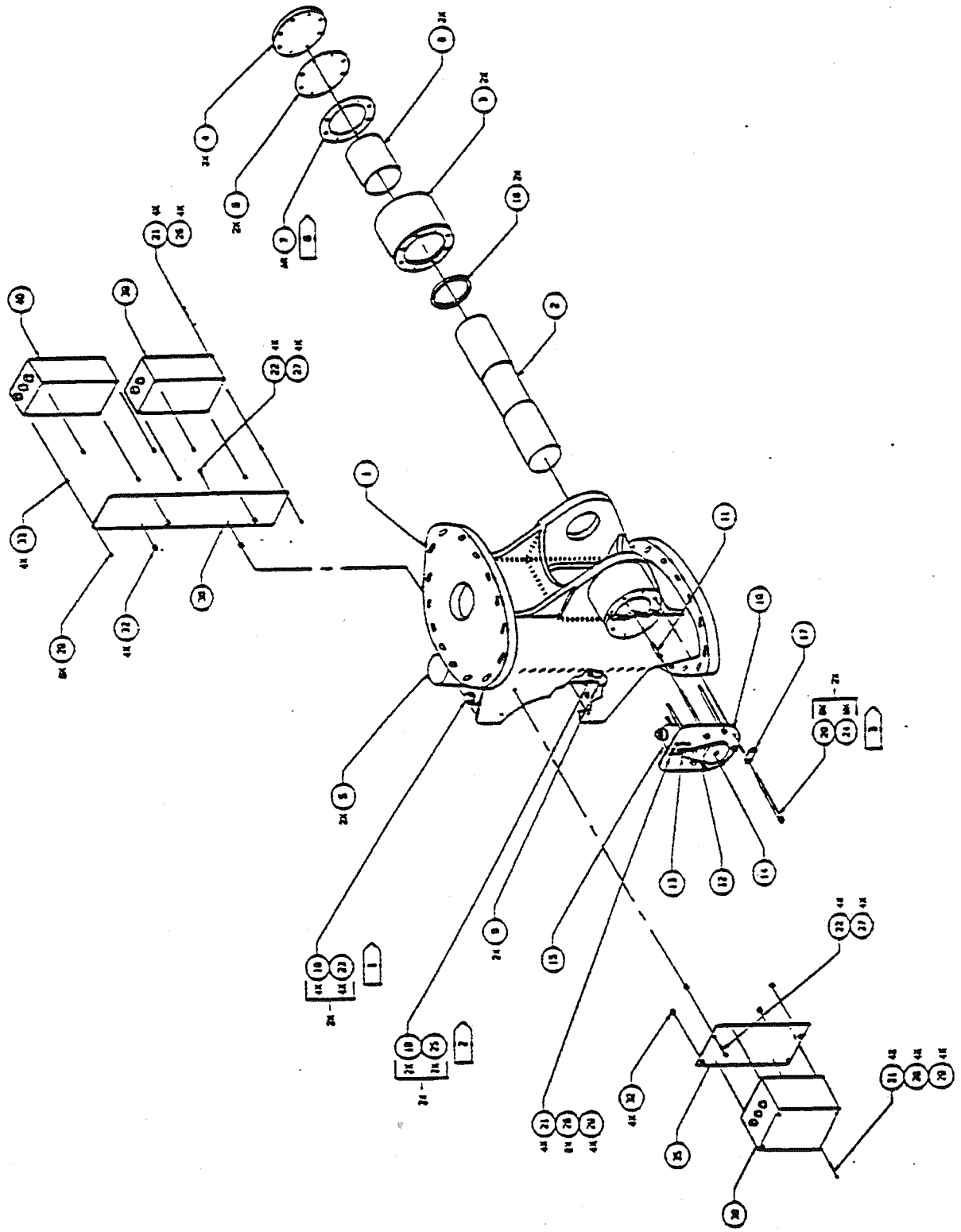

Figure 5-4. Assembly of AWT-26/P2 hub

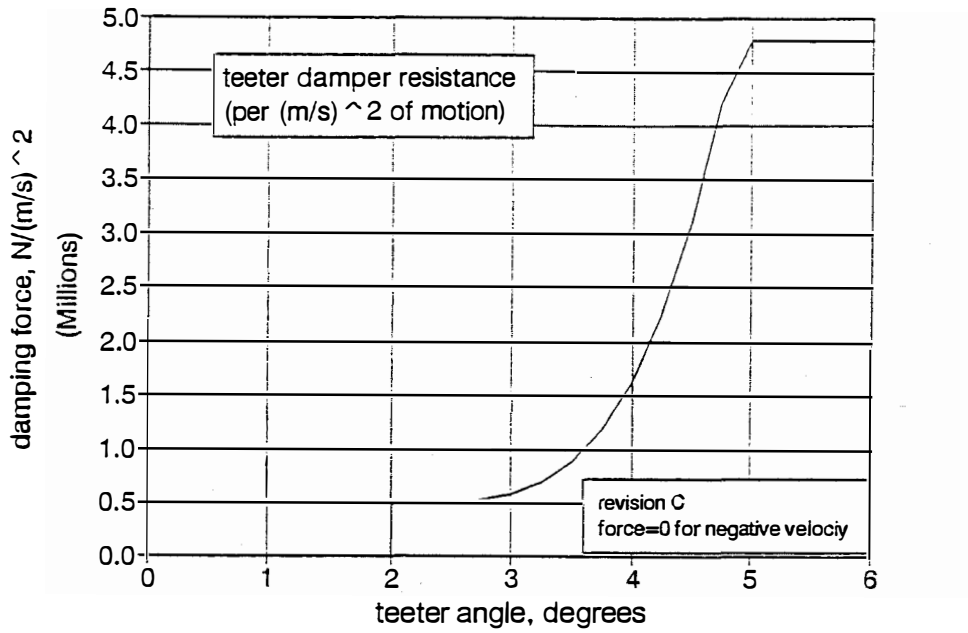

Figure 5-5. AWT-26/P2 teeter damper characteristics

5.3 Low-Speed Shaft

The low-speed shaft transmits the torque and other loads to the gearbox and mainframe. It is mounted in bearings that carry radial and thrust loading. The P1 machine uses split pillow block bearings and the gearbox on the upwind end of the shaft. The P2 design integrates the shaft, gearbox and bearings and is shown in Figure 5-6. This design allows for easier installation and alignment as well as improved structural characteristics.

The low-speed shaft on both machines has a circular cross section that transitions to a rectangular section downwind of the downwind bearing. This facilitates the teeter pin clamp-up design as well as teeter damper and hard-stop contact points. The clamp-up is achieved with an end cap using six bolts (AWT-26/P1) or eight bolts (AWT-26/P2) into the end of the shaft.

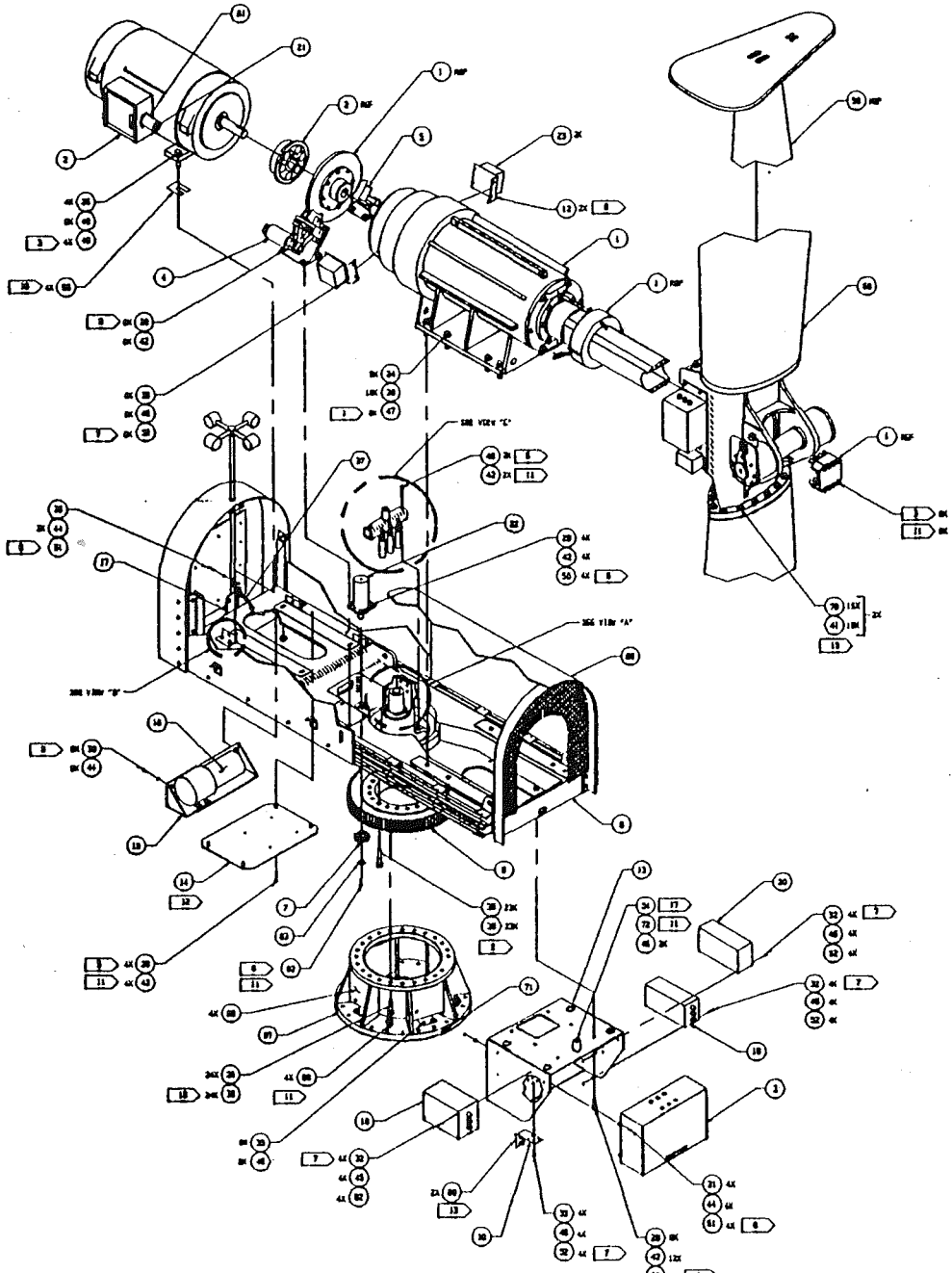

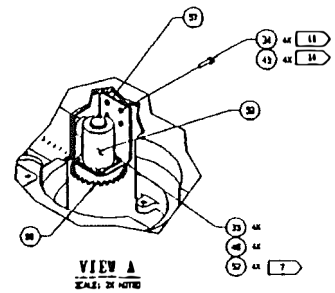

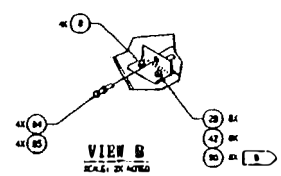

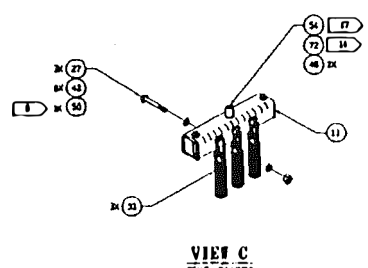

Figure 5-6. Assembly of AWT-26/P2 nacelle

5.4 Gearbox

For both AWT-26 prototypes the gearbox is a two-stage planetary (Flender PZ170) with a gear ratio of 31.5:1. On P1, the gearbox hangs on the end of the-low speed shaft with torque arms connecting to the mainframe. The P2 gearbox is flange mounted to a structural snout which also houses the main bearings. The assembly drawing is shown in Figure 5-7. The snout is foot mounted to the mainframe.

The gearbox is filled with oil for cooling and lubrication. Oil temperature and flow sensors are provided for control system monitoring. P1 has an electric motor-driven pump and radiator cooling system, while P2 has a simpler and less expensive mechanically driven pump that splashes oil inside the snout and to the bearings. Oil fill and drain ports are provided, along with a site glass and lifting eyes.

The gearbox provides a high-speed shaft output which is transmitted to the generator through a rubber element coupler.

5.5 Mainframe

The mainframe provides support for all of the drivetrain components and carries loads into the tower through the yaw bearing and tower top fitting. The mainframe has machined surfaces for mounting of gearbox/bearings, generator, brake brackets, yaw drive, and yaw bearing.

The P1 mainframe was fabricated from structural steel beams and plates. The P2 design was cast, providing a stiffer structure and improved fatigue life and is shown in Figure 5-8.

5.6 Electrical System

5.6.1 Generator

The induction generator is a three-phase, 480-volt unit, rated at 275 kW, and is an open drip-proof type. The insulation is class H, with a 449T frame type. The generator has three temperature switches installed to detect excessive operating temperatures and a heater to prevent moisture damage.

The three phases and a ground are carried from the windings via 6C-3/0 AWG cables and from the frame via 1C-2/0 AWG cable.

The generator is foot mounted to the mainframe and connected to the gearbox via a rubber-element coupler.

5.6.2 Slip Ring Unit

The function of the slip ring is to carry electrical power from the nacelle (stationary frame) to the rotor (rotating frame). This power is used to run the electromagnets that hold the tip brakes closed during operation.

There are three current-carrying rings fixed to the low-speed shaft. Electrical contact is made to each ring with a pair of brushes. The brush-carrying assembly is fixed to the gearbox snout. The rings rotate inside the brush assembly without the use of bearings. A removable cover is used to provide environmental protection and allow for brush replacement. A heater is installed to prevent the accumulation of moisture.

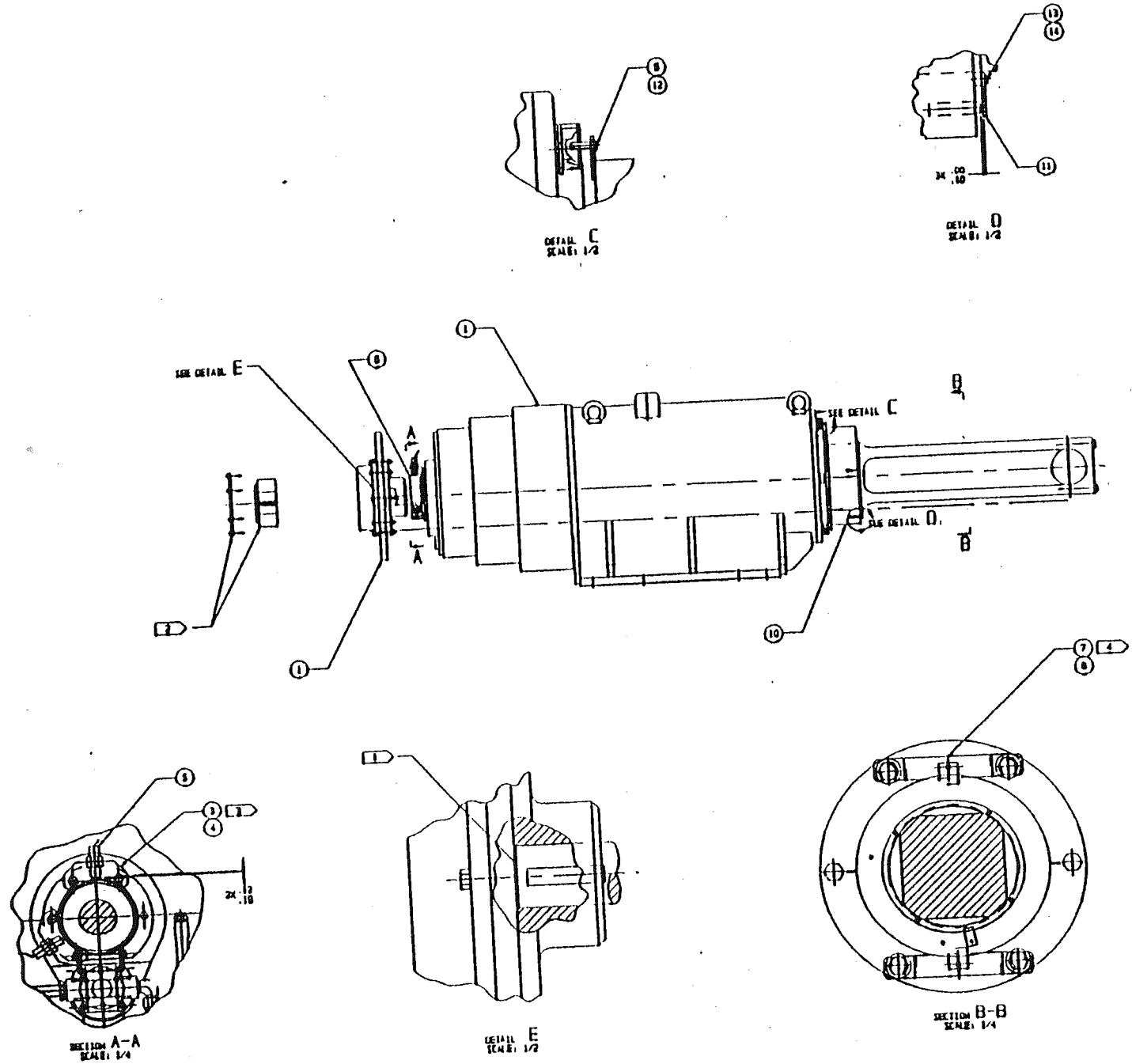

Figure 5-7. Assembly of AWT-26/P2 gearbox

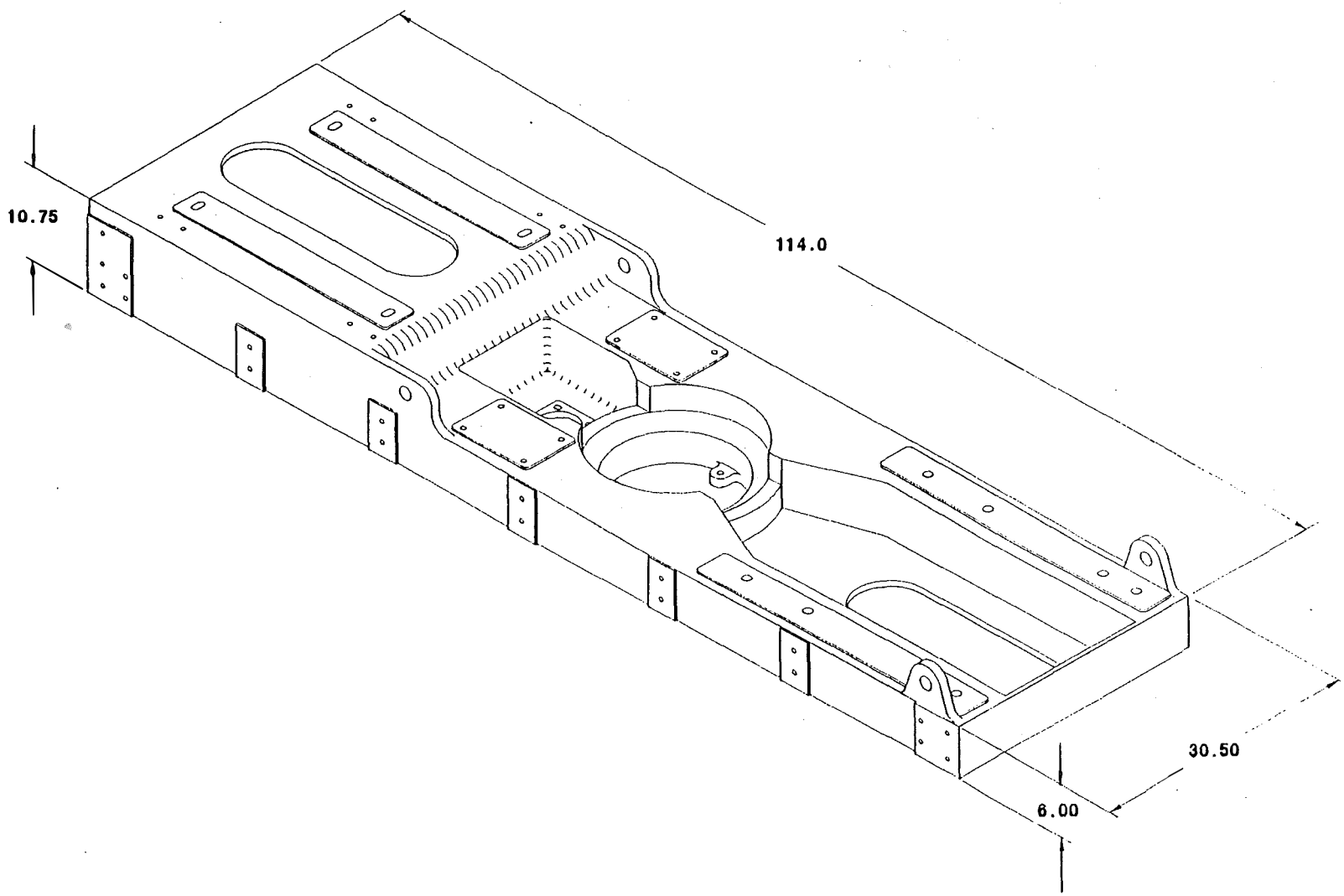

Figure 5-8. AWT-26/P2 mainframe

One ring carries the AC line, one the AC neutral, with the third as a spare. The AC power is fed into a rectifying circuit on the hub that converts the power to DC.

Additionally, the slip ring cover carries the proximity switches that detect the rotor position and main shaft rpm from a slotted disk. The slotted disk is mounted to the ring assembly, turning with the rotor.

5.6.3 Electrical Connectors

The generator is connected to the utility grid by means of solid-state thyristors. These and the associated logic are contained in the soft-start device. This device uses the solid-state switches to control the current flow in the motor/generator during starting (motoring up to operating speed), and then the switches are turned fully on and the generator is hard-connected to the utility grid. This has the advantage of not having contacts and coils to wear out as in conventional electro-mechanical contactors. Also, the torque characteristics of the start can be carefully controlled.

The system, once on line, has a short time delay before the power factor correction capacitors are put on-line. They are removed from the line during stops at the same time as the soft-start is opened. A vacuum contactor increases reliability as arcing is intense when capacitors are switched. The lack of oxygen to support the arc contributes significantly to keeping arcing to a minimum.

The power factor correction capacitors are 60 kVAR and are sufficient to ensure a unity power factor at no load and a power factor greater than 0.95 at full load. The capacitors are fused, explosion proof, have oil- and PCB-free dielectric, and contain bleeder resistors to remove charge when not in service.

5.6.4 Control System

The AWT-26 control system is based on a pair of programmable logic controllers (PLCs). One PLC is located on the ground in the switchboard and the other is on the nacelle. Distributed control is used with high-speed, critical computing done on the nacelle PLC, with the start, stop and other logic executed on the ground in the switchboard PLC. A PLC on the nacelle allows all input/output functions to occur with only one small cable connecting the two processors. The controllers communicate via a high-speed, asynchronous serial data link. If either controller fails or if the serial data link fails the turbine will shut down immediately. Schematic diagrams of the basic control logic for the three modes (start, run, and stop) are shown in Figures 5-9, 5-10, and 5-11.

The nacelle PLC controls the hydraulic power unit, brakes, tip brakes, droop cable unwind device, wind speed data collection, high- and low-speed shaft data collection and machine alarm functions.

The switchboard PLC controls the soft-starter, power factor capacitors, operator interface terminal, and safety systems. Additionally, it keeps track of many system parameters and will cause a shutdown if the parameters are exceeded.

The operator interface terminal (OIT) is a video interface allowing the monitor and control of all wind turbine functions. Information available includes wind speed, average wind speed, power, average power, machine operating mode, kilowatt hours produced, hours run, hours available, etc. Control functions include full manual control of yaw, brakes and starting systems.

The switchboard PLC can be interfaced to either a serial supervisory control and data acquisition system (SCADA) or a discrete SCADA system. All control, alarm and data functions can be accessed on the serial SCADA interface.

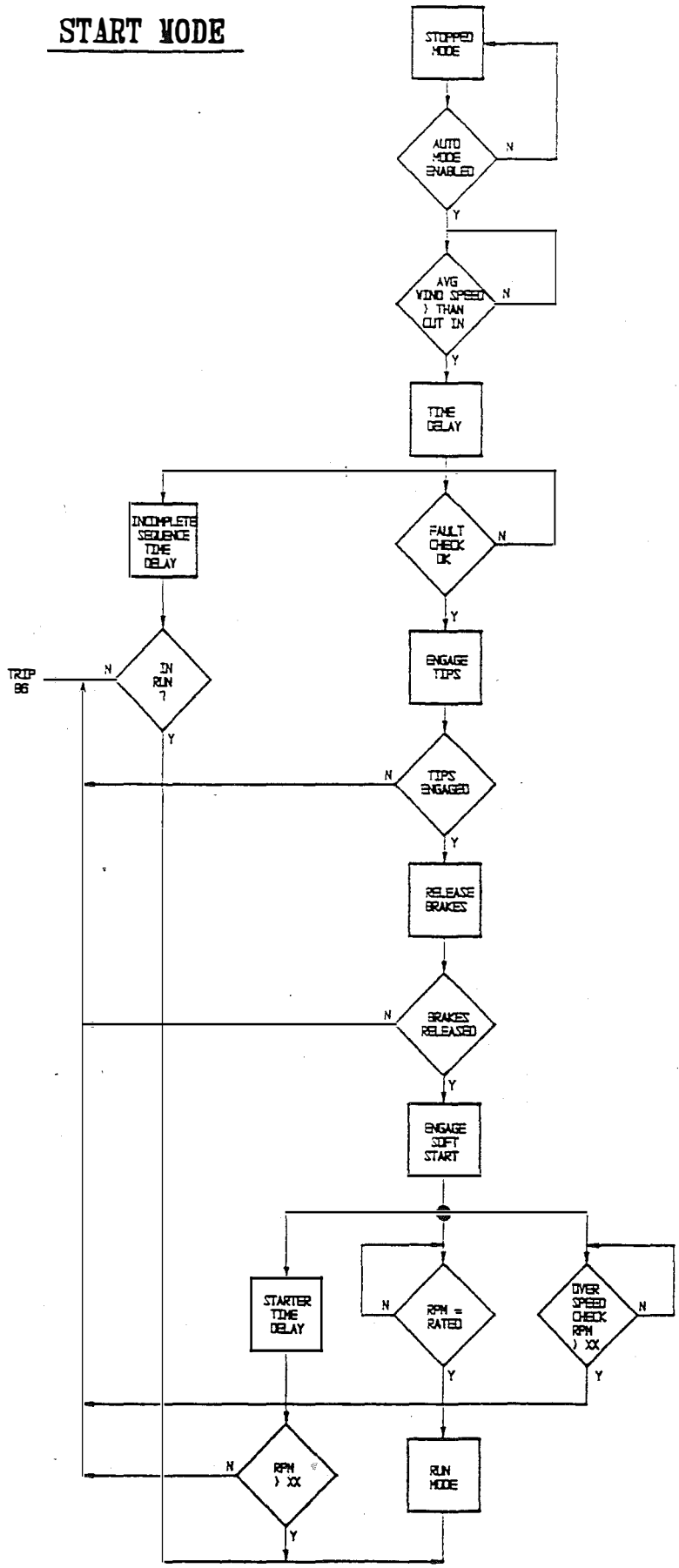

Figure 5-9. Schematic of AWT-26/P2 control system: start mode

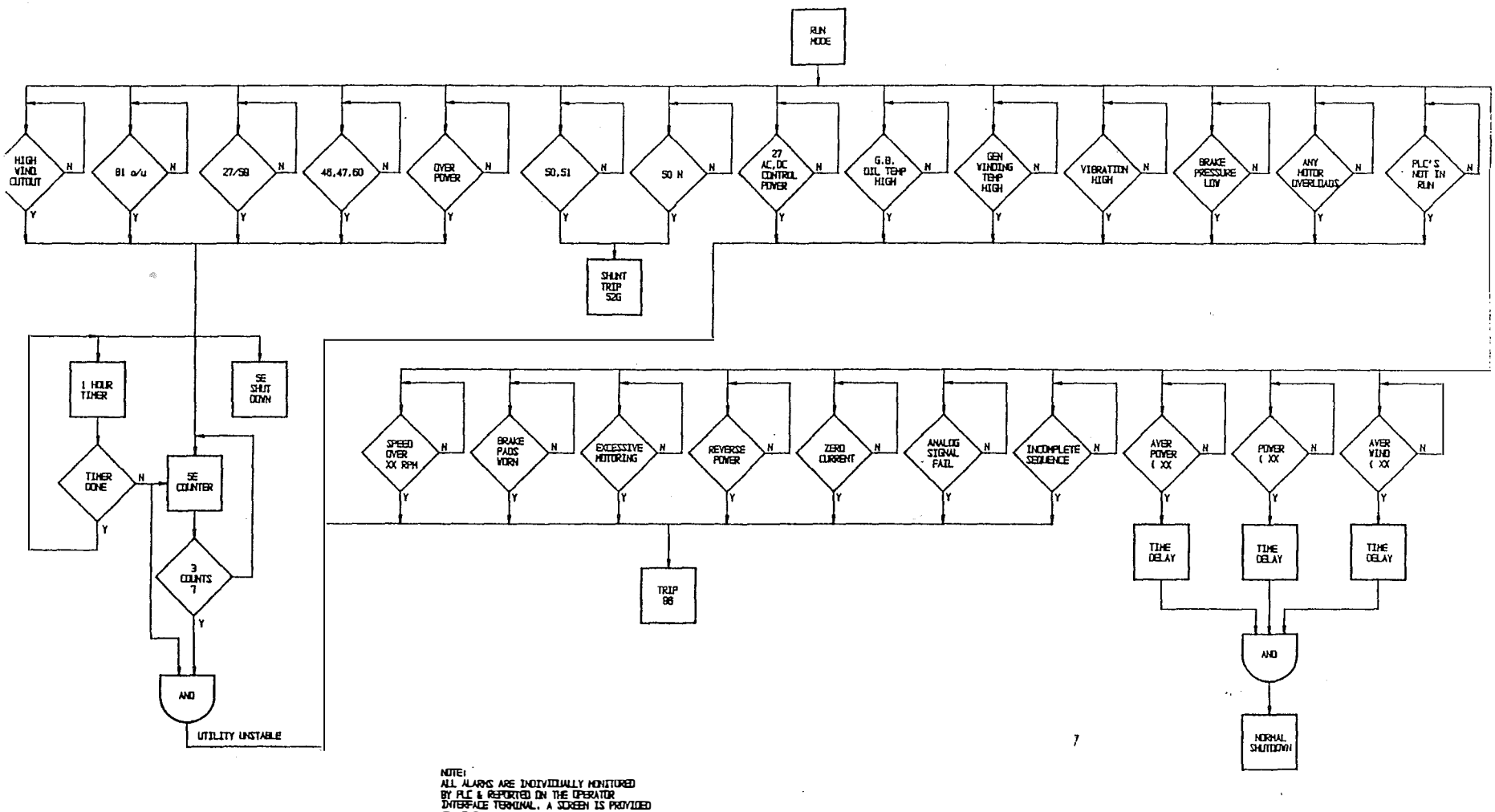

Figure 5-10. Schematic of AWT-26/P2 control system: run mode

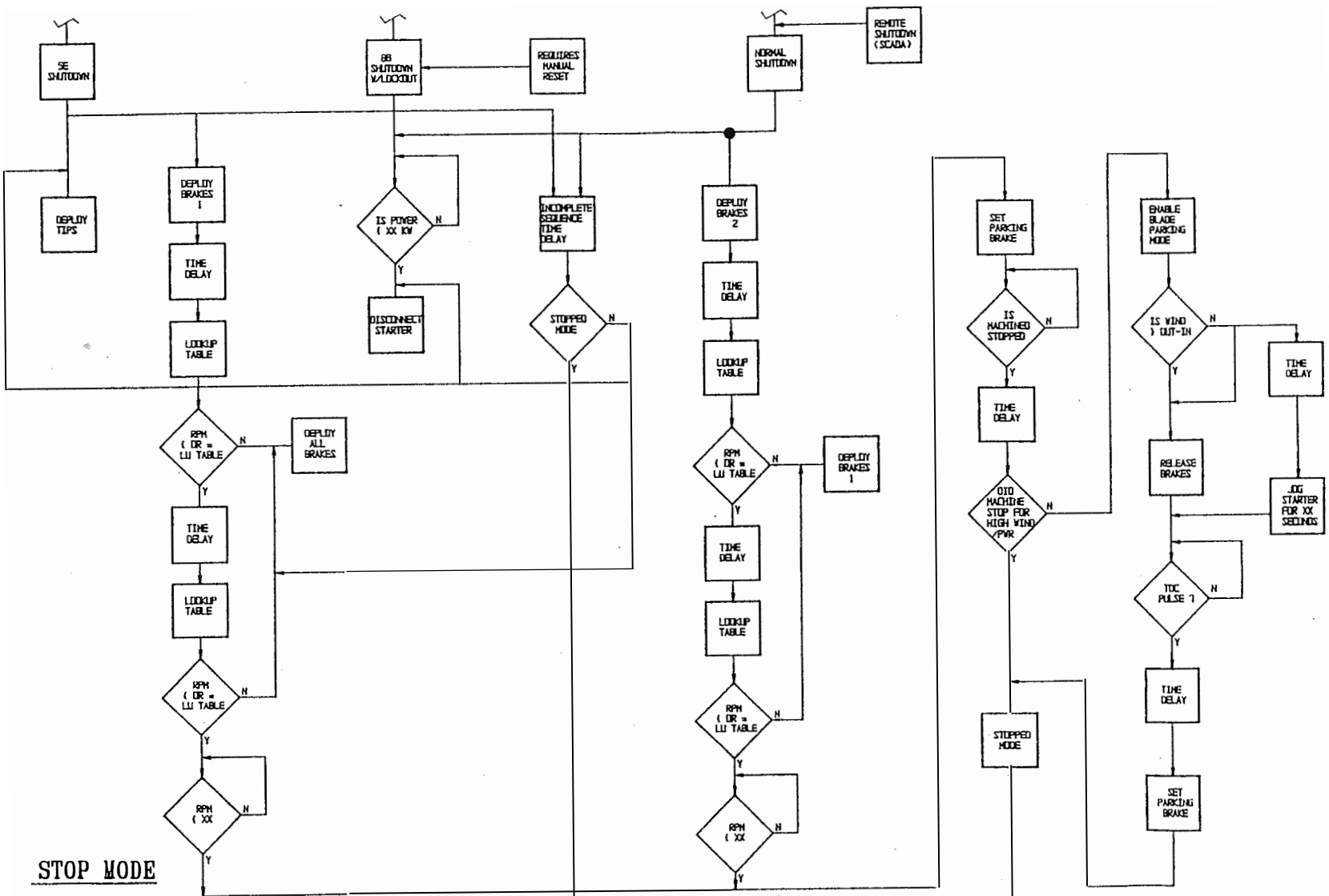

Figure 5-11. Schematic of AWT-26/P2 control system: stop mode

5.6.5 Generator Protection

The generator is protected from utility line electrical faults by a microprocessor-controlled, three-phase protective relay called the line protection relay (LP1). The LP1 is located in the switchboard and provides the following protection for the generator:

- loss of one or more phases;
- phase reversal;
- phase unbalance;
- phase shift;
- under voltage;
- over voltage;
- line under frequency; and
- line over frequency.

The generator has over-temperature sensors in each winding, and the turbine will shut down if the stator windings begin to overheat. Additionally, the stator windings are fitted with heaters to reduce condensation during off-line periods.

5.6.6 Utility Protection

The utility line is protected from the generator by two methods. The first method is generator overcurrent. The main circuit breaker (52G) in the switchboard contains overcurrent trips and will disconnect the generator from the utility line if the generator current exceeds a preset value for a certain period of time. Another circuit breaker is located on the 480-volt line at the pad mount transformer. When tripped, it disconnects the entire system at the transformer.

The second method of protection is the ground fault relay (GFR) in the switchboard. This device monitors the three phase line currents to see that they are balanced and equal to zero. A short circuit will cause an imbalance of the line currents and will trip the main circuit breaker.

The soft-start (42G) in the switchboard is provided with logic to cause the main circuit breaker to trip if one of the SCR's fails closed.

5.6.7 Lightning/Surge Protection

The utility line is bypassed with surge protectors (SC1 & SC2) and lightning arrestors (LA1 & LA2) at the service entrance in the generator switchboard and at the generator terminals. This protects the switchboard from surges and low-energy strikes, and also protects the generator windings.

The 120 VAC control voltage to all critical components is filtered and bypassed with protection for any power line abnormality. The switchboard and nacelle control circuits have individual protection.

The system is grounded in such a way as to minimize lightning damage. However, there is no protection that can be provided for a direct strike of high-energy lightning.

5.7 Hydraulic and Pneumatic Systems

Hydraulic and pneumatic systems are used to provide power and actuation to the brake and yaw drive systems. Pneumatic pressure is used only for the P1 brake release. The P1 yaw drive and P2 brake and yaw systems are hydraulic.

The hydraulic system diagram for P2 is shown in Figure 5-12. The hydraulic power unit can supply pressure to either the brake system or the yaw system, but not both simultaneously. When the brakes are released, the normal- and fast-stop valves are closed with a check valve, allowing pressure to be pumped into the brake canisters, thus compressing the springs. For brake application these valves are returned to their normal, open positions, allowing fluid to drain back into the tank.

During a normal stop sequence, the normal stop valve is opened while the fast-stop valve remains closed. The normal-stop relief valve allows the pressure to drop back only as low as a preset value, thus limiting the applied brake torque level. During a fast stop, both valves are opened, dumping pressure quickly down to zero. These sequences are illustrated in the results of the section titled Field Test Results.

The pump control pressure switch monitors the fluid pressure so that the pump can be turned on if brake pressure drops. The low-pressure switch is an alarm for excessively low brake fluid pressure.

A solenoid valve allows the diversion of hydraulic power to the yaw drive. This can be done only if the brakes are applied and the turbine is stopped. The yaw clockwise and yaw counter-clockwise valves allow the yaw drive to rotate in opposite directions at the command of the control system or the operator. The yaw lock can be applied independently of yaw selection, but only if turbine speed is below 30 rpm.

5.8 Mechanical Brakes

Mechanical brakes are used as the primary means of stopping the rotor for any reason. They are backed up by and assisted during all stops by the aerodynamic tip brakes. The P1 machine uses a disc brake mounted on the low-speed shaft between the upwind bearing and the gearbox. There are four sets of calipers, two for normal and fast stops, and two more for emergency stops.

The P2 machine uses a disc brake mounted to the coupler on the high-speed shaft as shown in Figure 5-7. There are two spring-activated, hydraulically released sets of brakes attached to the mainframe through cast aluminum brackets (see Figure 5-13).

5.9 Yaw Bearing and Drive

The yaw bearing allows free rotation of the nacelle assembly at the top of the tower. On both machines, the yaw bearing is a ball bearing type with a geared outer ring mounted to the tower top fitting. A pinion gear is mounted on the yaw drive output shaft and is engaged with the yaw bearing gear so that the nacelle can be driven continuously when the machine is parked. This function is primarily used as a droop cable unwind device, but can also be useful for maintenance tasks.

The P1 yaw drive is tight enough to be used as a lock. However, the P2 drive does not provide enough resistance and a manual lock is used. This lock is operated by manually driving (with a ratchet) a pin between two bolts protruding from the upper surface of the yaw bearing outer ring. The yaw bearing of the AWT-26/P2 is included in Figure 5-6.

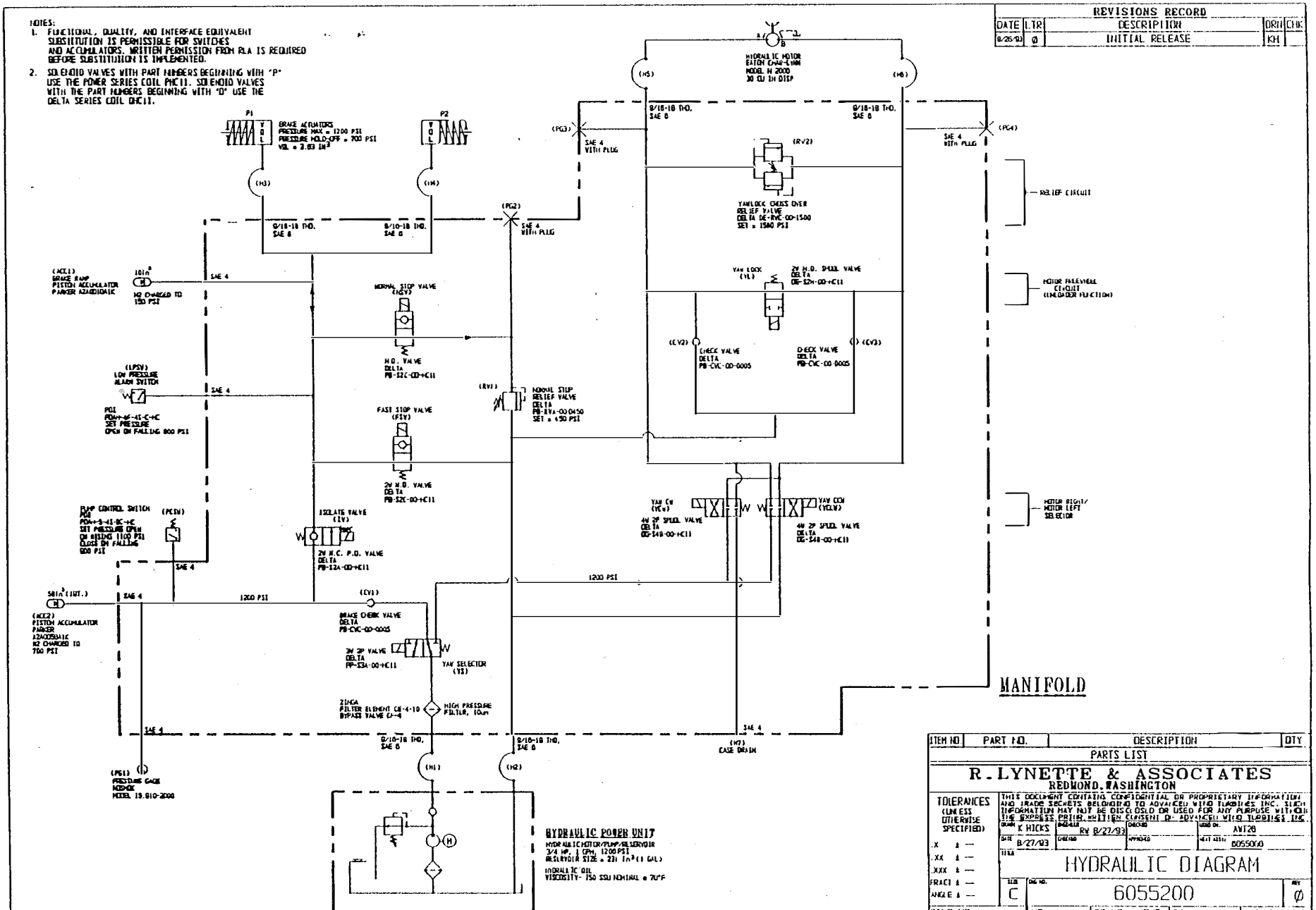

Figure 5-12. Hydraulic system of AWT-26/P2

5.10 Tower

The P1 tower is a freestanding, three-legged lattice tower providing a hub height of 80 feet (24.4 m). The legs are 8-inch (203-mm) tubes and the lattice members are 3-inch (76-mm) angles. The lattice members are bolted to a bracket welded to the tower legs. The tower tapers from the base to the top, with a change in slope at the midsection. The tower top plate is cast and machined.

Analytic studies of the wake behind the P1 tower led to a series of field tests intended to reduce the wake of the tower and thereby reduce the high frequency of the rotor. The P1 tower had a significantly higher solidity than the tower used on the ESI-80 turbines (which used 6.625-inch tubular legs with 2" angular lattice members). Linear analysis of the drag of the tower legs and lattice members indicated that the velocity deficit behind the tower could be reduced by 25% to 55% with the use of simple fairings around the legs and lattice members. Temporary fairings were fabricated from sheets of plastic, wrapped and stapled around the tower legs and lattice members. The fairings were oriented to be most effective when the wind was from the prevailing direction. An anemometer survey (data taken as one minute averages, and sorted to only accept wind directions near prevailing) showed a significant reduction in the velocity deficit, with no effect on the power curve.

Further studies showed that a cylindrical tube, at supercritical Reynolds numbers could also have a lower velocity deficit than the baseline truss tower and be omnidirectional. A 63-inch (1.600-m) diameter sheet metal shroud was fabricated and fastened around the truss tower to reduce the wake from the mid span of the rotor to the tip of the rotor. The peak velocity deficit of the shroud was estimated to be approximately 48% lower than the open truss and tests conducted with the tower shroud showed a dramatic reduction in the amplitude of the mainframe pitching cycles (see Section 6.3.1). Based on these results, a free standing cylindrical tube was chosen for the P2A tower design. The shrouds were eventually replaced with round lattice members per Dwg RL001-79, installed in late January 1994. The lattice members were 1.5-inch (38-mm) diameter solid rods, giving less than half the drag of the 3-inch angle sections they replaced.

The P2A tower was designed as a freestanding, tapered, cylindrical tube, providing a hub height of 80 ft. (24.4 m) The assembly drawing appears in Figure 5-14. A significant reduction in tower drag was anticipated, based on the results of tests conducted on the P1 tower. Industry experiences (MOD-1, WTS-4), however, warned that downwind rotors behind tubular towers tend to create a very low frequency "whumping" noise with the passage of each blade though the tower shadow. It was anticipated that the diameter of the tube would assure a fully turbulent wake without any coherent vortex structures that could instantaneously stall a blade and create the "whump" noise.

Early field tests of the P2A turbine indicated that the "whumping" noise was present at operation in wind speeds above about 37 mph (16.5 m/s). Three helixes of approximately 4-inch (100-mm) diameter irrigation hose were wrapped around the tower in the region of the blade to insure a fully turbulent wake behind the tower. The "hose strakes" reduced the "whump" at low wind speeds but were not effective in high winds. Helical strakes were designed from .125-inch thick sheets of plastic to reduce the coherence of the tower wake by providing a sharper edge than the hose. The dimensions of the strakes were based on research done on the MOD-1 turbine (Reference 28). Three strakes were installed with a height of ten percent of the tower diameter and a helix angle such that each strake climbed five tower diameters to complete one wrap around the tower. Originally the strakes covered the tower from one tower diameter below the tip of the blade to a height level with the mid span of the blade. This configuration worked in wind speeds up to about 47 mph (21 m/s). The strakes were extended to four tower diameters below the tip of the blade to provide a satisfactory reduction in "whumping" for all operational wind speeds. This strake geometry, fabricated from sheet metal, was subsequently used on the P2B tower.

The tower of the P2B configuration is a steel tube of constant 36-inch, (914-mm) diameter, guyed at a height of approximately 97 ft (29.6 m). The height of the rotor shaft above the ground is 144 ft (43.891 m). Further details of this design are shown in Figure 5-15.

The design of the towers was governed by fatigue strength and natural frequency requirements. In both prototypes the fundamental frequency is just above the one per rev. frequency. Each tower is equipped with a climbing ladder, safety cables, and a work platform.

NOTES:

1. INSTALL HEX HEAD SCREWS AND WASHERS. HAND TIGHTEN THE LOCKING NUTS. FINAL ALIGNMENT OF THE BRAKE CALIPER AND TIGHTENING OF THE FASTENERS TO THE REQUIRED TORQUE WILL BE PERFORMED AT INSTALLATION OF THE ASSEMBLY.
2. TAG WITH PART NUMBER AWT-6058200Ø.
3. INTERPRET DRAWING IN ACCORDANCE WITH ANSI Y14.5M-1982.

REVISIONS RECORD					
DATE	LTR	DESCRIPTION	DRN	CHK	DATE
7-26-93	Ø	INITIAL RELEASE	BH		

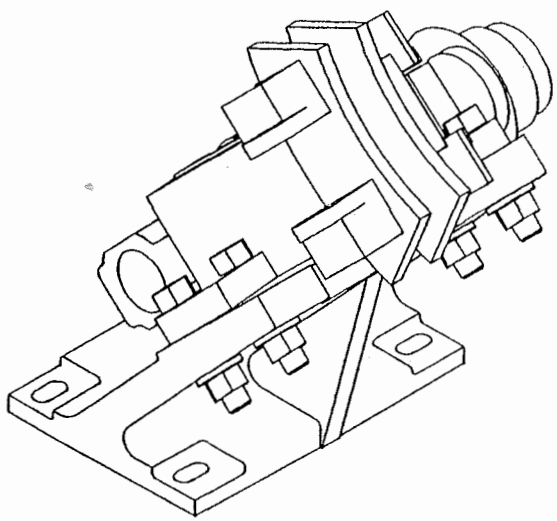

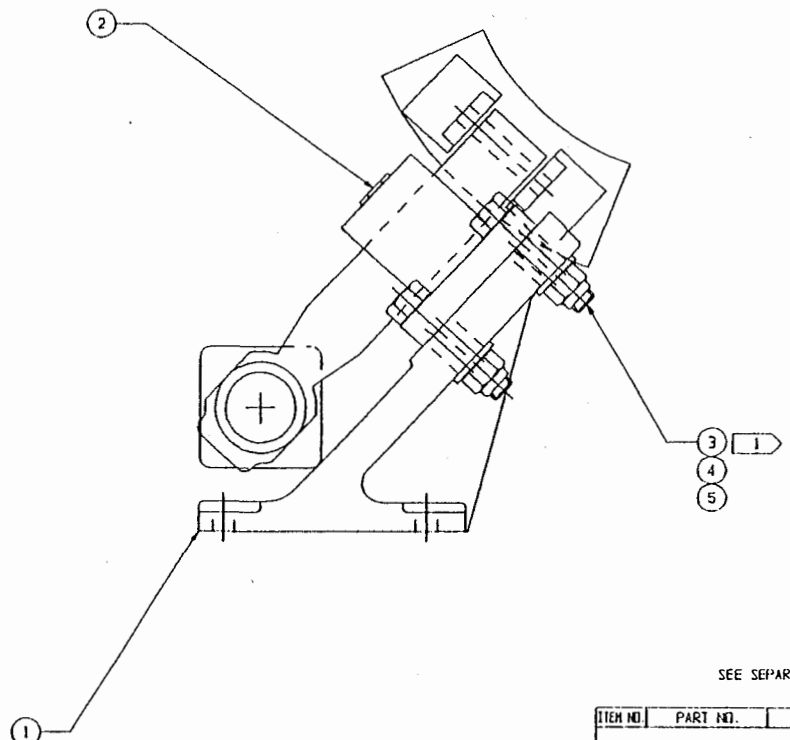

SEE SEPARATE PARTS LIST ON SHEET 1 OF 2

ITEM NO	PART NO.	DESCRIPTION	QTY.

PARTS LIST

R. LYNETTE & ASSOCIATES
REDMOND, WASHINGTON

TOLERANCES (UNLESS OTHERWISE SPECIFIED)
.X ± —
XX ± —
XXX ± —
FRACT ± —
ANGLE ± —

DRAWN	DATE	CHECKED	DATE	APPROVED	DATE	USED ON	NEXT ASSY
B. HOLZE	7/15/93	BH	7/15/93	JH	7/26/93	AWT-26	6050000
		RW	7/27/93	DB	7/27/93		

TITLE: R.H. BRAKE CALIPER ASSEMBLY

SIZE	DWG NO.	REV
C	6058200	Ø

FILE NO. 050200-2-PRI | WT: 53 LB | SCALE: 1/2 | DIM. INCHES | SHT 2 OF 2

Figure 5-13. Mechanical brakes of AWT-26/P2

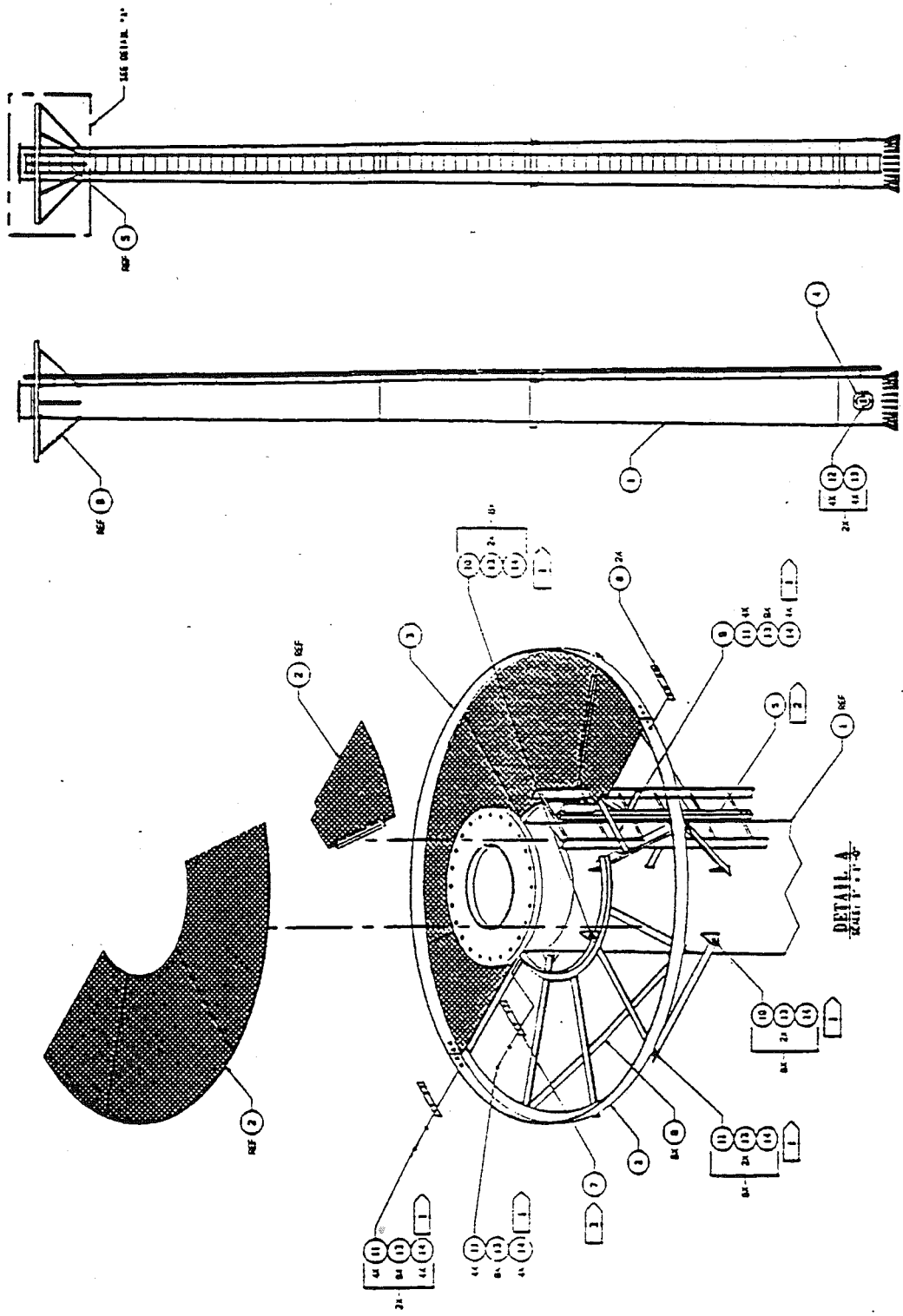

Figure 5-14. Assembly of AWT-26/P2 tower

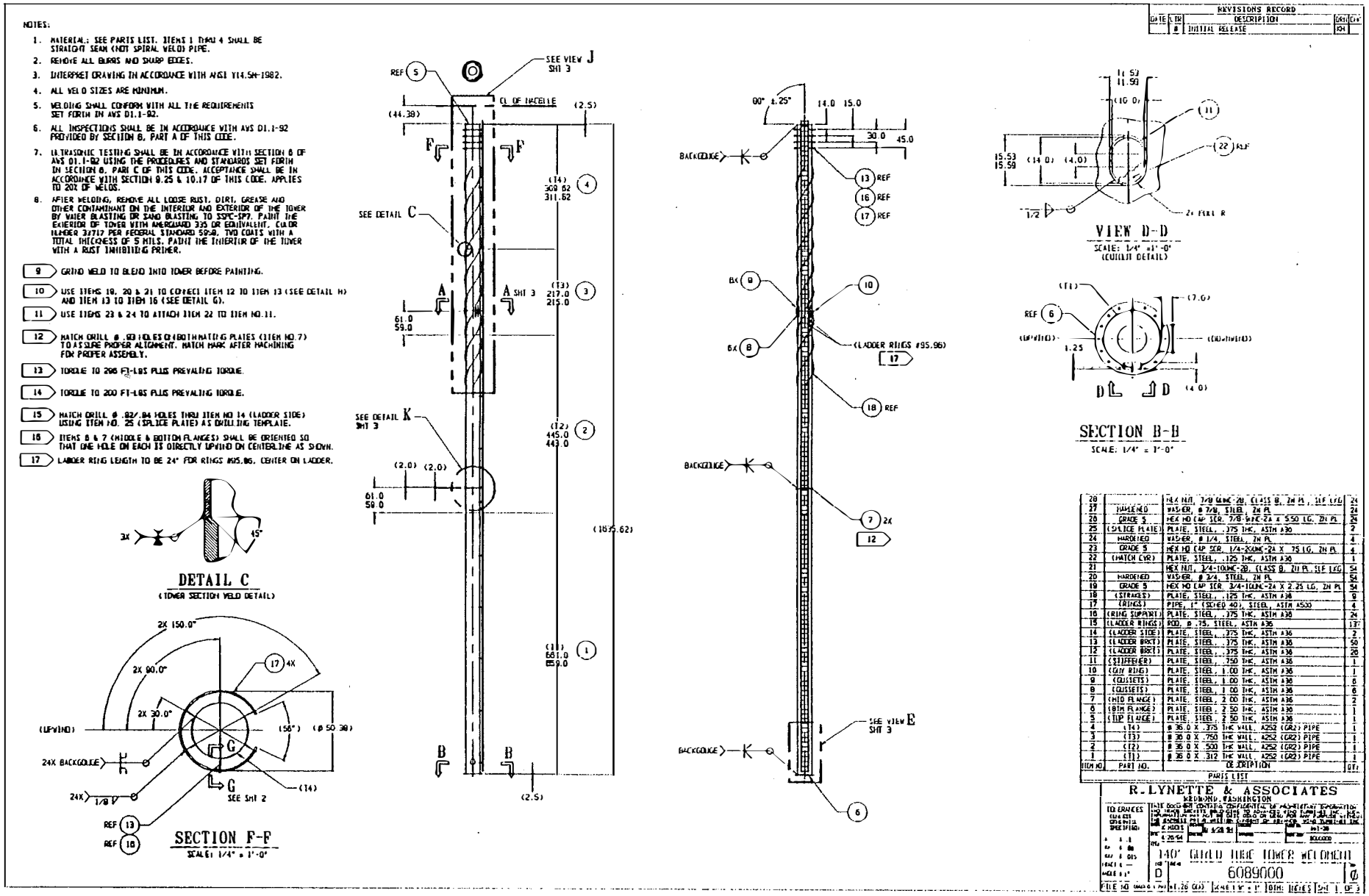

Figure 5-15. Assembly of AWT-26/P2B tower

6.0 Field Test Results

6.1 Test Program Review

This section of the report presents an overview of the test programs for both the AWT-26/P1 and P2 prototype turbines. Each program was broken into three phases: 1) assembly and component qualification tests, 2) installation tests, and 3) operational tests. An overall review of each of these test phases is presented in the following sections.

6.1.1 Assembly Integration Tests

The overall objectives for this phase of the test program were to verify that the turbine nacelle had been assembled correctly, all systems were properly integrated and operating as designed, and the turbine was ready for shipment to the test site. Tests were performed to achieve each of the following objectives:

1. to demonstrate all controller algorithms, as limited by the test configuration;
2. to demonstrate that all aspects of the generator "soft-start" algorithm were working within acceptable limits;
3. to demonstrate routine and emergency brake application sequences;
4. to determine the routine and emergency brake breakaway torques (P1 only);
5. to demonstrate that all nacelle and rotor instrumentation channels were operational;
6. to demonstrate that the yaw drive and yaw brake operate satisfactorily;
7. to demonstrate proper operation of the gearbox lubrication system (P1 only);
8. to determine the blade stiffness (P1 only);
9. to determine the blade/rotor mode shapes and frequencies (P1 only);
10. to conduct a modal survey of the drivetrain (P1 only);
11. to determine the weight and center of gravity (cg) of the nacelle;
12. to demonstrate that the drivetrain and all rotating components were balanced and aligned to within acceptable tolerances; and
13. to verify the turbine was properly assembled.

6.1.2 Qualification and Verification Tests

The purpose of these tests was to verify that critical components were built as designed and to provide baseline data against which future wear measurements could be made.

The rotor blades were subjected to the following tests:

a) geometry inspection;
b) weight and balance measurement: and
c) pitch calibration.

The following tests were carried out on the tip brakes:

a) wind tunnel tests (P1 only, see University of Washington Aerodynamics Laboratory report #1500);
b) tip vane static bending tests (P2 only); and
c) tip magnet pull tests (P2 only).

The hub and mainframe were subjected to the following:

a) X-ray inspection;
b) magnetic particle test;
c) 100% dimensional check of castings; and
d) 100% dimensional check of machined parts.

The gearbox was subjected to the following:

a) noise test; and
b) oil temperature test

The teeter damper characteristics were documented by the manufacturers.

The brake calipers were subjected to the following:

a) on/off cycling test; and
b) operating pressure test

The hydraulic system was tested over the temperature range of -8°F to 70°F by the vendors and approved by RLA.

The yaw bearing QA test data were supplied to RLA by the supplier and are on file. Inspection of the yaw bearing for wear will be accomplished if and when the unit is removed and returned to the supplier.

Measurements of the teeter bearing were made at the assembly facilities prior to final assembly of the hub. In addition, the condition of the bearing was checked and documented with photographs and measurements were made at several intervals during the test period.

6.1.3 Installation Tests

The objective of this portion of the testing was to verify that the wind turbine had been installed properly at the test site and was ready for operation . Specific tests were conducted to achieve each of the following objectives.

1. Calibrate and initialize all instrumentation.

2. Verify that the data acquisition system was operational.

3. Verify that the yaw drive and yaw brake were operational.

4. Verify that routine and emergency braking sequences and loads were within acceptable limits to the extent possible prior to rotation.

5. Verify all controller algorithms to the extent possible prior to rotation.

6. Verify appropriate loss of load response to the extent possible prior to rotation.

A detailed first rotation checklist and test procedure was developed to control the testing. Test results and the test procedure were recorded in the test notebook.

This portion of the testing demonstrated that the time required to test the turbines in the assembly facility prior to shipment to the site was extremely well spent. Very few problems were identified in this testing, and the turbines were erected and cleared for wind-powered operation relatively quickly after arriving on site. Weather and logistics problems would have substantially lengthened the test period had tests or configuration changes been required prior to installing the turbines on the towers.

6.1.4 Operational Tests

The objective of this portion of the testing was to verify that the wind turbine had been installed properly at the test site and was ready for operation. Specific tests were conducted to achieve each of the following test objectives.

1. Optimize starting algorithms through operational testing.

2. Verify all aspects of control system performance through operational testing.

3. Demonstrate adequacy, reliability, and operation of all routine and emergency braking sequences.

4. Determine loads during all routine and emergency shutdown modes, including loss of utility grid power.

5. Develop a power versus wind speed curve for various pitch settings.

6. Investigate the variation in system performance and loads with different blade pitch angles.

7. Investigate the variation in system performance and loads while the rotor was freewheeling with both tip brakes deployed.

8. Investigate system performance and loads with a mass unbalanced rotor.

9. Investigate the effects of off-yaw operation on system performance and loads as well as yaw stability and teeter stability (P1 only).

10. Investigate causes and solutions of 7-per-rev. (7P) problems.

11. Verify that loads during operation were as expected.

12. Identify any problems with the turbine which reduce its ability to operate reliably and unattended.

Test documentation required initiating turbine start-ups to gradually increase peak rotor speeds and then initiating a shutdown and verifying that all systems were functioning as required. In addition, the wind speeds at which the turbines could be operated were restricted until satisfactory operation and loads had been demonstrated at lower wind speeds. Both of these controls were extremely valuable in limiting the severity of problems when they first occurred. The problems encountered and the subsequent configuration changes are listed in Tables 6-1 and 6-2.

In addition to the above-noted configuration changes addressing particular problems, the gearbox on P1 was changed to increase the rotational speed from 57.1 to 61.3 rpm. This allowed a direct comparison of the performance of the rotor at the two speeds. There were also several other minor configuration changes such as changing the gearbox breather on P1 to prevent oil from escaping, and modifying the tip mechanism to eliminate bushing wear problems.

Table 6-1. Problems Encountered with P1 and Subsequent Modifications

Problem	Configuration Change
Tip brakes opening further than anticipated	Redesign to alter relationship between center of mass and center of pressure
Brake torque lower than expected	Change brake pads and springs, add caliper
Slow response to loss of load	Change capacitor sizing and response of line loss relay
Higher than anticipated torque at transition from motoring to operating mode	Revised starter software
"7P" problems	Reduced tip mass Added trailing edge mass (temporary)
	Modal tests
	Reduced tower shadow using tower shroud, which was replaced with round lattice members
	Changed to lighter generator

Table 6-2. Problems Encountered with P2 and Subsequent Modifications

Problem	Configuration Change
Thumping noise due to tubular tower vortex	Strakes on tower
Higher than expected teeter activity	Dampers with higher damping coefficient
Hydraulic yaw lock not adequate	Mechanical yaw lock

6.1.5 Documentation

The AWT-26 System Test Program was conducted and reported in accordance with the test documentation shown in Figure 6-1. Lower level documentation for the conduct of Phase 1, System Integration Testing, consisted of a series of test plans, test procedures, and test data sheets. The test data sheets summarized the test objectives, established the prerequisites for running the test, provided a test procedure and matrix, established success criteria, and allowed for the recording of test results. When a test was run, the actual results or the names of files containing the data were recorded in the appropriate location on the data sheets. For tests requiring more detailed procedures than the data sheets could accommodate, separate procedures were prepared. Each procedure established the expected results for the test and provided an appropriate form for recording the data. For ease of reference, data sheets, results, procedures, and other test documentation were maintained in a Test Notebook.

Lower level documentation for the conduct of Phases 2 and 3 testing at the Tehachapi site was also maintained in a series of notebooks. This documentation included a pre-rotation checklist and procedure, test data sheets, a test log maintained by the site manager and other personnel at the site, a data notebook, an instrumentation notebook, and test results. Each test data sheet had an associated data channel hookup list which established the data channels that were to be recorded during the test and their priority.

The test log was maintained by site personnel on a daily basis. The daily activities at the site, tests conducted, visitors to the site, turbine configuration changes, and other activities were recorded in the Test Log.

The data notebook contained the information necessary to ensure that high-quality traceable data were collected during the test program. It includes completed data channel hookup lists showing the dates a particular set of channels were connected as well as calibration information for strain gage channels, and the data log sheets. The data log sheets were completed for each data file collected and provided the information needed to locate the file on magnetic media as well as any video record of the test.

6.2 Performance Data

For the purposes of this discussion, "performance" will be taken to refer to the power curve (electrical) or power curve characteristics of the turbine. Various loads, dynamics and transients will be discussed in separate sections. A number of power curves for various blade pitch and rotor speed combinations were developed over the course of the power curve testing, which was conducted as part of this program. Specifically, P1 was first operated at two rotational speeds; at 57 rpm (2/93 - 12/93) and at 61 rpm (12/93 - 6/94). 61 rpm operation resulted in undesirable turbine dynamics, and so P1 was returned to 57-rpm (6/94) for extended operation. P2A has been operated at 57 rpm with three different blade pitch settings, resulting in peak electrical power levels ranging from 230 to 310 kW. The 310 kW pitch setting was used for extended operation of P2A. Blade pitch is measured as the angle between the chord-line at the blade tip, and the plane of rotation of the blades (positive pitch ≡ towards feather or leading edge upwind, negative pitch ≡ towards stall or leading edge downwind).

All of the following performance measurements were obtained using a Power Curve Monitor (PCM), which records 1-minute averages of wind speed and direction, generator power, and atmospheric temperature and pressure. The general data quality control and reduction procedures are outlined in the following paragraphs.

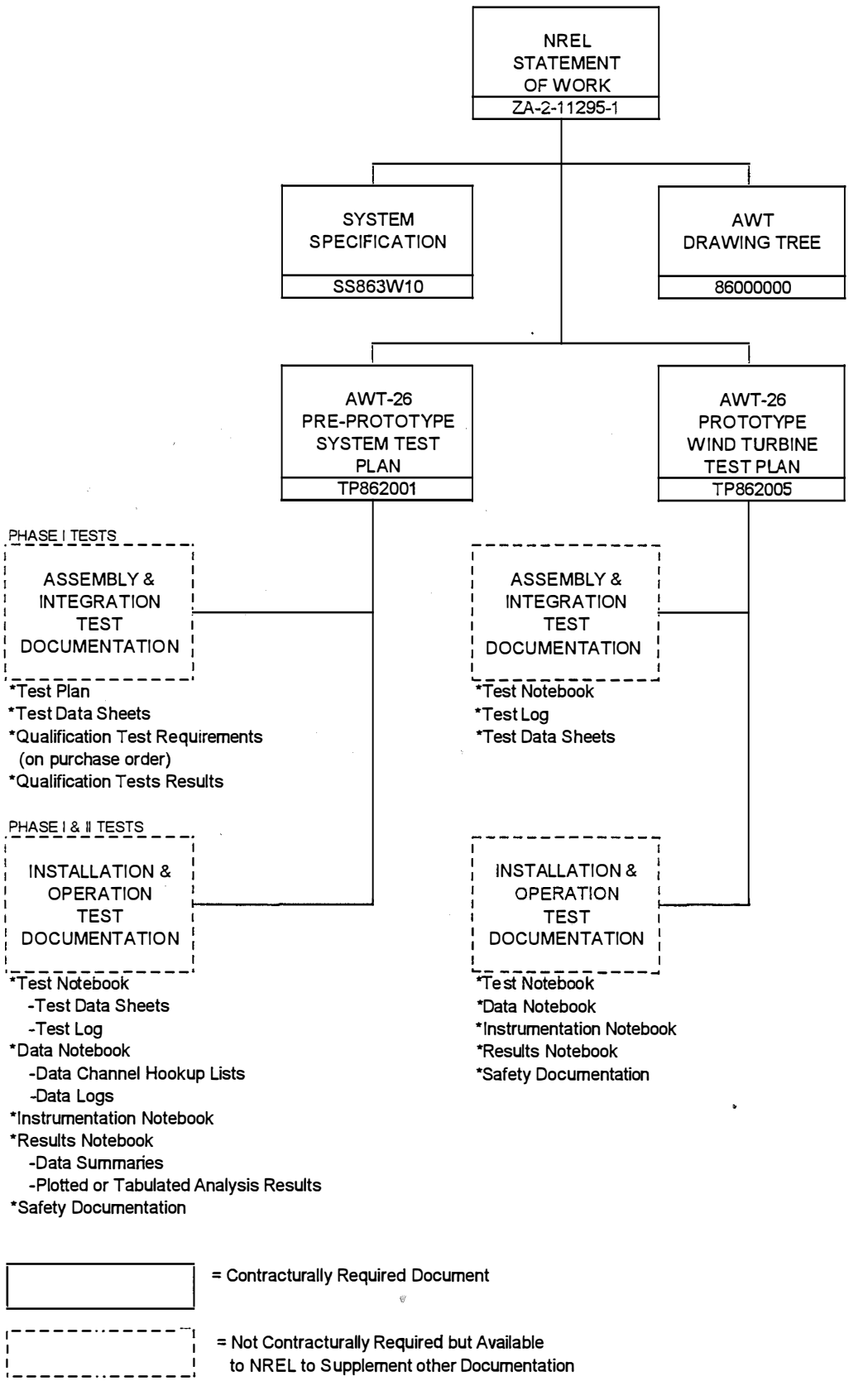

Figure 6-1. Qualification and/or field test program documentation

In order to accurately measure a power curve, two fundamental variables must be known simultaneously - electrical power output and wind speed. Accurate measurement of the electrical power output is relatively straightforward - the current and voltage are measured simultaneously and power is determined with a calibrated transducer.

Determination of the wind speed at the rotor is not a simple matter, because the operation of the turbine rotor significantly alters the wind speed at the plane of rotation of the rotor. The following procedure was used to relate the wind speed measured at an upwind anemometer to the wind speed at the turbine location:

1. A reference anemometer is located on a meteorological tower (MET) at hub height and upwind from the turbine in the direction of the prevailing wind.

2. Using an anemometer mounted at hub-height and outside of any of the blockage effects from the nacelle or rotor, the wind speed at the rotor location is measured with the turbine off. These two wind speeds are simultaneously recorded at both locations over an extended period of time, and stored as 1-minute averages.

3. The two readings are then binned based on wind direction, and scatter-plots are used to check that the relationship is approximately linear over a range of wind speeds. The values are used to generate a correlation factor for each wind speed and wind direction range. These correlation factors then represent a statistical relationship between the wind speed at the reference anemometer (which can accurately be measured during turbine operation) and the wind speed at the turbine location (which cannot accurately be measured during turbine operation).

4. The power curve is then gathered based on the reference anemometer signal. These results are binned and averaged and the correct correlation factor for the given wind direction range is then applied to the reference anemometer signal to determine the correct wind speed for the final power curve.

5. The correlation factor is defined below in Equation 6-1. Note that when this correlation is applied to the MET anemometer signal, which is measured during turbine operation (as indicated in Equation 6-2), the MET anemometer signal is canceled out of the expression. Thus, it is very important that the turbine anemometer used to form the correlation is accurate, well calibrated and not within the local flow field caused by nacelle or rotor blockage.

$$f = WS_{nacelle} / WS_{met} \qquad \text{Equation 6-1}$$

where: f = Correlation factor
$WS_{nacelle}$ = Wind speed measured at the nacelle
WS_{met} = Wind speed measured at the MET tower

$$WS'_{nacelle} = WS_{met} \times f \qquad \text{Equation 6-2}$$

where: f = Correlation factor (measured with machine parked)
$WS'_{nacelle}$ = Calculated wind speed at nacelle (used for power curve definition)
WS_{met} = Wind speed measured at the MET tower (measured simultaneously with turbine output to define power curve)

At a given wind speed, the turbine will produce higher power when the air density is greater, and so performance data must also be corrected to eliminate the effects of varying air density. PCM measurements of atmospheric temperature and pressure are used, along with the ideal gas law, to calculate air density for each 1-minute average recorded. Equation 6-3 is then used to correct the measured generator powers for density effects, where the present work uses a reference air density of 1.06 kg/m^3.

$$P_{corr} = P_{uncorr}/\sigma \qquad \text{Equation 6-3}$$

where: P_{corr} = Density-corrected generator power
P_{uncorr} = Uncorrected generator power
σ = Density ratio = ρ/ρ_0
ρ = Measured air density
ρ_0 = Reference (altitude) air density

In addition to the wind-speed and density corrections, other procedures are followed to insure high quality of power curve data. Data sheets from the turbine test site are used to identify weather conditions, blade operating conditions, and other factors which may affect performance. For each data collection period, scatter plots of wind speed versus power are made, and inspected for data quality. Careful selection of data sets eliminates data collected in poor weather (heavy rain, snow), data where blade soiling is undesirably high, and data points where the turbine came on or went off-line in the middle of a 1-minute average. Additionally, data points are removed for wind directions which place the MET tower in the wake of the turbine itself or of another nearby turbine.

6.2.1 P1 Performance

The reference anemometer for P1 was mounted on a MET tower approximately 36.6 m (120 ft) upwind of the turbine location. Figure 6-2 shows the P1 test site plan and the prevailing wind direction. Note that the MET tower was located along a line with a compass heading of 300° from the turbine. The prevailing wind direction is at a compass heading of approximately 322.5°. The anemometer that was used to simultaneously measure the wind speed at the turbine location was mounted on the nacelle, as indicated in Figure 6-3.

Table 6-3 shows an example of measured wind-speed correlation factors ($WS_{nacelle}/WS_{met}$) for a number of directional sectors. For the prevailing directional sectors, the correlation factor is less than unity (wind speeds are found to be 1% to 4% lower at the turbine than at the MET).

When the measured correlation factors (as shown in Table 6-3) were used to reduce P1 performance data, and drivetrain efficiencies were considered, an unrealistically high rotor power coefficient was obtained. This, along with recent wind speed measurements near the P1 site, has cast suspicion on the correlation factors of Table 6-3. While further work is planned to validate the wind speed correlation for the P1 site, it is expected that the correlation factor should be close to unity. Thus the final P1 performance curve reported in this work uses a wind-speed correlation factor of unity (wind speed the same at turbine and MET).

Table 6-3. MET/Nacelle measured Correlation for P1

Directional Sector	Number of 1-Minute Averages	Correlation Factor $WS_{nacelle}/WS_{met}$
0° - 15°	12	1.079
15° - 30°	60	1.056
30° - 45°	87	1.049
45° - 60°	67	1.027
60° - 75°	41	1.006
75° - 90°	46	1.000
90° - 105°	78	1.013
105° - 195°	Not Applicable	MET Tower Waked (data not used)
195° - 210°	147	1.051
210° - 225°	187	1.004
225° - 240°	85	0.996
240° - 255°	58	1.006
255° - 270°	57	1.015
270° - 285°	228	0.997
285° - 300°	1875	0.991
300° -315°	5875	0.967
315° - 330°	13558	0.958
330° - 345°	1275	0.970
345° - 360°	18	1.023

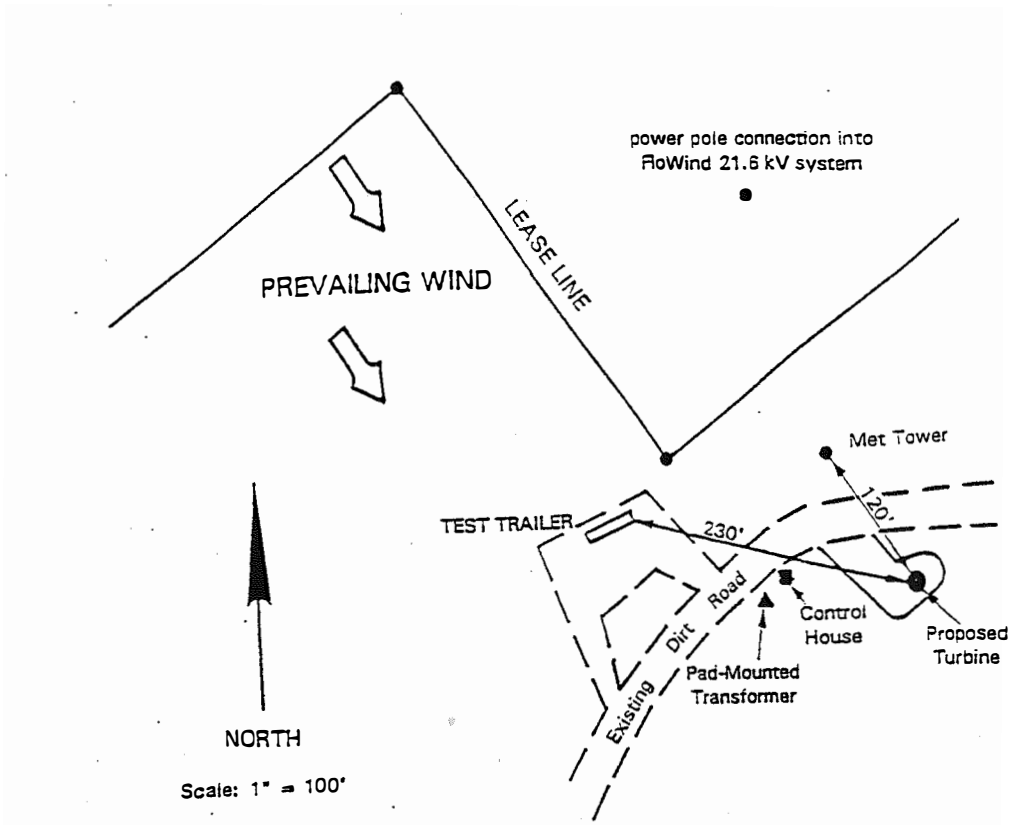

Figure 6-2. Plot Plan of P1 Test Site

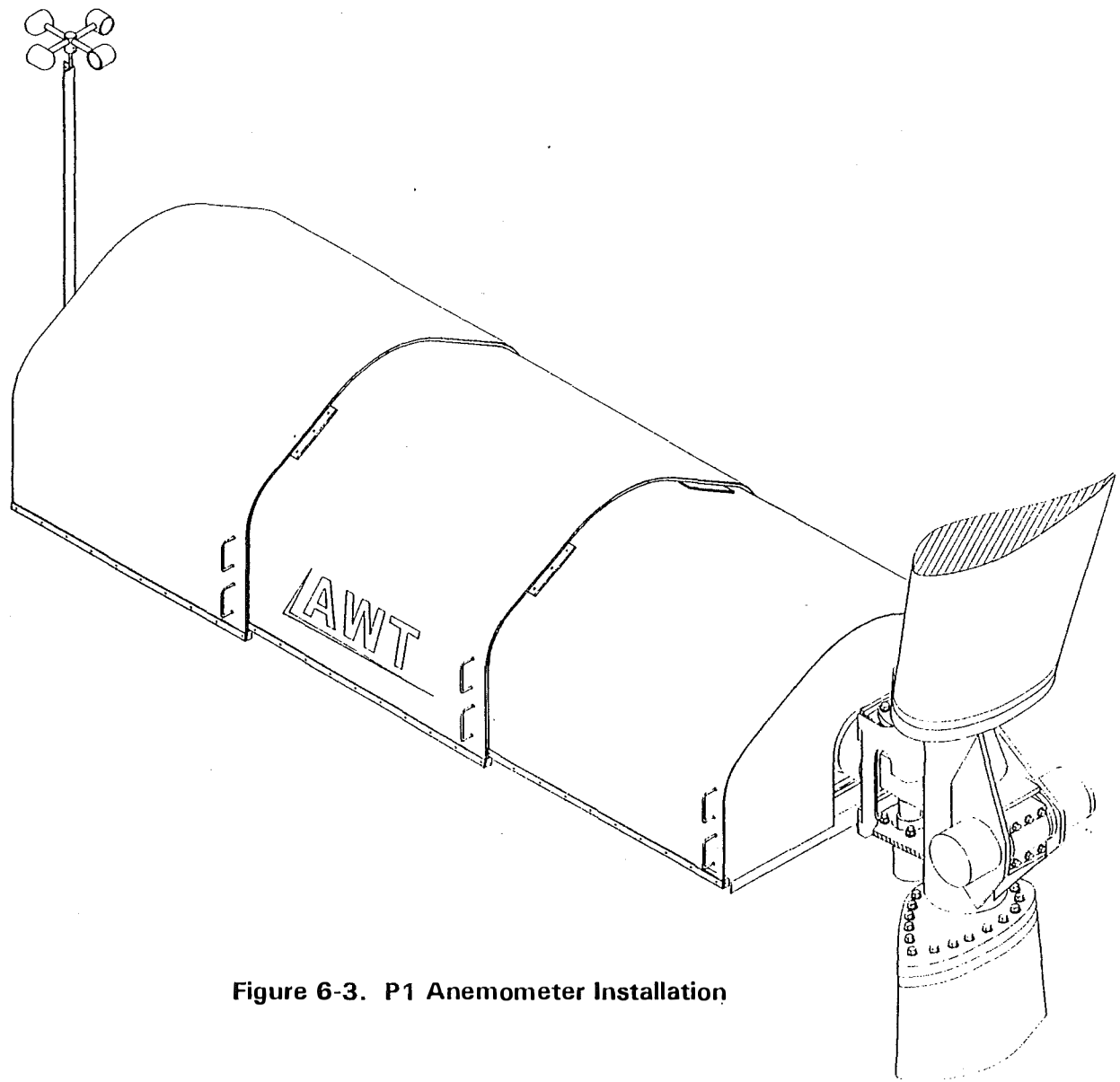

Figure 6-3. P1 Anemometer Installation

6.2.1.1 Effect of Rotor Speed on P1 Performance.

The P1 rotor was operated at two different speeds to investigate the impact of rotor speed on the power curve and overall system performance. P1 was originally run at 57 rpm. After approximately 10 months of operation at 57 rpm, the gearbox on P1 was replaced by a box with a gear ratio that resulted in a rotor speed of 60.8 rpm. For both rotation speeds, the blades were pitched so as to achieve a peak power of approximately 275 kW.

Figure 6-4 shows both the 57 rpm and 60.8 rpm power curves. Note that these curves used the correlation factors as shown in Table 6-3, and should be used for a relative comparison between performance at rotation rates, and not as an absolute measure of performance (performance of P1 at 57 rpm will be addressed in the next section).

Operation at the higher rotor speed resulted in a much more significant drop off in power at the higher wind speeds, as the rotor progressed more deeply into stall. In addition, vibration and transient accelerations of the nacelle increased markedly as rotor operation exceeded peak power and moved onto the region of the power curve with a negative slope. This increase in loads was unmistakable and clearly evident in all the high wind loads data which were recorded. It is believed that the more abrupt reduction in power was the result of local blade section aerodynamics which resulted in a decrease in teeter and yaw stability (negative lift curve slope).

Although operation of P1 at 60.8 rpm would produce more annual energy than operation at 57 rpm (at sites with average wind speeds 5.8 m/s or greater), this would come at the expense of higher loads and undesirable dynamics. As a result, the 57 rpm gearbox was reinstalled early in June 1994. P1 was run in this configuration for extended performance testing.

6.2.1.2 P1 Power Curve at 57 RPM

Extended performance testing of P1 at 57 rpm was conducted at a pitch setting such that the peak generator power output was approximately 320 kW. Figure 6-5 shows a sample uncorrected power curve for P1 operating at 57 rpm. Each data point represents a 1-minute average power and wind speed value. Approximately 732 hours of valid power-production data were recorded for this configuration, between the dates of 8-31-94 and 11-21-94. The resulting P1 power curve is shown in Figure 6-6, and in tabular form in Table 6-4. A wind speed correlation factor of unity was used to generate the P1 power curve (wind speeds assumed the same at the turbine as the MET tower).

6.2.1.3 P1 Energy Production Characteristics

The P1 power curve shown in Figure 6-6 was used to calculate annual energy production for sites with annual average wind speeds ranging from 12 to 19 mph (5.4 to 8.5 m/s). The results are summarized in Table 6-5. These annual energy production levels assume 100% availability, and clean blades, and refer to Rayleigh wind speed distributions at turbine hub height.

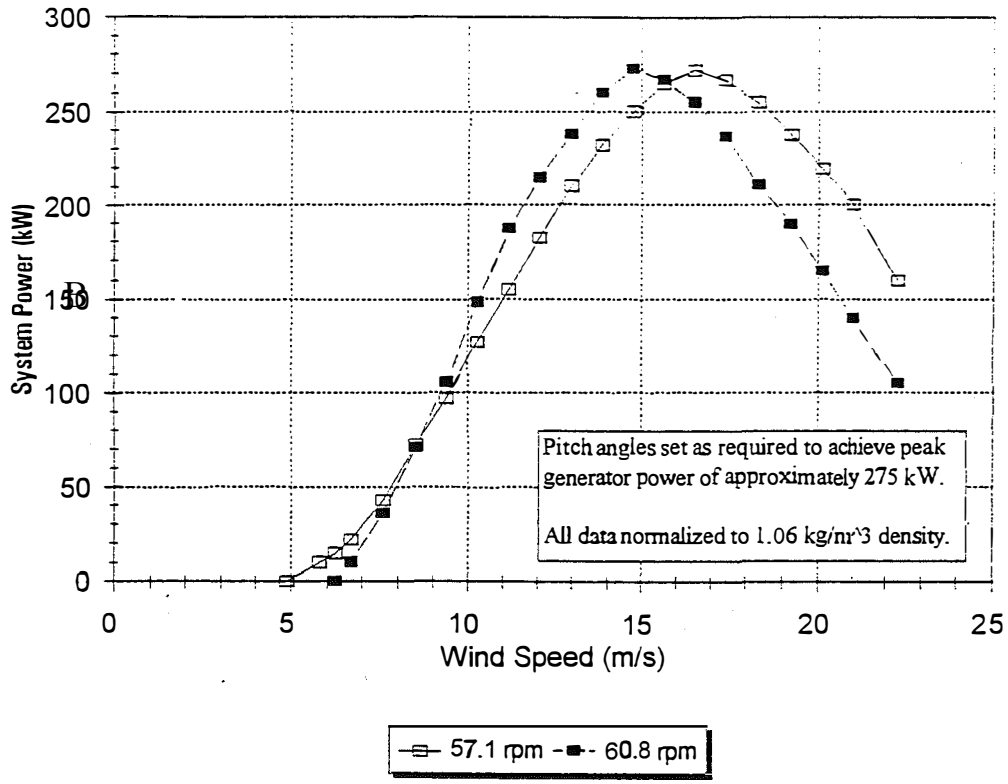

Figure 6-4. P1 Power Curves for 57.1 rpm and 60.8 rpm Operation

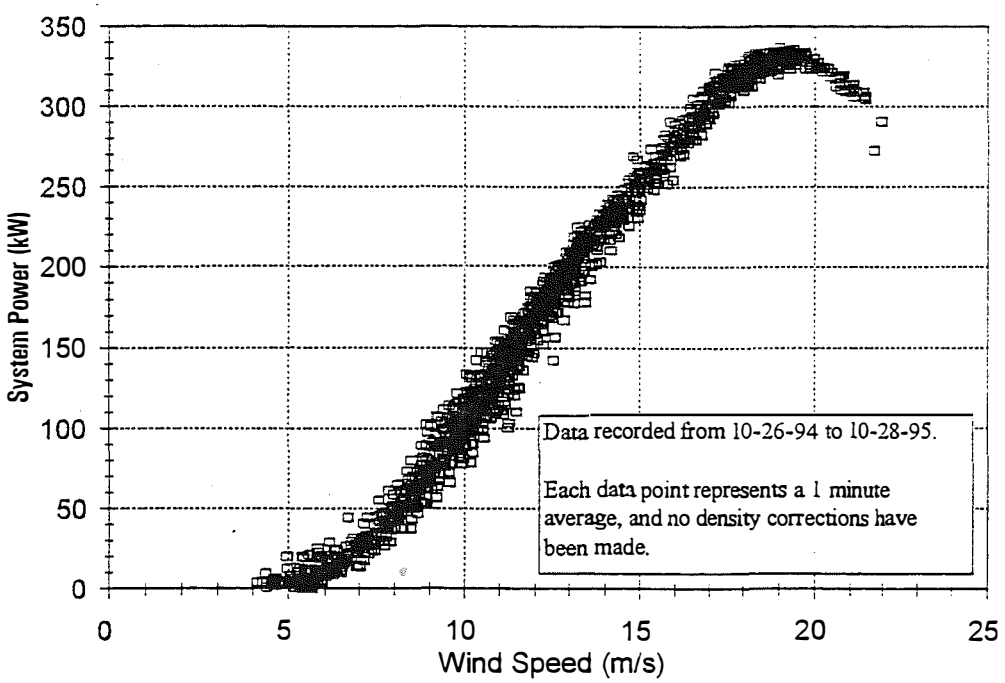

Figure 6-5. Uncorrected 57 rpm P1 Power Curve

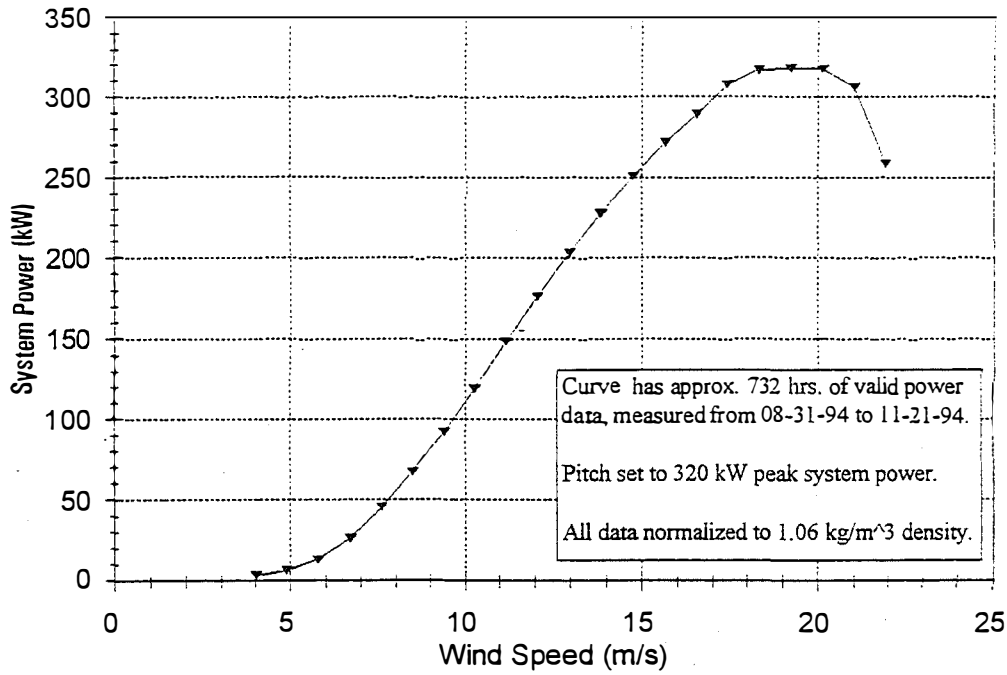

Figure 6-6. Power Curve for P1 at 57 rpm

Table 6-4. Tabulated Power Curve of P1 at 57 rpm (Normalized to 1.06 kg/m^3 Density)

Wind-Speed (m/s)	Wind-Speed (mph)	System Power (kW)
4.0	9	3.3
4.9	11	6.7
5.8	13	13.1
6.7	15	26.4
7.6	17	45.5
8.5	19	67.5
9.4	21	92.2
10.3	23	119.0
11.2	25	148.3
12.1	27	176.4
13.0	29	203.5
13.9	31	228.1
14.8	33	251.2
15.6	35	271.8
16.5	37	288.9
17.4	39	307.4
18.3	41	317.3
19.2	43	318.1
20.1	45	317.4
21.0	47	306.1
21.9	49	258.0

Table 6-5. Annual Energy Production Estimates - P1 at 57 rpm

Average Wind Speed, Rayleigh Distribution at Hub-Height (m/s)	Average Wind Speed, Rayleigh Distribution at Hub-Height (mph)	AEP for Measured P1 Performance (kWh)
5.4	12	241,100
5.8	13	308,300
6.3	14	380,900
6.7	15	458,100
7.2	16	537,600
7.6	17	618,100
8.0	18	697,900
8.5	19	776,000

6.2.2 P2A Performance

The reference anemometer for P2A was mounted on a MET tower approximately 39.6 m (130 ft) upwind of the turbine location. Figure 6-7 shows the P2A test site plan and the prevailing wind direction. The MET tower was located on a line approximately 295° up wind of the turbine, and the prevailing wind direction was approximately 292°.

The turbine anemometer which was used to collect wind-speed correlation data was originally mounted on the nacelle in a similar fashion to P1 (12-21-93 to 1-13-94). With this arrangement approximately 60 hours of data were recorded to measure the correlation factor ($WS_{nacelle}/WS_{met}$). For the prevailing directions correlation factors ranged from 1.06 to 1.12 (wind speeds 6% to 12% higher at the turbine than the MET tower).

To gain greater confidence in performance evaluation, additional correlation data were recently measured at the P2A site with the P2A turbine removed and the turbine-location anemometer at hub height on top of the P2A tower. From 3-20-95 to 5-10-95 approximately 350 hours of correlation data was measured. As shown in Table 6-6, this resulted in correlation factors of 1.037 to 1.065 for the prevailing directions. Comparing all correlation measurements for the P2A site, a constant correlation factor of 1.06 (wind speeds 6% higher at the turbine than the MET tower) was selected and used for all the P2A performance data presently reported.

Table 6-6. MET/Nacelle Correlation for P2A (measured from 3-20-95 to 5-1-95)

Directional Sector	Number of 1-Minute Averages	Correlation Factor WS_{turb}/WS_{met}
0° - 30°	627	1.079
30° - 50°	297	1.083
50° - 225°	Not Applicable	MET Tower Waked (data not used)
225° - 240°	457	1.054
240° - 255°	564	1.056
255° - 270°	820	1.059
270° - 285°	1264	1.057
285° - 300°	4121	1.065
300° - 315°	7338	1.064
315° - 330°	8090	1.037
330° - 345°	640	1.029
345° - 360°	Too Few Data Points	Not Applicable

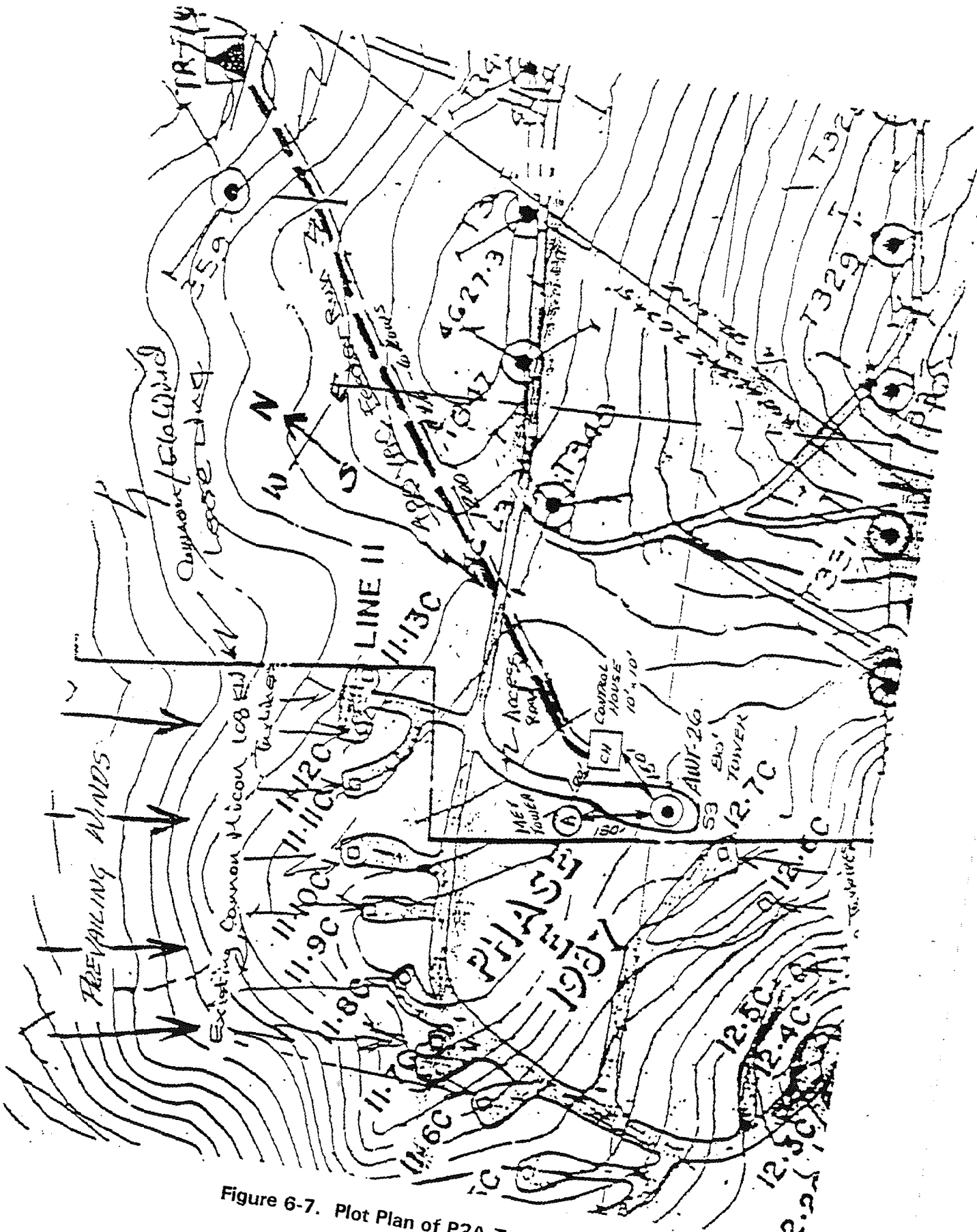

Figure 6-7. Plot Plan of P2A Test Site

6.2.2.1 Effect of Pitch Setting on P2A Performance

The P2A turbine was operated at one rotor speed only (57 rpm), but during the course of the test program three different blade pitch settings were investigated. The pitch settings resulted in different peak power levels ranging from 230 kW to 310 kW. This investigation, in conjunction with the different rotor speeds that were tested on P1, forms a valuable database for understanding the effect of blade pitch and rotor speed on the AWT-26 turbine.

When the turbine was initially installed, blade pitch was set to -1.13°. Approximately 19 hours of power curve data were collected at this setting, which resulted in a peak power of approximately 230 kW. After preliminary system checkout procedures had been completed, the blades were repitched to 0.37° and 2.7 hours of data were recorded, showing a peak power of approximately 270 kW.

The blades were then repitched to 1.27°, which resulted in a peak power of 310 kW, and the turbine was left in this configuration for extended performance testing.

6.2.2.2 P2A Power Curve at 310 kW Peak Power

P2A was run for extended performance testing at the 1.27° pitch setting. Figure 6-8 shows a sample of uncorrected power curve data for P2A. Each data point represents a 1-minute average power and wind speed. Note that the P2A data forms a wider band of scatter than is seen in Figure 6-5 for P1. This trend has been consistently observed between the two turbines.

Approximately 300 hours of valid power-production data were recorded for this configuration, between the dates of 3-4-94 and 6-3-94. Figure 6-9 shows the resulting P2A power curve, corrected for density and with a constant wind speed correlation factor of 1.06, as discussed above. The P2A power curve is given in tabular form in Table 6-7.

6.2.2.3 P2A Energy Production Characteristics

The P2A power curve shown in Figure 6-9 was used to calculate annual energy production for sites with annual average wind speeds ranging from 12 to 19 mph (5.4 to 8.5 m/s). The results are summarized in Table 6-8. These annual energy production levels assume 100% availability, and clean blades, and refer to Rayleigh wind speed distributions at hub height.

6.2.2.4 Comparison of P1 and P2A Performance

Figure 6-10 shows a comparison of the measured power curves for P1 and P2A, both at 57.1 rpm, and near the same peak power. At wind speeds below 12 m/s (27 mph) the power curves are largely in agreement, with the P2A curve being only slightly higher than the P1 curve. Above 12 m/s the P2A curve falls consistently below the P1 curve. These differences in the power curves are reflected in the annual energy production estimates. Comparison of Tables 6-5 and 6-8 shows that at a 5.4 m/s (12 mph) site P2A will produce 1.4% more annual energy than P1, and at an 8.5 m/s (19 mph) site P2A will produce 1.6% less than P1.

There are several reasons that the P1 and P2A curves are not in exact agreement:

1. They are pitched to different peak powers (by 10 kW), and so must diverge near the peaks.

2. The different towers and other mechanical differences result in different structural and aerodynamic responses.

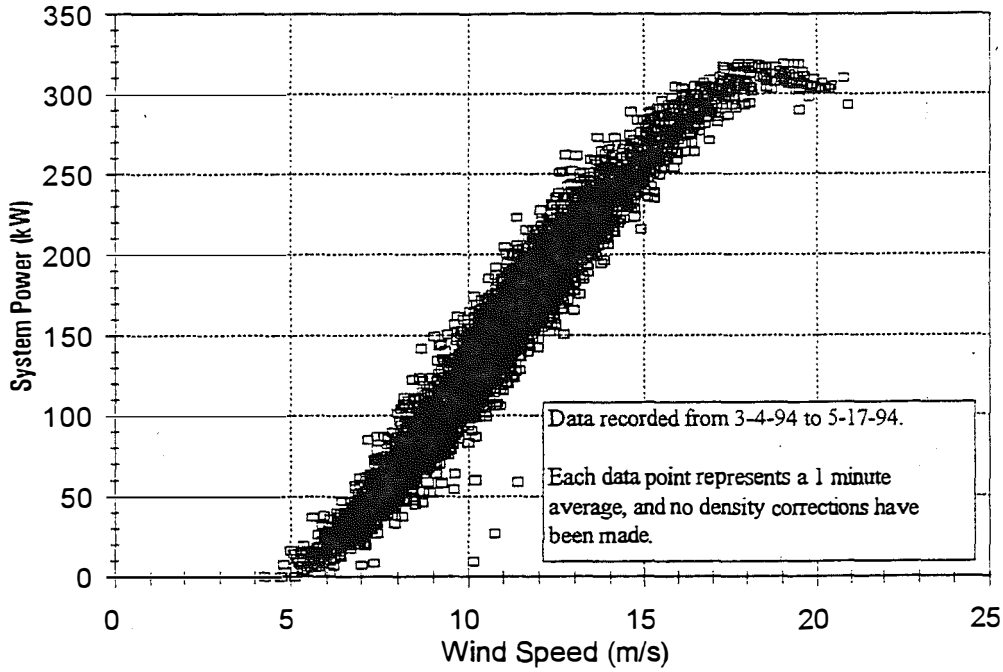

Figure 6-8. Uncorrected P2A Power Curve (57 rpm, pitch = 1.27°)

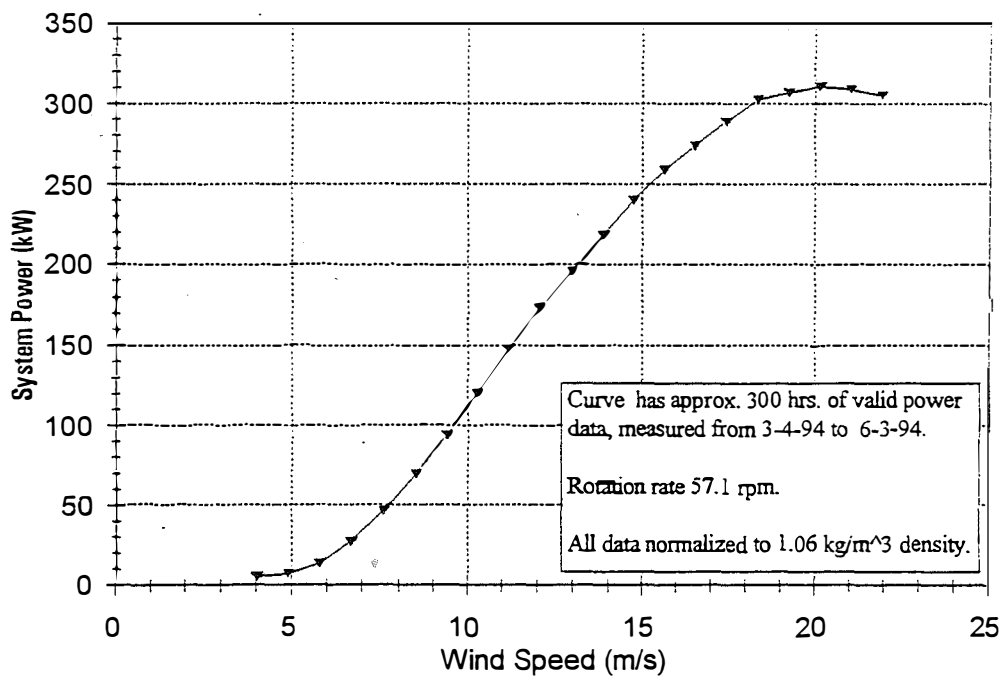

Figure 6-9. Power Curve for P2A at Pitch = 1.27°

Table 6-7. Power Curve for P2A at Pitch = 1.27° (Normalized to 1.06 kg/m^3 Density)

Wind-Speed (m/s)	Wind-Speed (mph)	Svstem Power (kW)
4.0	9	5.2
4.9	11	7.1
5.8	13	13.5
6.7	15	26.8
7.6	17	46.5
8.5	19	69.6
9.4	21	93.8
10.3	23	120.1
11.2	25	147.7
12.1	27	172.9
13.0	29	195.9
13.9	31	218.3
14.8	33	240.6
15.6	35	259.2
16.5	37	274.2
17.4	39	289.2
18.3	41	302.6
19.2	43	307.2
20.1	45	310.9
21.0	47	308.7
21.9	49	305.7

Table 6-8. Annual Energy Production Estimates - P2A at Pitch = 1.27°

Average Wind Speed, Rayleigh Distribution at Hub-Height (m/s)	Average Wind Speed, Rayleigh Distribution at Hub-Height (mph)	AEP for Measured P2A Performance (kWh)
5.4	12	244,400
5.8	13	310,600
6.3	14	381,500
6.7	15	456,700
7.2	16	533,600
7.6	17	611,400
8.0	18	688,500
8.5	19	763,700

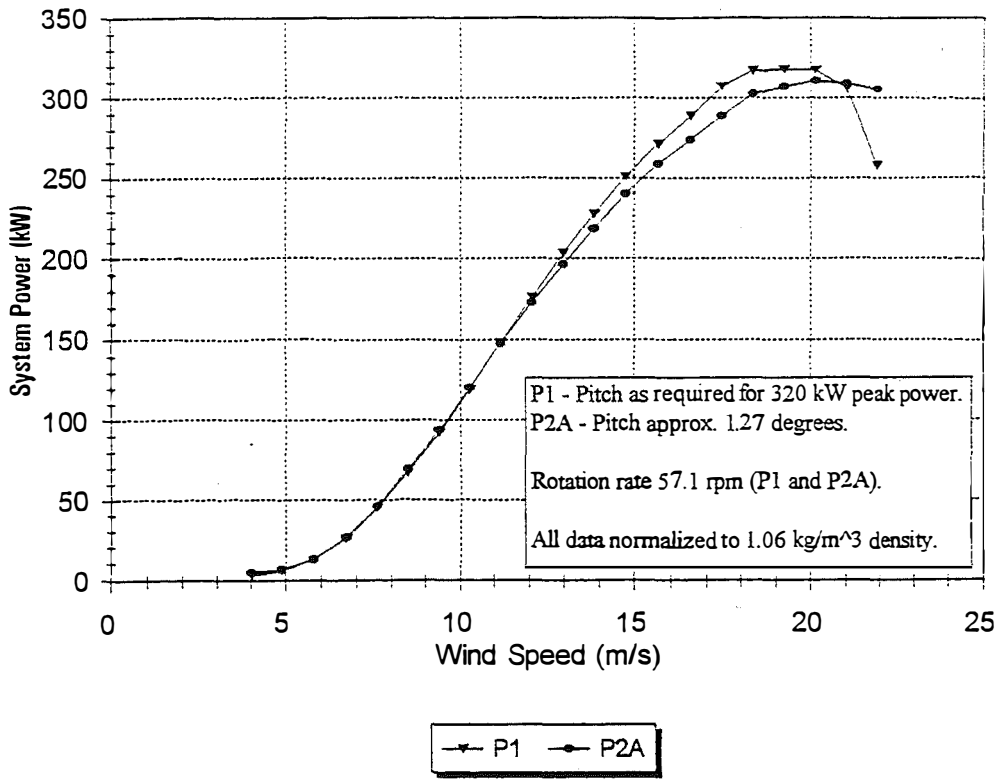

Figure 6-10. Comparison of Power Curves for P1 and P2A

3. The tests were conducted at two different locations, each with its own wind-speed adjustments. Although these were measured, testing at two different locations adds an additional degree of uncertainty when making comparisons.

Given the above, the P1 and P2A power curves are in very close agreement with each other.

6.3 Structural Response

6.3.1 AWT-26/P1

The AWT-26/P1 machine demonstrated considerable blade edgewise bending at a frequency of 7P. Much attention was given to this phenomenon because it was perceived as affecting the fatigue life of several components, and the entire test program became oriented towards reducing this particular response. A number of configuration changes were made in order to reduce the 7P response.

The level of 7P response in the P1 wind turbine was less than that observed on the REP machine (see Figures 6-11, 6-12 and 6-13). The reason for this may have been the lower turbulence on the P1 site (12% compared to 22%) and the reduced vertical wind shear (an exponent value of about 0.05).

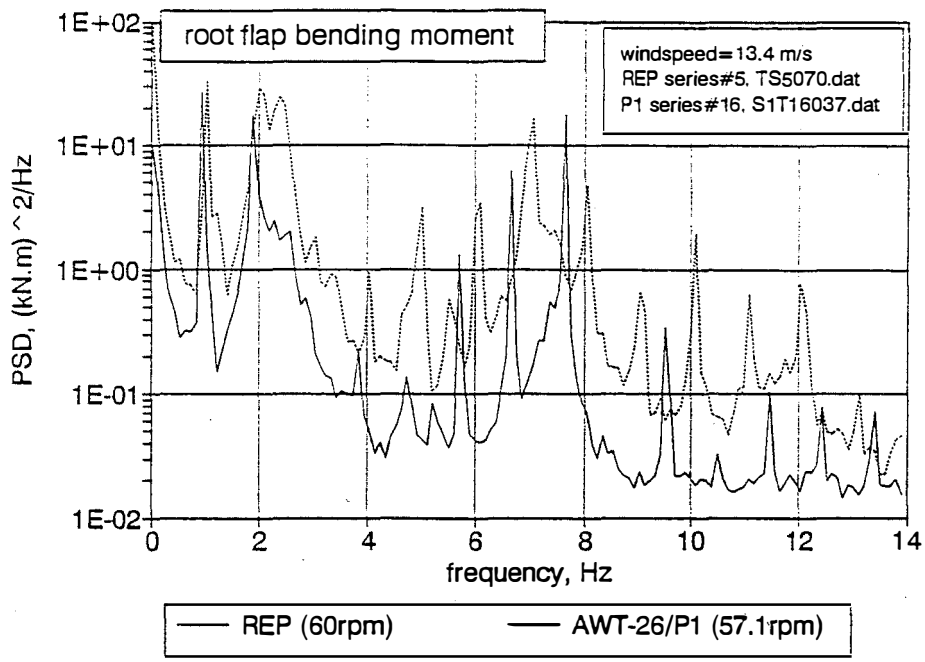

Figure 6-11. Comparison of REP versus AWT-26/P1: root flap bending

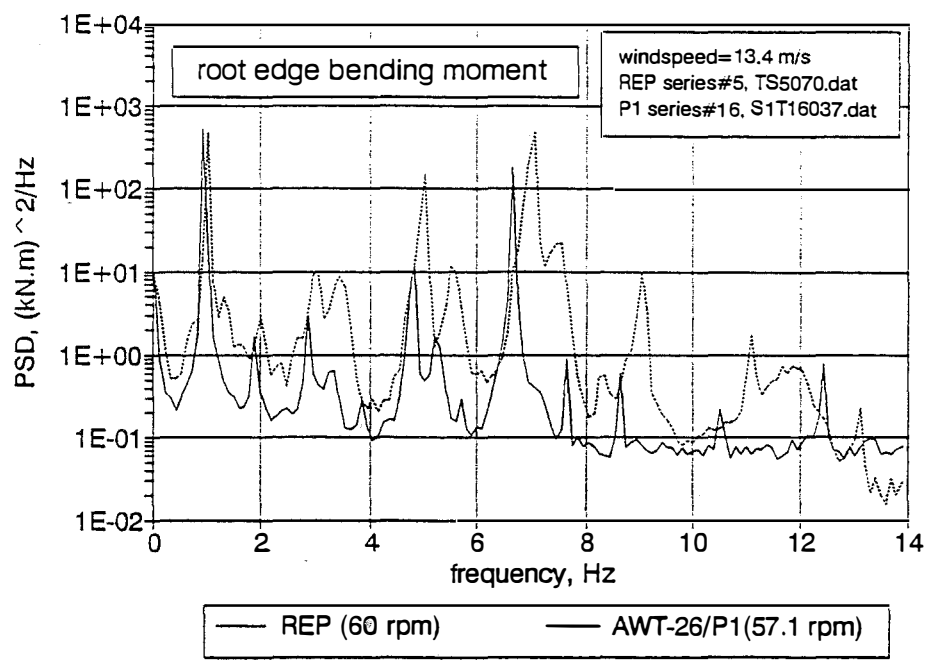

Figure 6-12. Comparison of REP versus AWT-26/P1: root edge bending

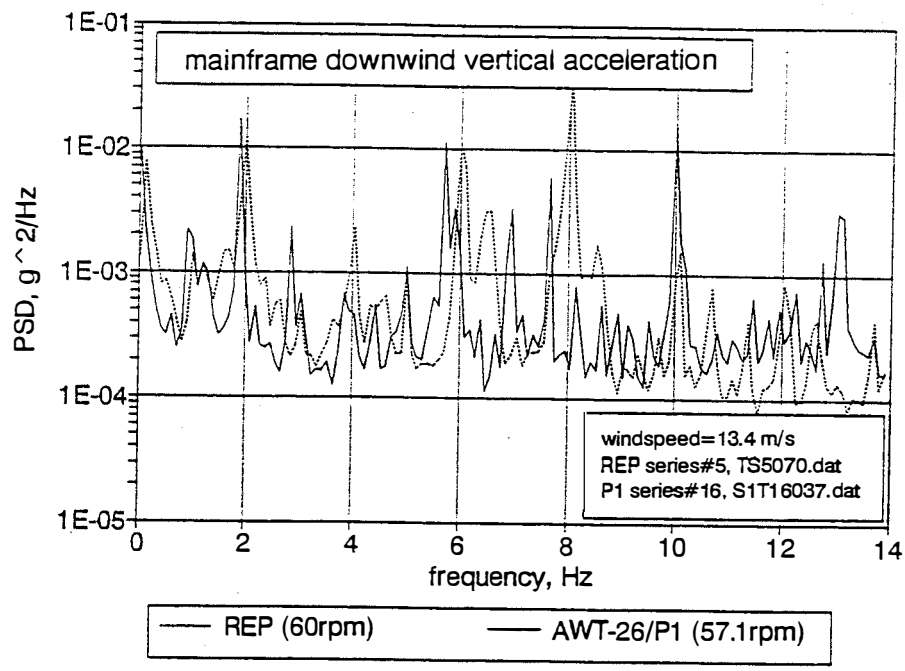

Figure 6-13. Comparison of REP versus AWT-26/P1: mainframe downwind vertical acceleration

Because of the several configuration changes and the continuing difficulties experienced with the data acquisition system, it was not possible to collect a good baseline set of data for the AWT-26/P1. It should be mentioned, however, that efforts were made to reduce the source of the 7P excitation -- the tower shadow. It was found that replacement of the angle section cross-bracing members on the upper half of the tower by tubular members did reduce the response at 7P. This was probably due to the lower drag of the tubular members and a reduced overall tower shadow and is demonstrated in Figure 6-14.

6.3.2 AWT-26/P2

The results obtained from the AWT-26/P2 indicated a substantially reduced blade edgewise bending at 7P (by at least one decade on the power spectral densities). In fact, there was as much response at 5P as at 7P. This is illustrated by the power spectral densities in Figures 6-15 through 6-18 (compare the AWT-26/P2 response to the REP response). An explanation of the difference between the two machines must lie with the different structural characteristics and/or the different tower shadow intensities.

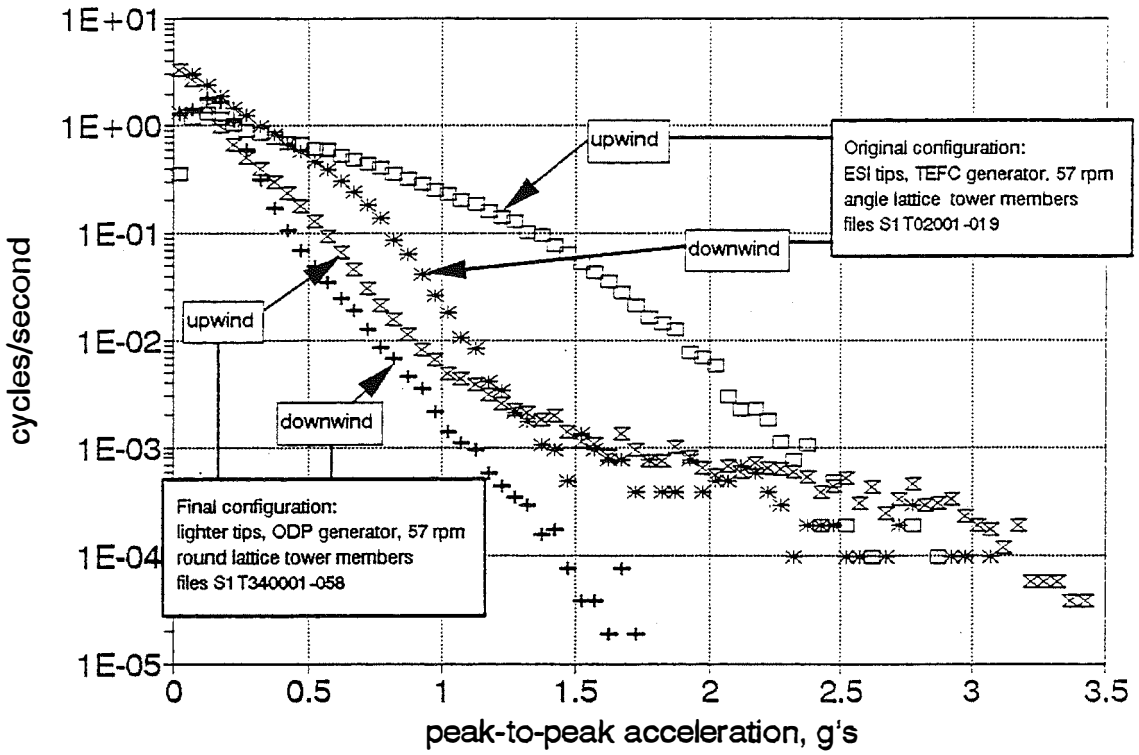

Figure 6-14. Effect of tower modifications on P1 nacelle pitching.

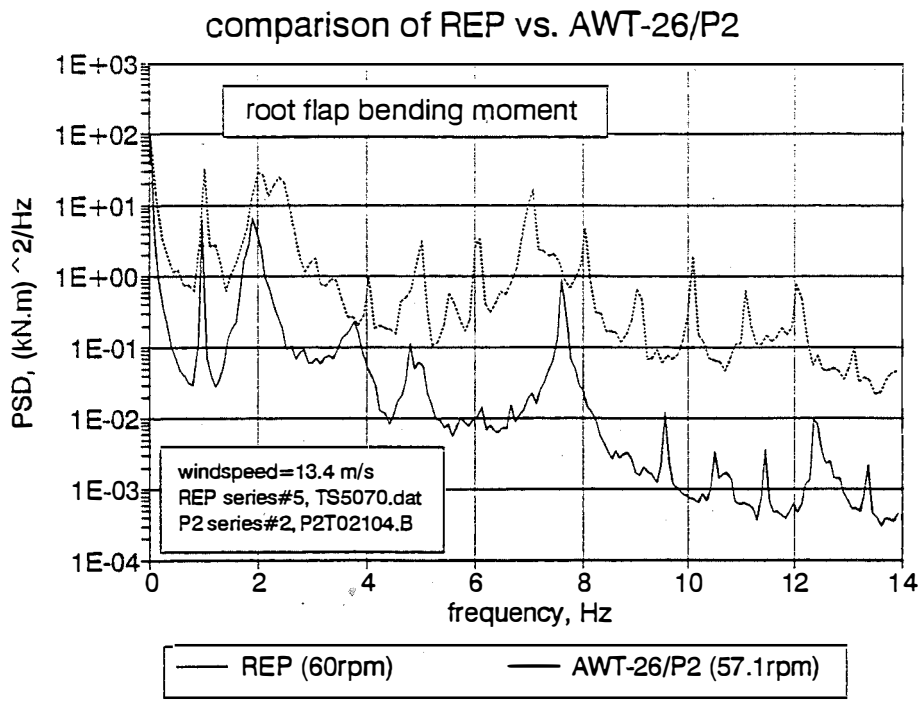

Figure 6-15. Comparison of REP versus AWT-26/P2: root flap bending

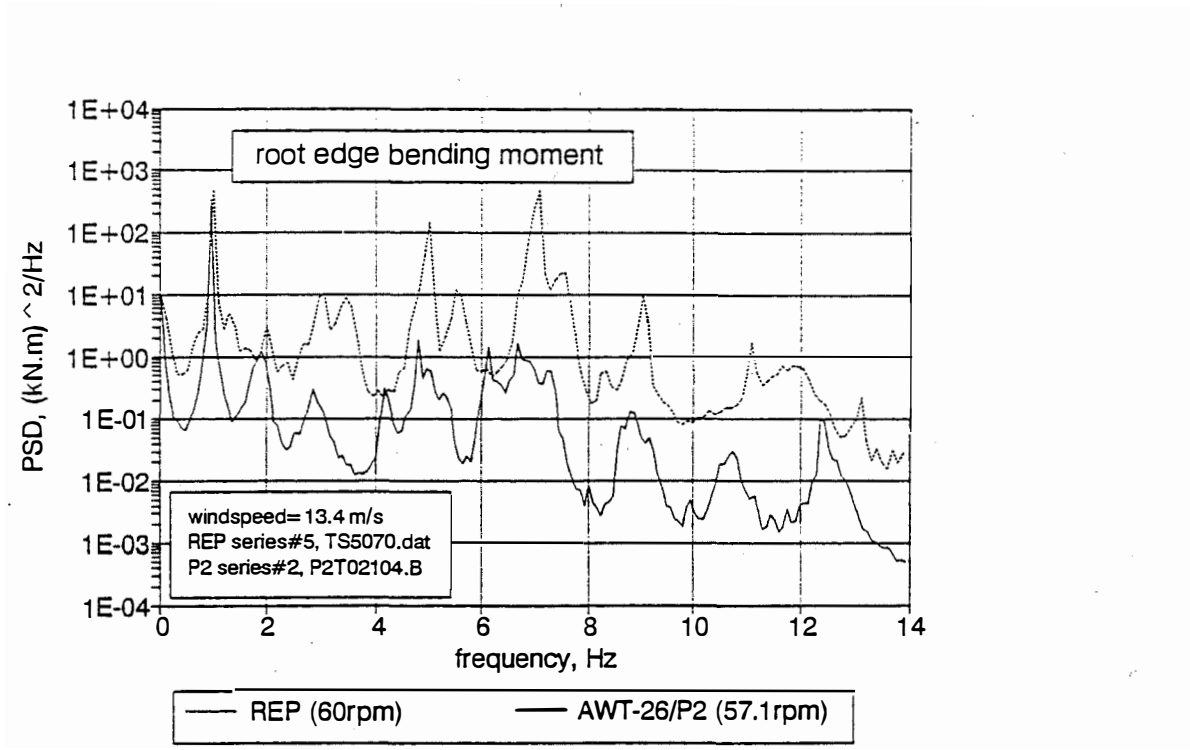

Figure 6-16. Comparison of REP versus AWT-26/P2: root edge bending

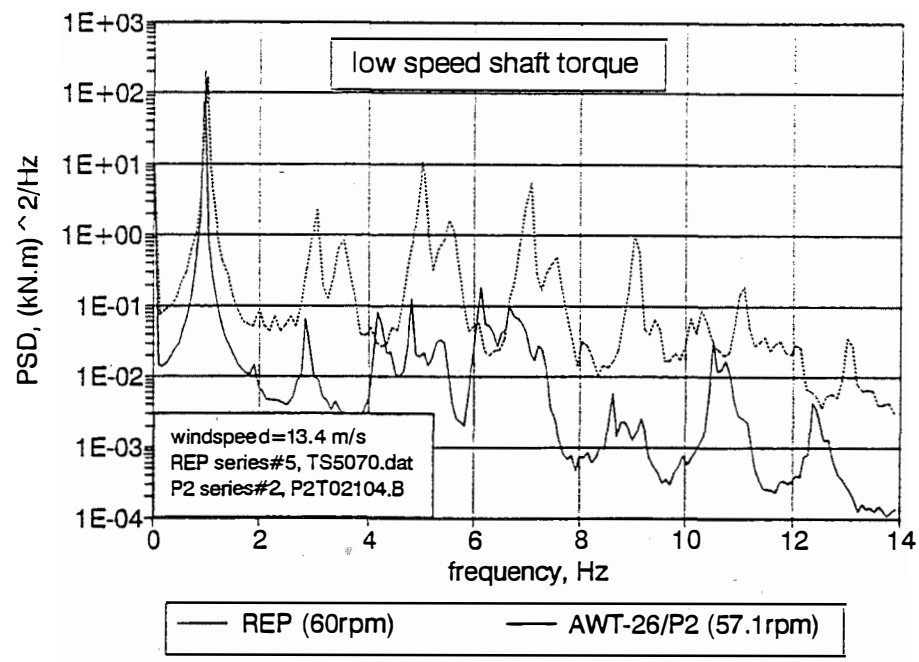

Figure 6-17. Comparison of REP versus AWT-26/P2: low-speed shaft torque

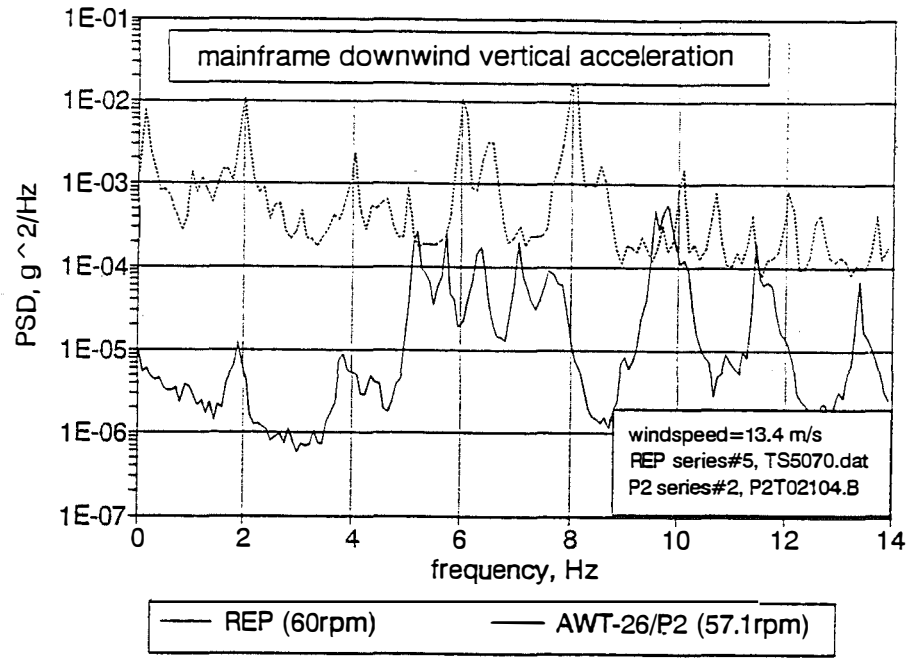

Figure 6-18. Comparison of REP versus AWT-26/P2: mainframe downwind vertical acceleration

The data collection from this machine has focused primarily on obtaining a baseline data set that could be used for design load validation. By relating the data to wind speed and to turbulence level, it is hoped to apply the data base to other site conditions and other wind regimes.

6.4 Mean Loads

A mean loads data set has been gathered for a pitch setting of +1.27° at a mean air density of 1.04 kg/m^3. Plots of root flap bending, root edge bending, shaft torque, and teeter standard deviation versus wind speed are presented in Figures 6-19 through 6-22.

These mean loads and their associated standard deviations may be compared with the corresponding design peak values and cycle spectra presented in Section 4. If the maximum deviation is assumed to be as high as 4.0 times the standard deviation, then the design loads are still not exceeded.

6.5 Fatigue Loads

A data set of cyclic loads was developed for one value of pitch setting and air density. The distribution of wind speeds used for this data set is shown in Figure 6-23 and shows that the P2 distribution exceeds the Rayleigh distribution specified for design except at low winds. The average turbulence intensity versus wind speed is plotted in Figure 6-24.

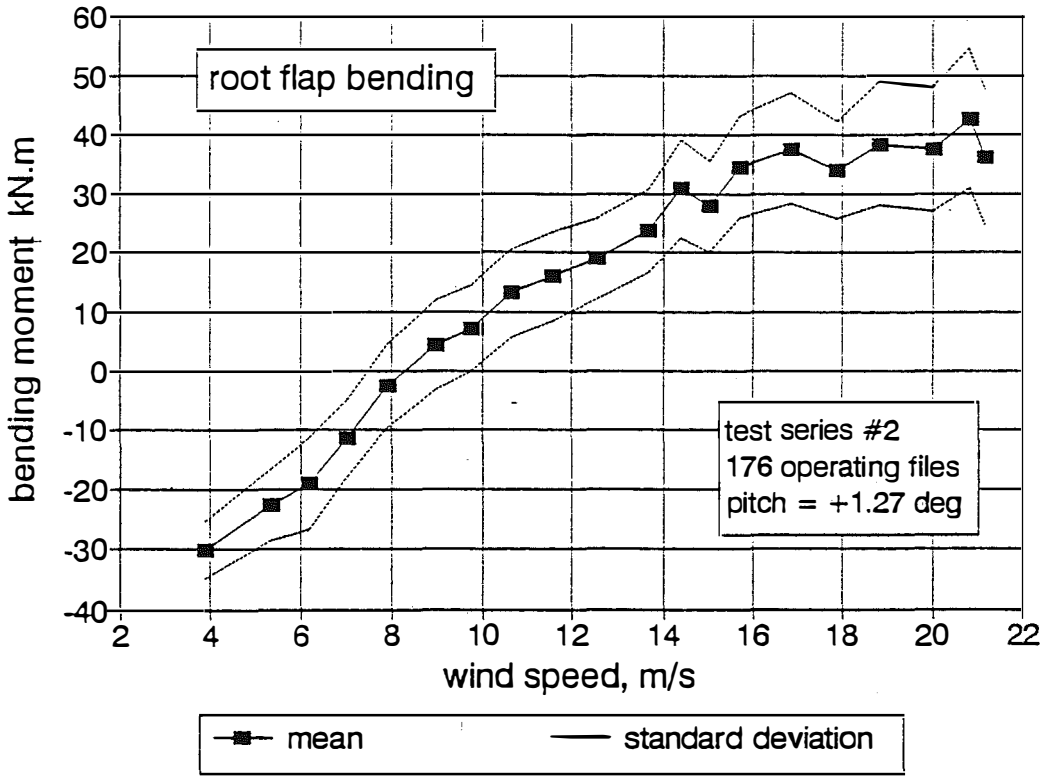

Figure 6-19. AWT-26/P2 mean test loads: root flap bending

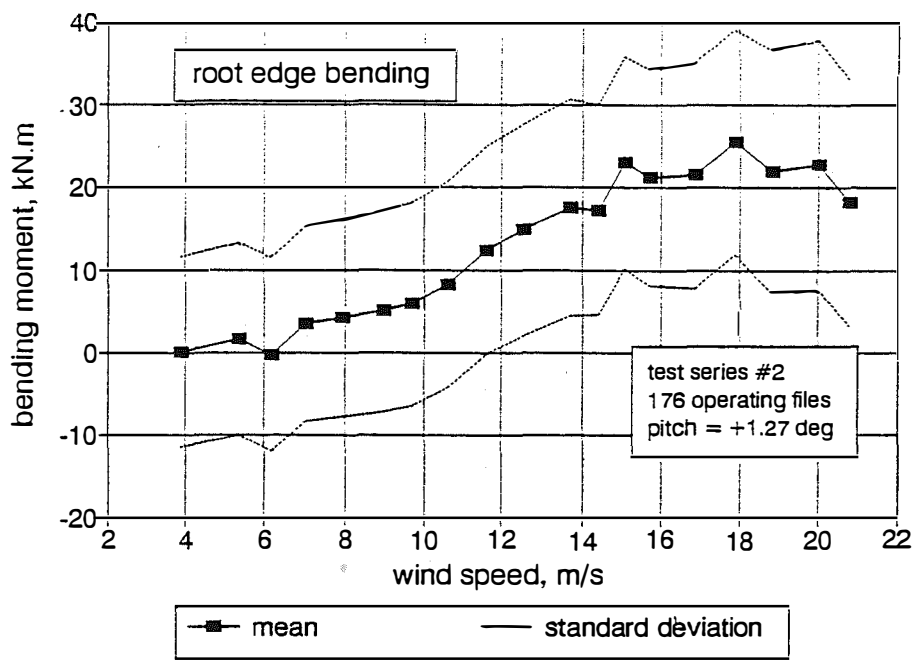

Figure 6-20. AWT-26/P2 mean test loads: root edge bending

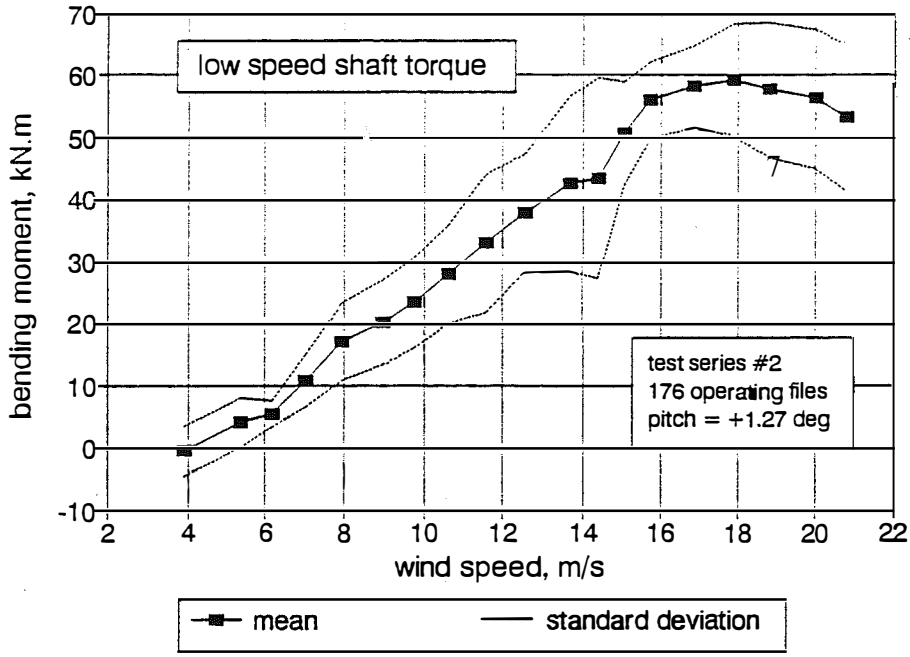

Figure 6-21. AWT-26/P2 mean test loads: low-speed shaft torque

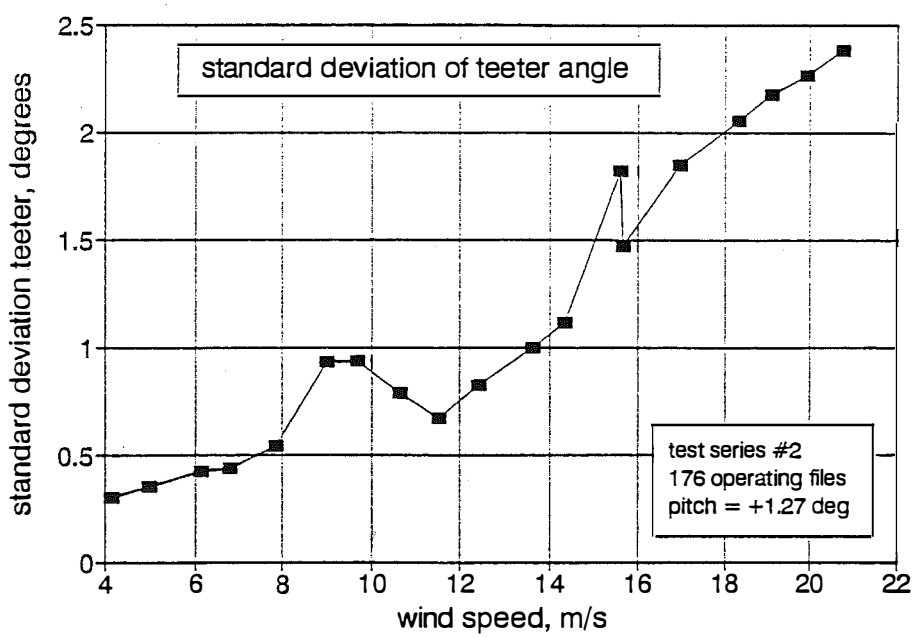

Figure 6-22. AWT-26/P2 mean test loads: standard deviation of teeter angle

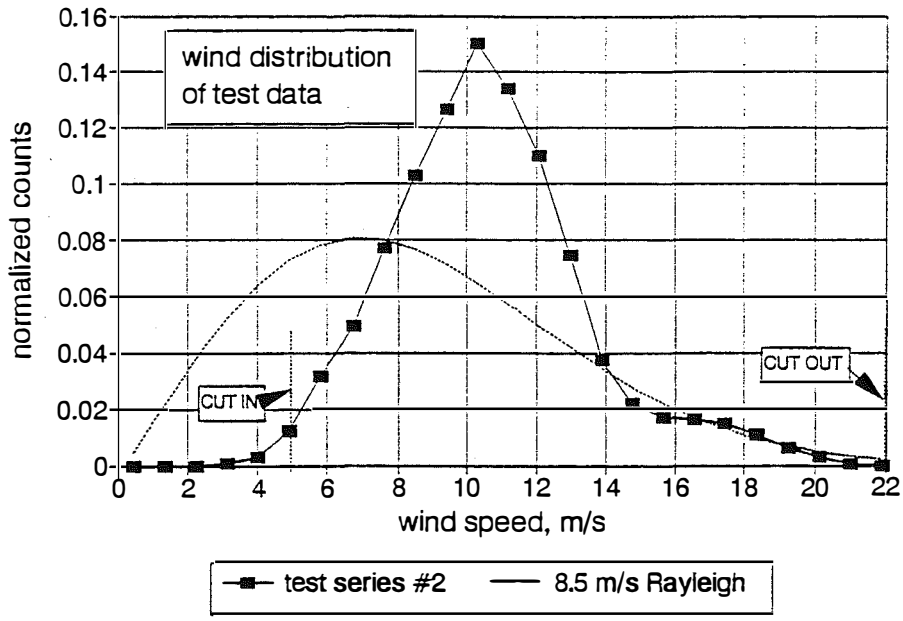

Figure 6-23. Wind distribution for AWT-26/P2 series #2 tests

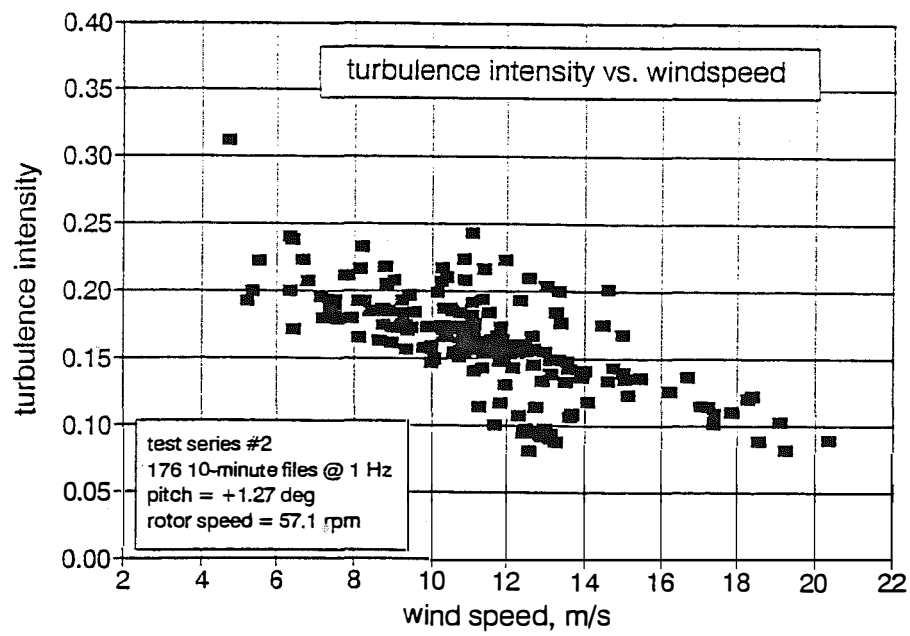

Figure 6-24. AWT-26/P2 test results: turbulence intensity versus wind peed

Figure 6-25 shows how the distribution of rainflow-counted cycles of root flap bending varies with wind speed. The distributions from P2 are compared with the combined distribution from REP on the same figure and indicate that the design spectrum exceeded the measured spectrum. Figures 6-28 and 6-29 show the same trends for the root edge bending and for the shaft bending. The difference in levels can be attributed to two possible causes: a more pronounced 7P response in the REP machine, and the more severe turbulence characteristics at the REP site. It is theorized that the damaging turbulence events seen regularly by the REP machine are approached during high wind conditions at the P2 site.

The early tests of the P2 machine indicated that it was fairly active in teeter. Figure 6-26 is a plot of the teeter cycle distributions for four wind speed ranges during the first test series. At the high wind speeds, the large teeter excursions occurred frequently. This problem was addressed primarily by increasing the resistance of the teeter dampers. At the same time the peak power was increased by changing the blade pitch, and strakes were added to the tower as a noise reduction measure. Figure 6-27 shows that dramatic reductions in large amplitude teeter excursions were achieved. The high wind results in this figure are very low due to the upwind turbines having been shut down for this period. However, data showing the effect of these changes on loads such as blade root moments, were not available.

Figures 6-28 and 6-29 present the corresponding fatigue cycle results for the blade root edge bending and low-speed shaft torque. These results are similar to those for the blade root flap bending in Figure 6-25. In the case of torque, the tower shadow effect seems to be particularly strong at the high wind speeds, causing an increase in this part of the load spectrum.

6.6 Transient Loads

The machine start and stop sequences were thoroughly tested to verify that the loads were within those specified for design. A sample trace of shaft torque and generator power during a start in a 10.3-m/s wind is shown in Figure 6-30. Figure 6-31 shows the corresponding traces of yaw and teeter angle.

The P2 machine has two stop modes, normal and fast. A plot of the normal stop sequence appears in Figure 6-32 and a plot of the fast stop appears in Figure 6-33. The peak shaft torque during a fast stop is within 90 kN.m (66,000 ft.lbs). This is well within the peak value specified for design (145 kN.m).

The oscillations at approximately 5.4 Hz in the shaft torque during braking, apparent in Figures 6-32 and 6-33, are probably due to the natural frequency of the rotor and gearbox relative to a restraint at the high speed brakes. This natural frequency is higher than the corresponding frequency of the operating machine when the flexibility of the high speed shaft is included. This "ringing" phenomenon is quite normal.

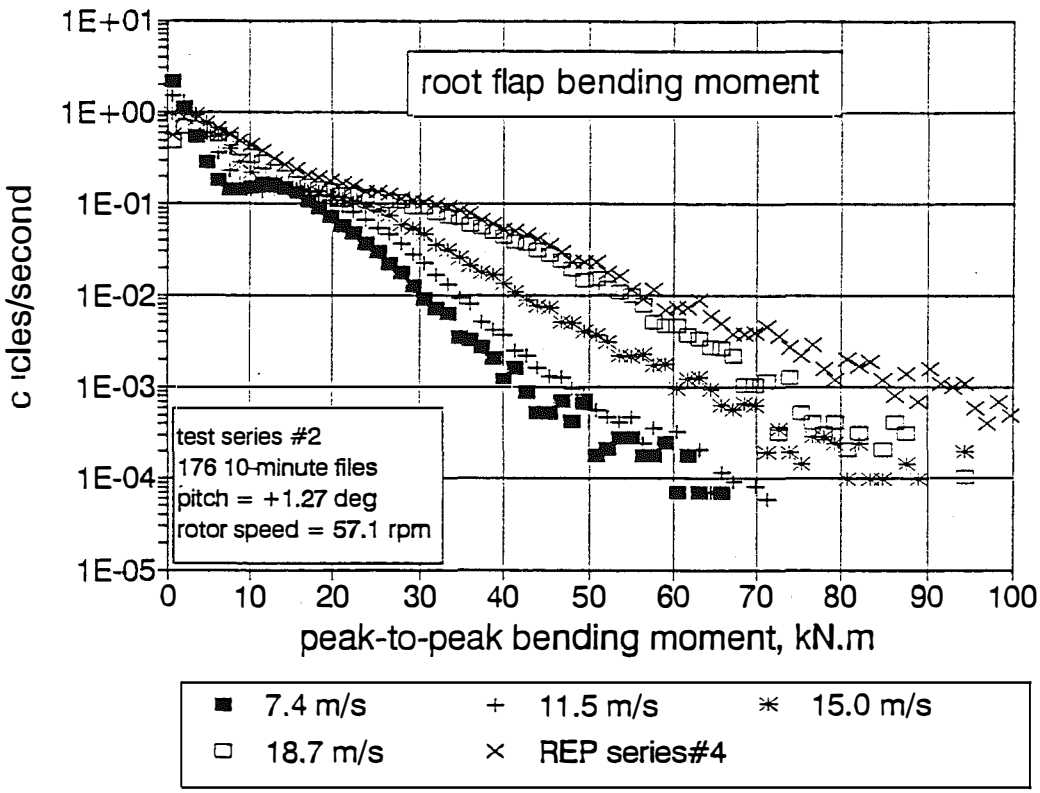

Figure 6-25. AWT-26/P2 cycle count test results: root flap bending

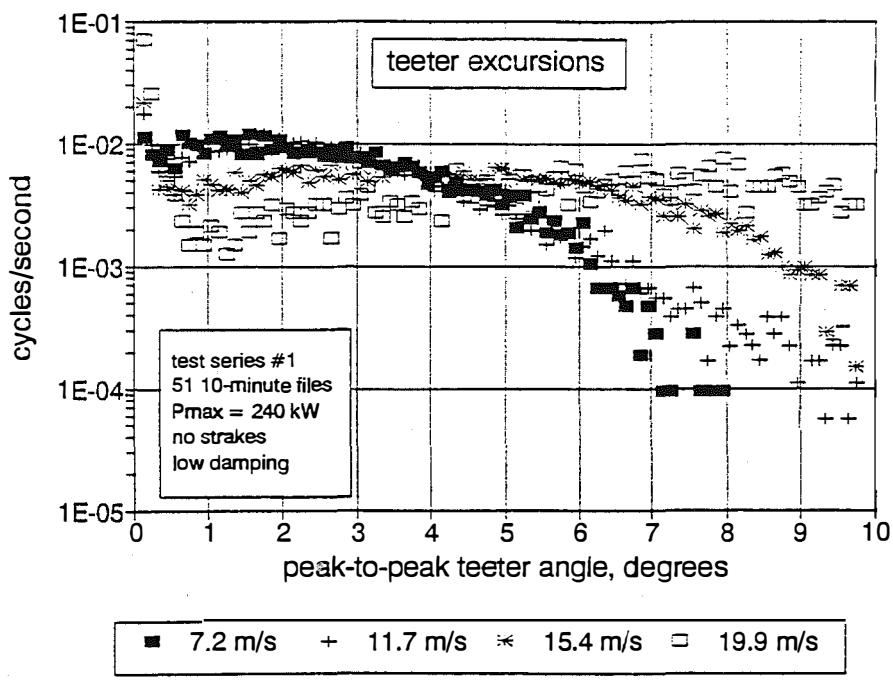

Figure 6-26. AWT-26/P2 cycle count test results: teeter excursions

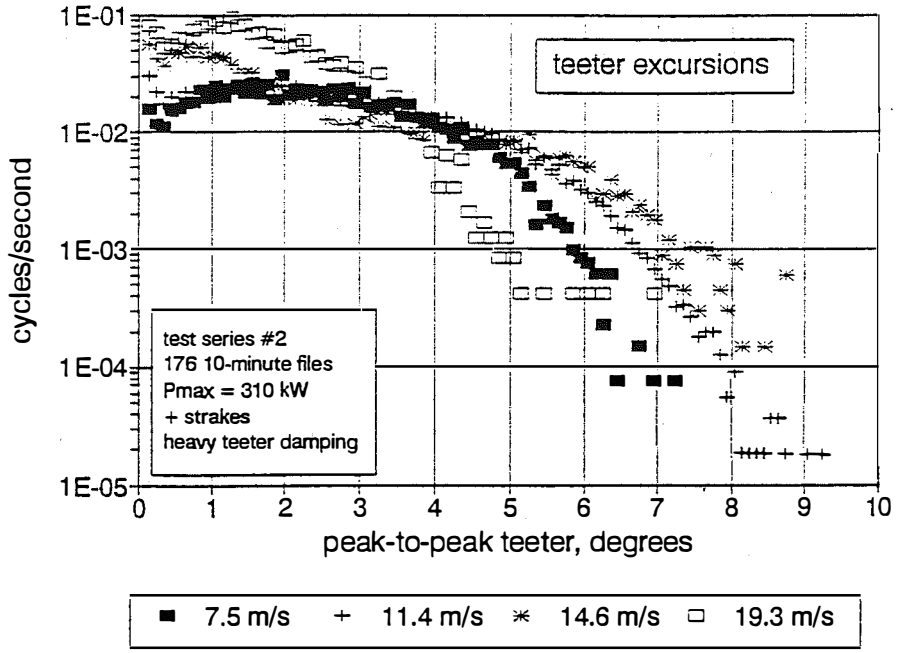

Figure 6-27. AWT-26/P2 cycle count test results: teeter excursions, series #2

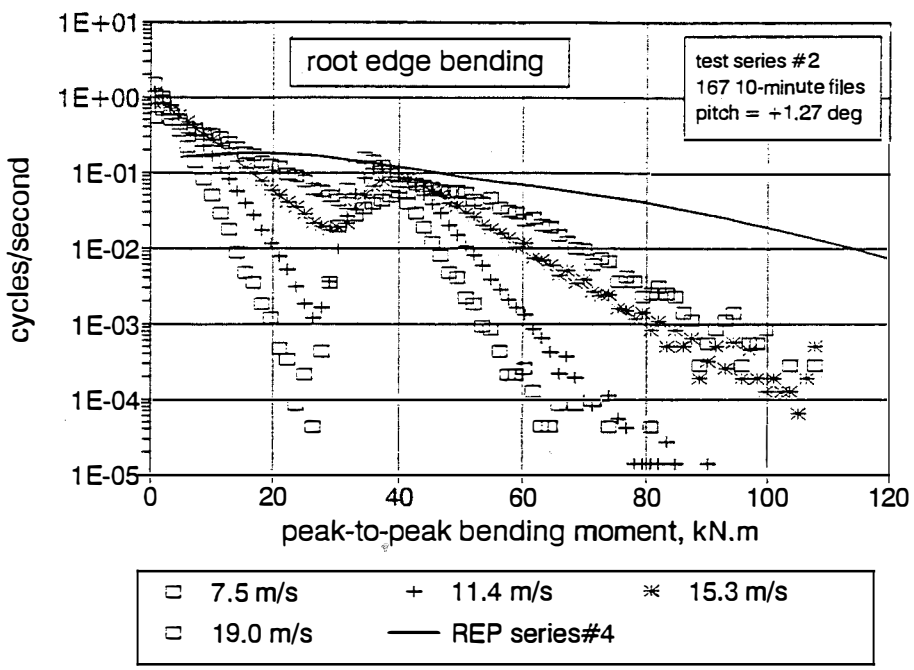

Figure 6-28. AWT-26/P2 cycle count test results: root edge bending

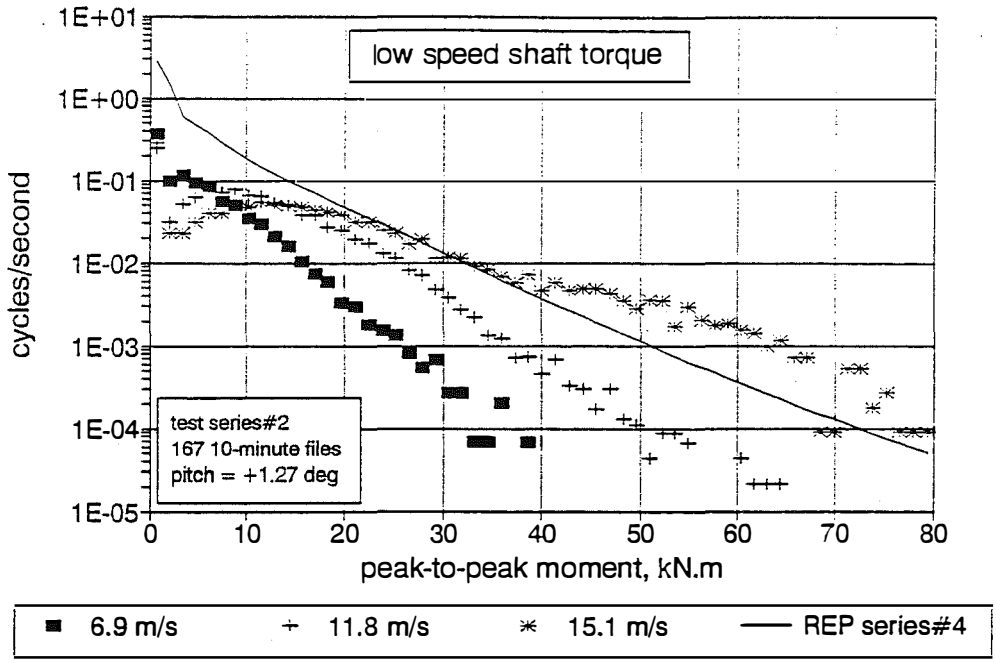

Figure 6-29. AWT-26/P2 cycle count test results: low-speed shaft torque

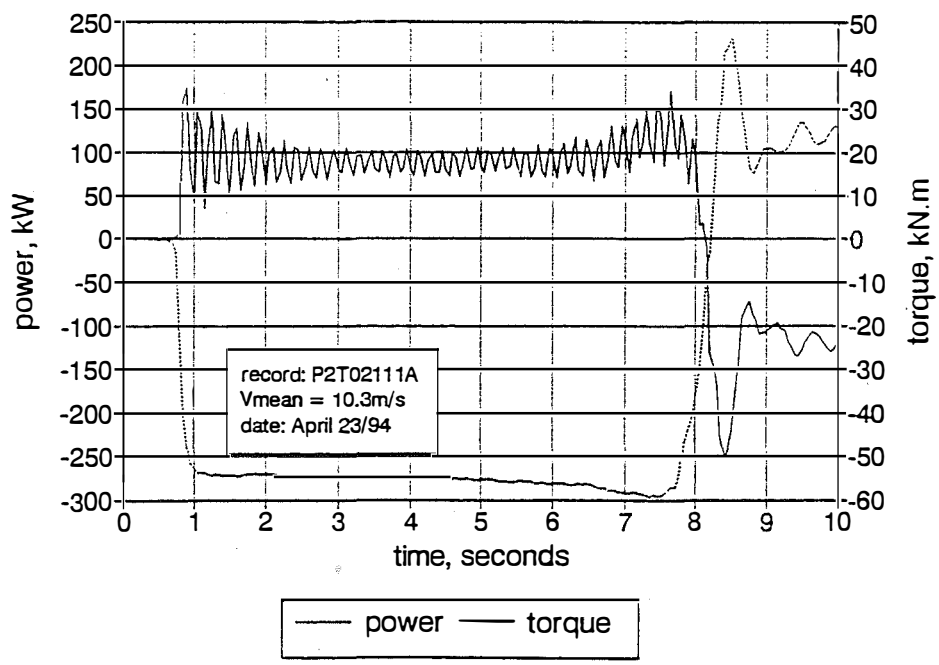

Figure 6-30. AWT-26/P2 typical startup: power and torque

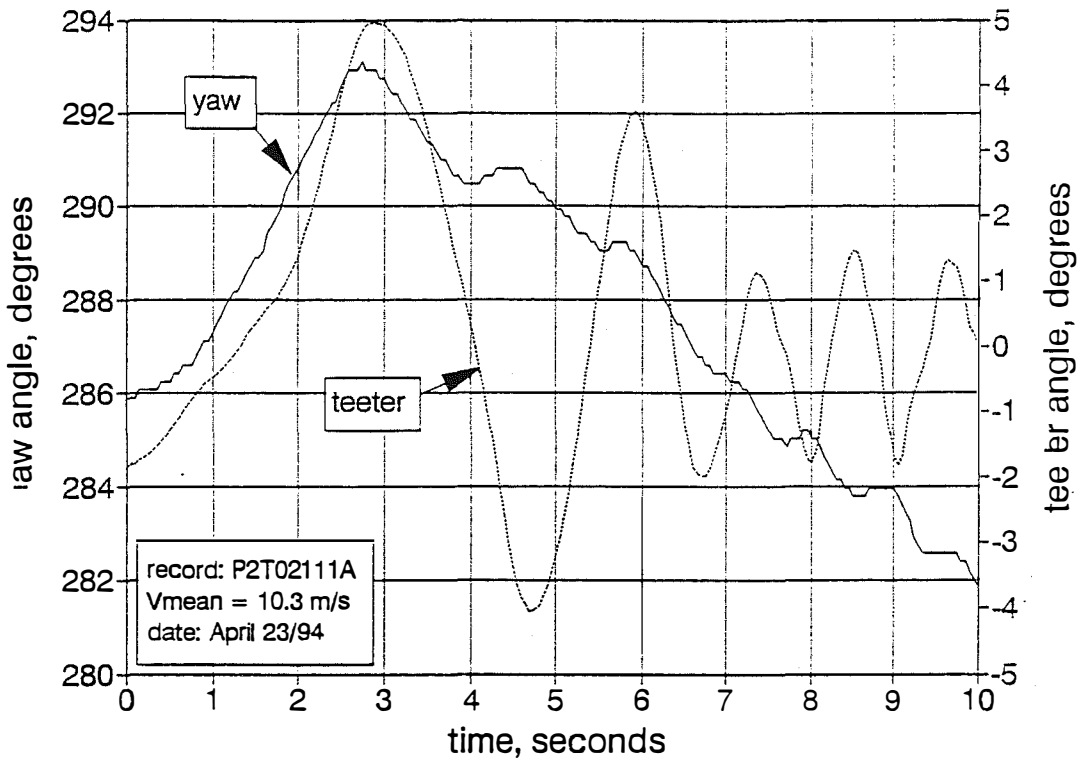

Figure 6-31. AWT-26/P2 typical startup: yaw and teeter motion

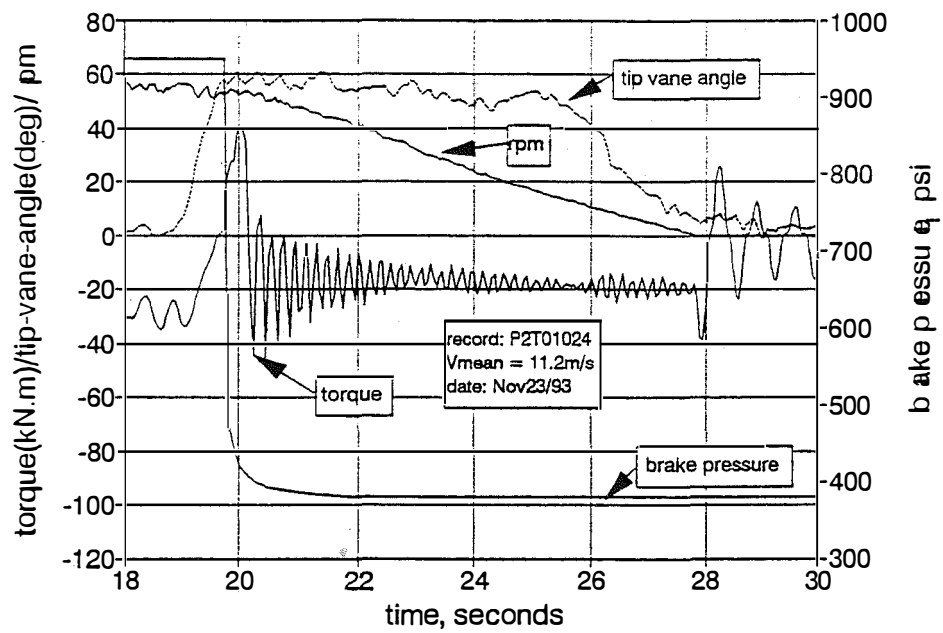

Figure 6-32. AWT-26/P2 typical normal stop: torque, rpm, tip vane angle, and brake pressure

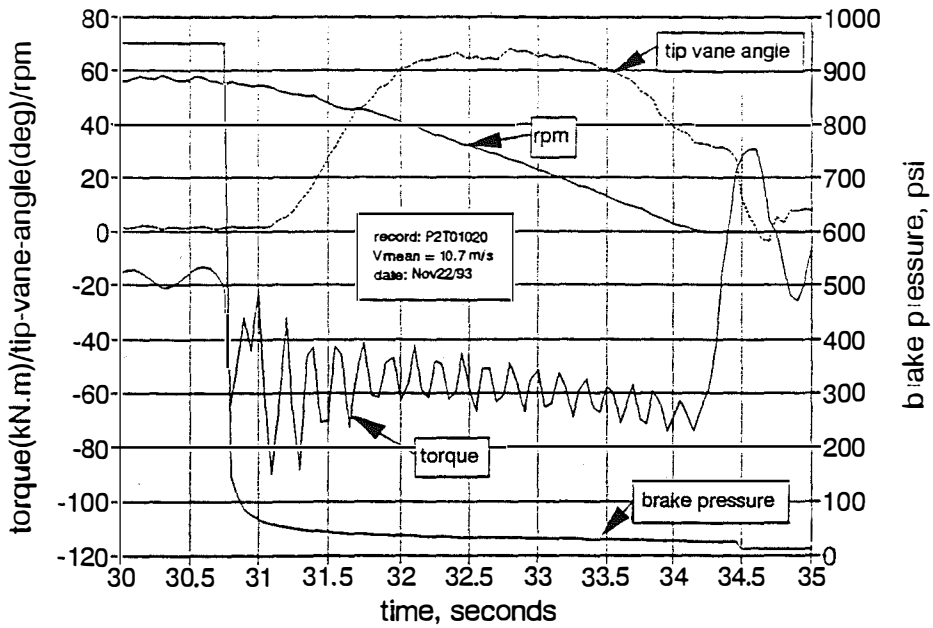

Figure 6-33. AWT-26/P2 typical fast stop: torque, rpm, tip vane angle, and brake pressure

7.0 Model Simulation

7.1 Modeling Tools

7.1.1 Finite Element modeling

Much of the detailed stress analysis was done using the Algor code (ref. 17). Components that were modeled included the hub, teeter pin, mainframe, gearbox housing and snout, tower top plate, and parts of the tubular tower.

These analyses used static loads that had been previously identified from prototype testing and/or dynamic simulation. For most of the components the model was constructed of four-sided plate elements with some load applied through a number of stiff beams. The results of the modeling was used to identify the maximum stressed due to both peak loads (for ultimate strength checks) and due to unit loads (for fatigue strength checks). An example of the Algor modeling of the hub is shown in Figure 7-1.

Algor was also used to predict the natural frequencies and modes of the isolated blade and of the complete system (rotor, nacelle, and tower). Although these results could be used to confirm the behavior of the stationary machine, the code could not simulate the behavior of the operating wind turbine. For this reason, most of the dynamic modeling was done with the codes described below.

7.1.2 Dynamic Simulation

Several computer models have been used in the course of this project to simulate the aerodynamic and/or the structural dynamic response of the wind turbine..

PROPPC is a FORTRAN code, originally developed at NREL, to calculate the performance and mean loads in horizontal axis wind turbines. It uses blade element theory and assumes flow occurs in independent annular stream tubes. The effects of hub and tip losses and tower shadow are included. The code has been well validated by several investigators.

FLAP is another FORTRAN code developed at NREL. It calculates the structural loads in a HAWT in either steady or turbulent flow with a prescribed yaw rate. The limitations of FLAP, and its derivative STRAP for teetered rotors, are that the tower is assumed rigid and blade edgewise bending is not considered.

FLAP was used extensively during the ESI-80 retrofit (REP) project to calculate blade forces. In general, FLAP tended to underpredict rotor loads, especially the blade edge loads and in turbulent flow. Results from FLAP are compared with ESI-80 results in the report on the ESI-80 retrofit project (Reference 4).

YAWDYN is a code developed at the University of Utah to model the behavior of a HAWT during yawing motions. The code was used in the preliminary stages of the project but, due to its limitations, was discontinued in favor of the Automatic Dynamic Analysis of Mechanical Systems, from Mechanical Dynamics, Inc. (ADAMS) code.

FAST is a code developed at Oregon State University, Corvallis, and is based on an earlier code named DRT. FAST includes more degrees of freedom than FLAP (it includes several tower modes), but still lacks blade edge bending. Some time was spent applying this code to the AWT-26/P2 and in tuning the model to reproduce the measured mean loads. However, time did not allow further efforts with this code to reproduce operating cyclic loads.

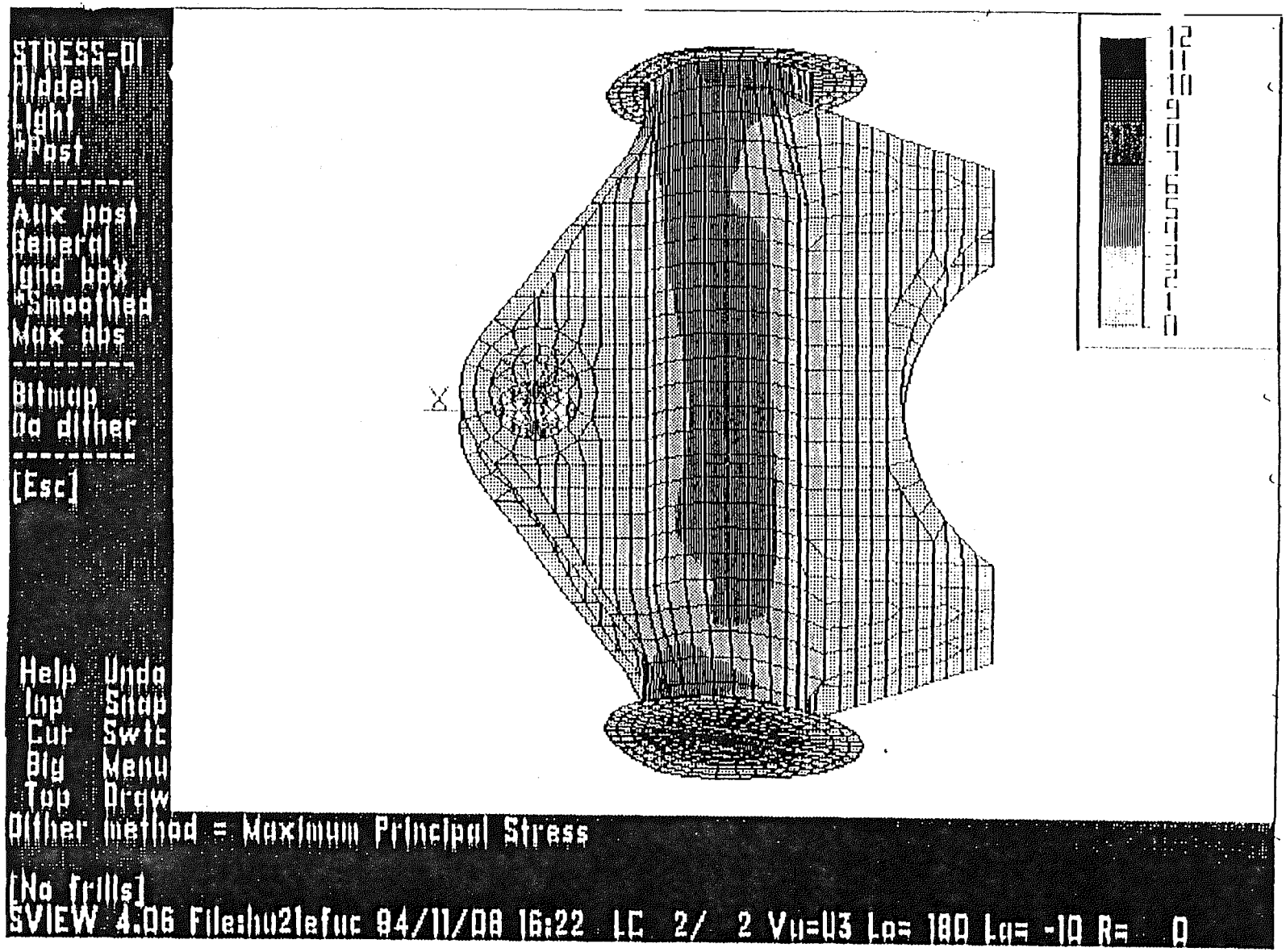

Figure 7-1. Algor finite element model of the AWT-26/P1 hub

In 1990, NREL began the application of ADAMS to horizontal-axis wind turbines. In 1992, RLA began cooperating with NREL to use ADAMS to simulate the response of the AWT-26. The perceived advantages of ADAMS were its complete nonlinearity, the representation of all degrees of freedom, the facility to link with user-written (aerodynamic) subroutines, and its commercial support.

Modeling with ADAMS began with the retrofitted ESI-80 and proceeded to the AWT-26/P1 and P2. Extensive results, which were obtained for each machine, are described in greater detail below.

An outline of the ADAMS model of the AWT-26/P2 is shown in Figure 7-2. The tower was idealized as eight rigid parts connected by "beam" elastic springs. The mainframe/drivetrain was modeled by three parts (corresponding to the generator, the gearbox/yaw bearing, and the main bearings), and by a rotating low-speed shaft. The rotor was modeled as a central hub (with teeter pin connection to the shaft) and elastic connections to the blade roots; the blades were modeled as eight parts and beam connections with an additional tip mass corresponding to the tip brakes.

7.2 Modal Tests

Modal tests were carried out on the isolated blade structure and on the complete P1 and P2 machines.

7.2.1 Blade Modal Tests

In May 1993, a blade from the ESI-80 retrofit project was transferred to the NREL structural test facility at the National Wind Technology Center, where it was instrumented and attached to a rigid support. A number of modal tests were conducted with tip vanes of differing masses and with different mass offsets. The purpose of these tests was to determine the physical characteristics of the isolated blade to confirm that part of the total ADAMS model. Some of the results of the tests are given in Table 7-1. More detailed results are available in Reference 7.

Table 7-1. Results of Modal Tests on Isolated Blade

	Tip Mass = 0		Tip Mass = 15.7 kg	
Mode	Test	ADAMS*	Test	ADAMS*
	(Hz)	(Hz)	(Hz)	(Hz)
1 flap	2.81	2.79	2.29	2.31
1 edge	7.68	7.81	6.38	6.47
2 flap	9.18	8.81	7.47	7.36

* ADAMS results were obtained using RLA's configuration BLADE21

Considerable coupling between the flapwise and edgewise bending was observed, especially in the "1 edge" and "2 flap" modes. This was due to the spanwise twist of the principal axes of the cross section. This twist was adjusted to improve the agreement between ADAMS/linear and the test results. The test results also allowed some adjustments to be made to the flap-wise and edge-wise stiffnesses used in the ADAMS and Algor models.

The effect of tip mass eccentricity appeared to be small with little coupling between either edge or flap bending with torsion.

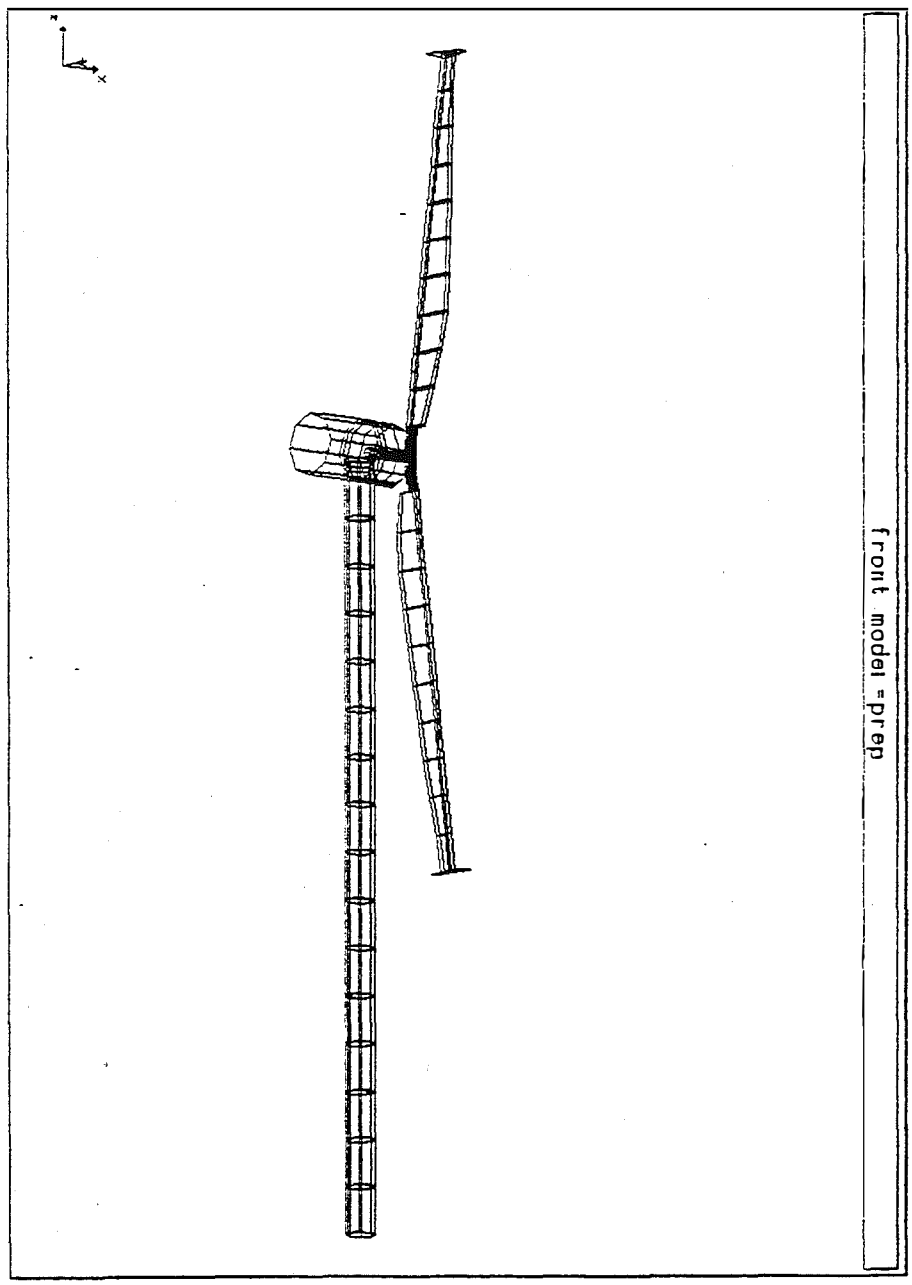

Figure 7-2. ADAMS idealization of AWT-26/P2

7.2.2 AWT-26/P1

Specialized Testing Services (STS) of Arleta, California, was contracted to carry out modal tests on the AWT-26/P1. Tests were performed on the rotor and nacelle in the Tacoma, Washington plant of Jesse Engineering in January 1993. Tests on the complete wind turbine were carried out in April 1993.

The results of these tests were not entirely satisfactory. While the natural frequencies of the fundamental modes were identified, there was ambiguity about the modes involving blade edgewise symmetric motion. The latter were considered important in the response of this machine.

In November 1993 a more complete modal survey was carried out by R. Osgood using specially designed equipment from NREL. Blades, drivetrain and tower were instrumented and a known excitation was applied to the tower and to the nacelle. This was done with blades vertical and with blades horizontal. Some of the results are given in Table 7-2. More detailed results are in Reference 5.

7.2.3 AWT-26/P2

In December 1993 modal tests similar to those performed on P1 were performed by R. Osgood of NREL on the AWT-26/P2. The results and comparison with the current ADAMS model are given in Table 7-3. More detailed results are in Reference 6.

Table 7-2. Comparison of AWT-26/P1 Modal Tests and ADAMS Predictions

	Blades Horizontal		Blades Vertical	
Mode	Modal test	ADAMS	Modal test	ADAMS
1 tower fore-aft	1.12 Hz	1.09 Hz	1.12 Hz	1.09 Hz
1 tower lateral	1.18	1.12	1.25	1.12
1 flap symmetric	2.44	2.35	2.44	2.35
flap asym + nacelle			5.42	4.68
1 edge symmetric	4.30	4.08	6.56	6.58
2 flap symmetric	7.23	7.25	7.23	7.26
1 edge sym-nacelle	7.40	7.40		
2 tower lateral	8.64	9.57	8.73	9.63

[ADAMS configuration used: PREP45]

Table 7-3. Comparison of AWT-26/P2 Modal Tests and ADAMS Predictions

	Blades Horizontal		Blades Vertical	
Mode	Modal Test	ADAMS	Modal Test	ADAMS
1 tower fore-aft	1.05 Hz	1.02 Hz	1.03 Hz	1.02 Hz
1 tower lateral	1.16		1.15	
1 flap symmetric	2.44	2.49	2.42	2.48
flap asym+nacelle			5.42	4.68
1 edge symmetric	5.18	5.20	7.05	7.65
2 flap symmetric	7.16	7.09	7.10	7.11
1 edge sym-nacelle	7.80	7.99		
2 tower lateral	8.25	8.41	8.00	8.41

[ADAMS configuration used: P2_39]

To obtain the above ADAMS/linear results, the following modifications were made to the initial model of the P2 wind turbine.

1. The elastic modulus of the blade was reduced by 5%.

2. The edgewise section moments of inertia of the blade were reduced by 5%.

3. The edgewise section moments of inertia of the hub and blade root were reduced by 20%.

4. The stiffness of the drive and mainframe was reduced by 10%.

5. The mass moment of inertia of the nacelle/drivetrain was increased by 20%.

6. A torsional spring of 90E6 N·m/radian was introduced at the yaw bearing.

It was noted that agreement between the tests and ADAMS predictions was better when the blades were horizontal, and also when the mode did not involve motion at either the yaw or the teeter bearings. One explanation might be that the motion during the tests was influenced by friction in those bearings.

7.3 Simulation of Operating Response

This subsection documents some of the progress in simulating the response of the AWT-26/P1 and (mainly) P2 prototypes using ADAMS. Further documentation can be found in Malcolm and Wright (Reference 1), and Wright, Osgood and Malcolm (Reference 2).

7.3.1 AWT-26/P1

Both the retrofitted ESI-80 and the AWT-26/P1 exhibited a 7P response in the blade edgewise symmetric bending. Efforts made to simulate this response were met with limited success. It was found that only when the tower shadow deficit was increased to 50% did the simulation come close to the field data.

Figures 7-3 through 7-6 compare measured and predicted power spectral densities (PSD) for both flap and edge bending moments. Whereas there is good agreement for the flap bending, the measured edgewise response at 7P is underpredicted by the ADAMS model.

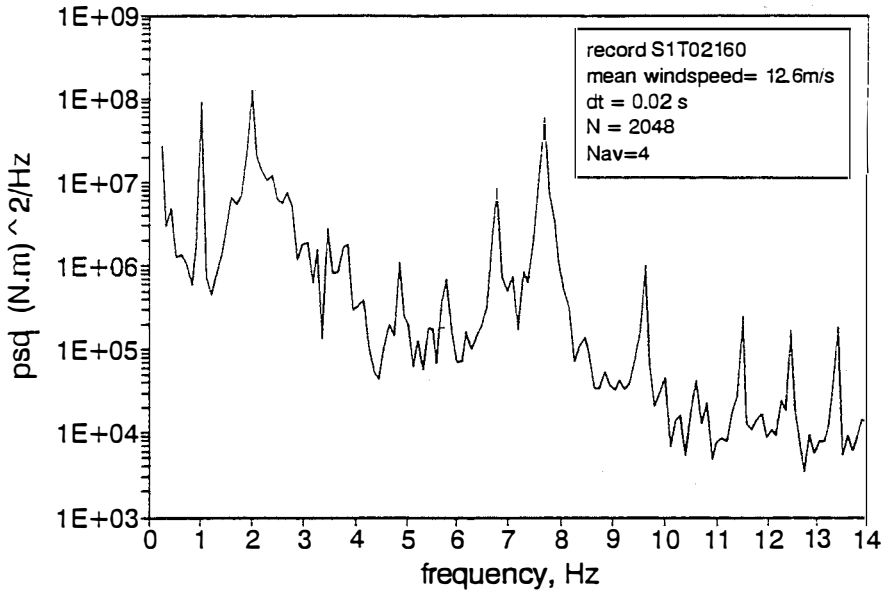

Figure 7-3. Measured PSD of root flap bending from AWT-26/P1

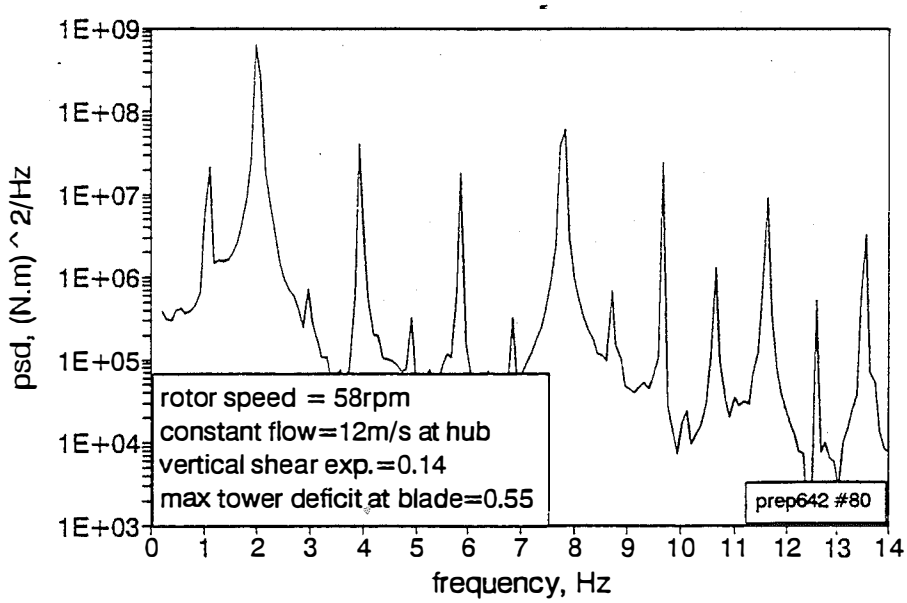

Figure 7-4. ADAMS prediction of PSD of root flap bending for AWT-26/P1

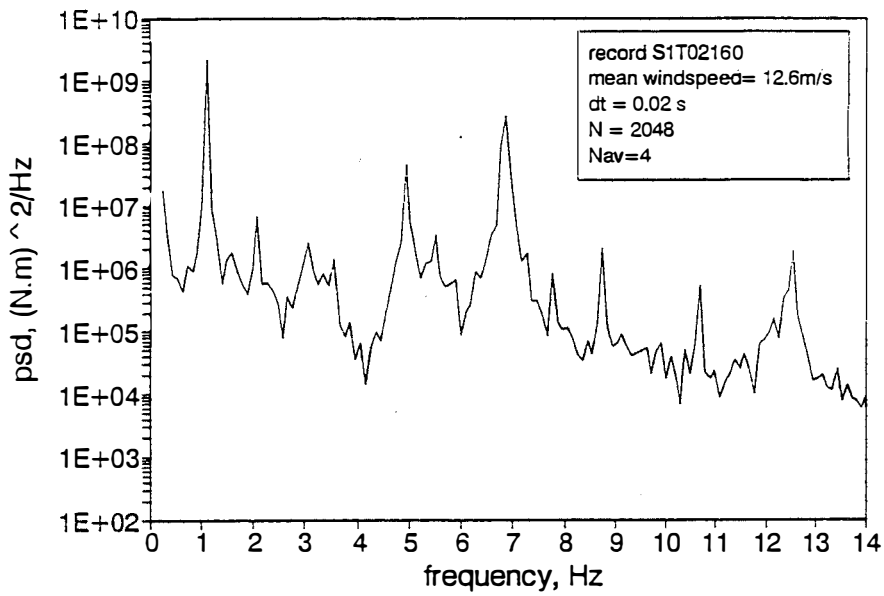

Figure 7-5. Measured PSD of root edge bending from AWT-26/P1

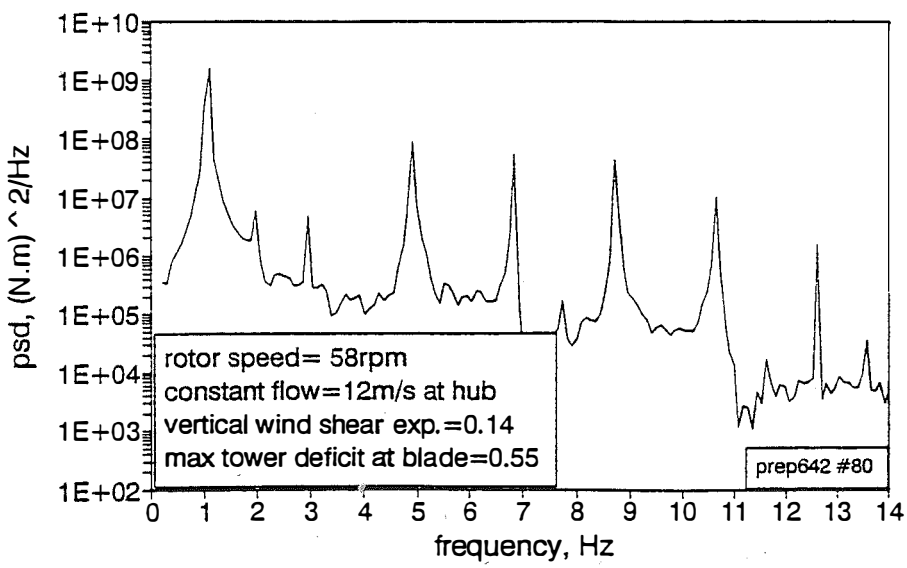

Figure 7-6. ADAMS prediction of PSD of root edge bending for AWT-26/P1

The ADAMS prediction of edgewise response at 7P improved considerably if the bending stiffness of the upper one third of the tower was halved (see Reference 2). This adjustment also brought the ADAMS/linear prediction of the "1 edge symmetric-nacelle" static natural frequency into better agreement with the modal test data (see Section 7.2.1). While this finding is significant, it suggests that the modeling of the tower properties is not fully understood.

7.3.2 AWT-26/P2

The dynamic response of the P2 prototype was, in general, more benign than that of P1. The response in edgewise bending at 5P and 7P was much less pronounced. The reasons for this were considered to be the reduced tower shadow (from the tube in place of the 4-sided truss) and the different structural characteristics of the tower, mainframe, and low-speed shaft.

Figures 7-7 and 7-8 show both measured and predicted results for flap and edge bending in a hub-height wind speed of 12 m/s. Both sets of data have been azimuth averaged so that only the deterministic parts are included. Also included in these figures is the corresponding aerodynamic loading; the ratio of the response to the loading is a measure of the dynamic amplification at each frequency.

Figure 7-9 plots the predicted edgewise harmonic responses against increasing rotor speed. This helps to identify rotor speeds that may correspond to a resonant condition. According to the model, it appears that resonance will peak at rotor speeds of 55 rpm or 65 rpm.

Information on these resonant conditions was also obtained by the application of an impulse to the ADAMS model and by analyzing the subsequent free motion (see Reference 1). Results are shown in Figure 7-10 which indicates the several series of natural frequencies that exist for this machine. A comparison of Figure 7-10, and some of the non-harmonic peaks in the field data from P2 is given in Table 7-4.

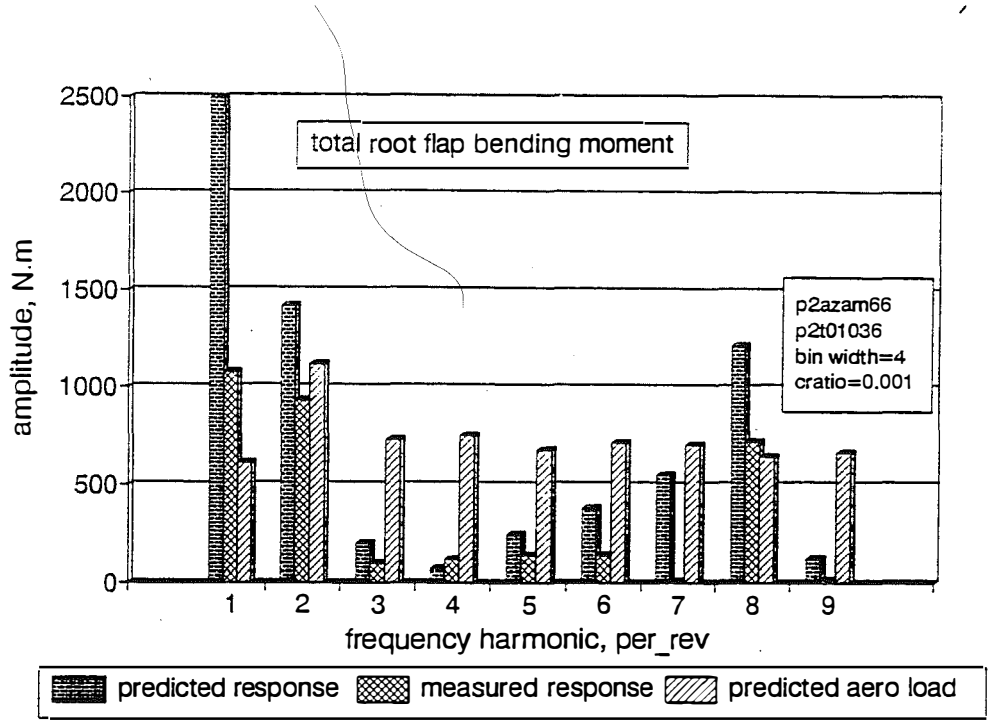

Figure 7-7. Measured and predicted flap bending harmonics for AWT-26/P2

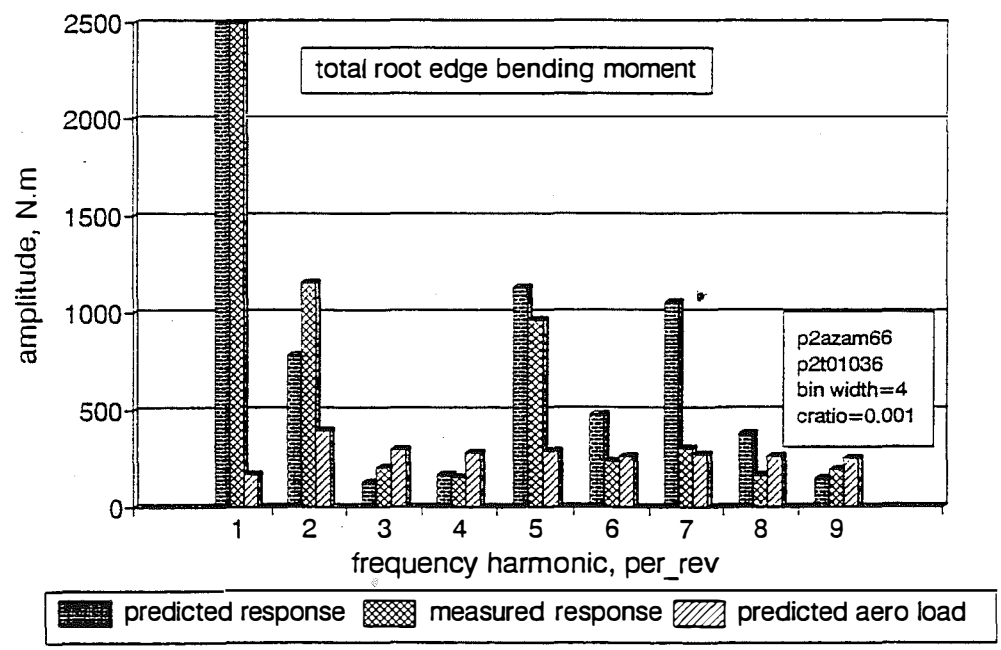

Figure 7-8. Measured and predicted edge bending harmonics for AWT-26/P2

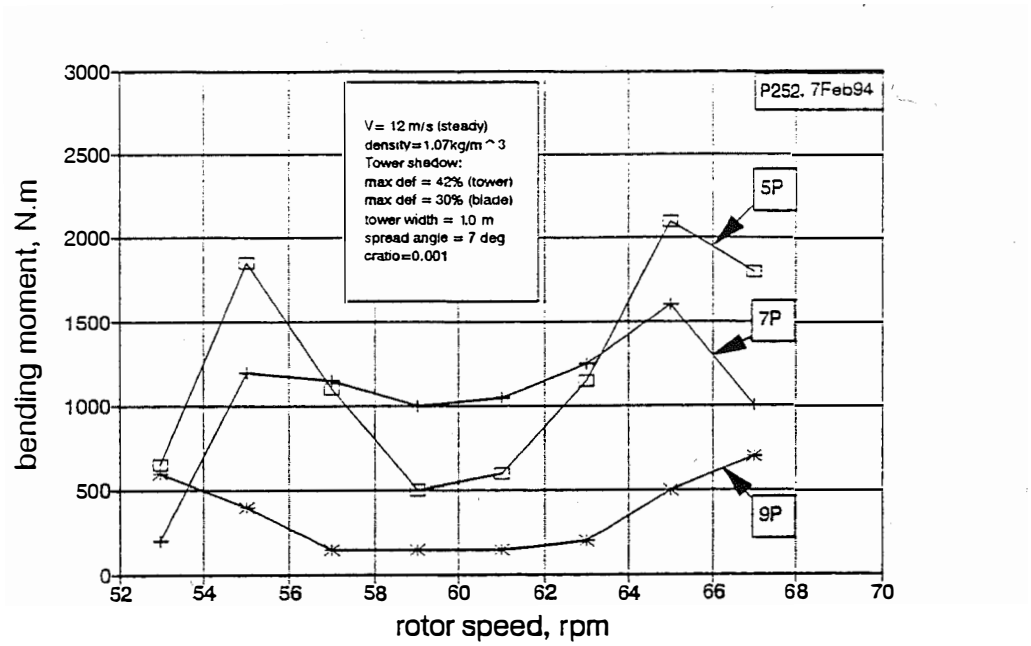

Figure 7-9. AWT-26/P2: predicted edgewise harmonic response versus rotor speed

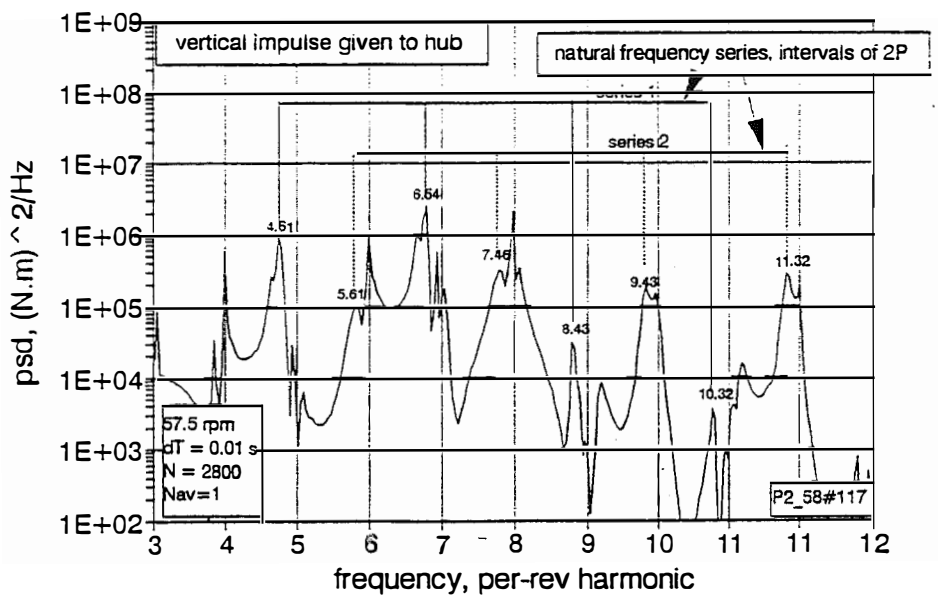

Figure 7-10. AWT-26/P2: predicted PSD of edgewise bending in free motion of moving rotor

Table 7-4. Operating Natural Frequency Predictions; ADAMS versus Field Data

	Edgewise Series 1		Edgewise Series 2	
	Field Data[1]	ADAMS[2]	Field Data[1]	ADAMS[2]
	4.21 Hz	4.61 Hz	5.43 Hz	5.78 Hz
	6.13	6.54	7.31	7.68
	8.03	8.43	9.23	9.58

Mode	Field Data	ADAMS[2]
1 tower	1.15 Hz	1.04 HZ
1 flap symmetric		2.79
2 flap symmetric		7.35

Note: (1) field data file: P2T01048.C
(2) ADAMS model: P2_58, run #117, April 12 '94

The simulation of the response of the AWT-26/P2 in turbulent winds was also investigated. Full field models of turbulent winds corresponding to Kaimal turbulence and also a more vigorous "San Gorgonio" environment were obtained from NREL. Most effort was directed at the San Gorgonio environment because results from that model were more likely to lead to critical fatigue and peak loads. Many numerical difficulties were encountered in that simulation; therefore, it has not been completed.

The attempts at simulation of the structural and aerodynamic response of the complete wind turbine have not yet been entirely satisfactory. One deficiency appears to be the discrepancy between the predicted natural frequencies and those indicated by field data. This is probably the cause of the under-prediction of the response of the AWT-26/P1. Another deficiency is the inability to use the ADAMS code to simulate a period of 10 minutes of operation in an extremely turbulent environment. Future releases of the code, faster computers, and more skillful application may correct this.

For the reasons given above, the simulation with ADAMS has not been incorporated directly into the design process. It has been considered more reliable to use the structural loads obtained from prototype field data.

8.0 Reliability And Maintainability

8.1 ESI-80 vs. AWT-26 Designs

Task 1.0 of the subcontract required the subcontractor (RLA) to analyze the ESI-80 wind turbine, to identify any problems associated with the machine, and to suggest solutions to those problems. This work has been documented in other reports, and will only be summarized in this section. The main objective of this section of the report is to show how each of the ESI-80 problems was addressed in the final design of the AWT-26.

The ESI-80 wind turbine had several dynamics, control, and hardware design problems. These are discussed below with an explanation of how each problem was addressed in the AWT-26 design.

8.1.1 Dynamics Problems

The ESI-80 had a random teeter/yaw instability during start-up. It was believed that this instability was the result of a start-up sequence that was too slow, allowing the machine to remain too long at a rotational speed at which this instability could occur. This resulted from the lack of aerodynamic damping during start-up and, perhaps, from insufficient teeter damping. The AWT-26 employs a much faster start-up sequence that enables the rotor to pass quickly through any potentially unstable rotation speeds and also results in greater aerodynamic damping. In addition, the AWT-26 teeter dampers have more damping than the ESI-80 dampers. These solutions have proven successful, and there has never been an instability during the hundreds of start-ups of the AWT-26 production prototypes.

The ESI-80 exhibited a 7P blade edgewise response also noticed in the AWT-26/P1 prototype. This issue is discussed in Section 6.3 of this report. The 7P response was reduced to acceptable levels in both the P1 and P2 prototypes by changing the nature of the tower shadow. Other factors that may have helped were the reduction of the tip brakes mass from the original 43 lbs (20 kg) to approximately 25 lbs (11.3 kg), and the increase in the coupling between the flap and edgewise blade motion.

8.1.2 Control Problems

The ESI-80 used two different controllers, one from American High Tech and an alternate from Second Wind, the Alpha 7. Both were unreliable, poorly documented, relatively inflexible, and provided poor control during connection of the wind turbine's generator to the grid. The AWT-26 uses a modified industrial PLC furnished by Eaton, Cutler-Hammer. The AWT control system was designed with the following fail-safe features:

- Tip brakes and mechanical brakes are powered in "off" position (i.e., loss of power activates brakes).
- All wiring is such that no signal is an alarm or shutdown.
- All relays are energized to operate; nonoperation is an alarm or shutdown.
- All critical functions are monitored for "state"; improper state results in alarm or shutdown.
- Analog signals out of range result in alarm or shutdown.

The connection of the ESI-80 to the utility grid was poorly managed, causing large torque transients to pass through the drivetrain. The AWT-26 employs a "soft-start", SCR-controlled connection to the utility line that minimizes such transients.

8.1.3 Hardware Problems

The ESI-80 had a number of hardware problems that were addressed in the AWT-26 design in the following ways.

Tip brake mechanism failures	Mechanism redesigned and new dampers used in place of unreliable ones used on the ESI-80.
Premature wear of rotor teeter bearings	The AWT-26 teeter system design increases the bearing surface area by 68% and increases the moment arm by 33%.
Teeter damper failures	The teeter dampers used for the AWT-26 have been designed by Enidine, a highly respected name in the specialty damper industry in the United States. There have been no problems with these dampers in service on the two production prototypes. A back up teeter damper, proven in many years of service on a competitor's wind turbine, has also been adapted for use on the AWT-26 in the event the current dampers have life problems.
Rotor slip rings failures	The AWT-26 uses a redesigned slip ring configuration, includes a weather cover, and has a redundant ring should there be a ring failure.
Gearbox failures and wear	The ESI-80 used a ball bearing in the upwind output shaft bearing that had limited radial capacity. This bearing was replaced with a roller bearing recommended by the subcontractor and there have been no further failures. The AWT-26 uses a gearbox that is rated at 180% of the ESI-80 gearbox, yet the loads have been increased by only 10 -- 15%. In addition, a consultant analyzed the life of all critical gears and bearings, and as a result, the gearbox supplier was required to increase the quality of several bearings in the gearbox.
High-speed brake high maintenance	The high-speed brake on the ESI-80, located on the upwind side of the generator, was pneumatically activated and employed multiple discs operated like a clutch. The AWT-26 mechanical brake is located on the downwind side of the high-speed coupler, and is a conventional disc-caliper system activated by a conventional hydraulic system.

Yaw bearing wear	The yaw bearing on the ESI-80 exhibited excessive wear. Investigation revealed that the bearings were not adequately maintained. After satisfactory maintenance procedures were implemented, no further wear occurred. Nevertheless, the AWT-26 yaw bearing is rated approximately 40% higher than the ESI-80 yaw bearing.
Tower loose bolts and cracks	The AWT-26/P2 tubular tower does not have the fasteners that were a problem in the ESI-80 truss towers. For machines that do incorporate a truss tower, all welding should be avoided and fasteners should be of the direct tension type
Controller failures	The AWT-26 uses a standard, rugged industrial controller in place of the custom units used on the ESI-80 wind turbines.

8.2 Failure Mode and Effects Analysis

A failure model and effects analysis (FMEA) was conducted for all of the components used in the AWT-26 wind turbine. The FMEA considered the impact on the system of all possible failure modes of each device. If the effect on the system was undesirable (e.g., was dangerous to personnel or caused secondary, costly failures), remedial design action was taken. An example of an FMEA is shown in Figure 8-1. Approximately 500 of these FMEAs were performed for the AWT-26. The analyses resulted in approximately 50 design changes, including the identification and correction of ten previously unidentified failure modes.

More information on and examples of the FMEA are given in the System Design Review Package.

8.3 Reliability and Maintainability Analysis

A detailed analysis of the expected reliability and maintainability costs for the AWT-26 was conducted and maintained throughout the design and development program. Table 8-1 shows the results of the most recent reliability and maintainability analysis. This analysis assumes that the wind turbines are deployed in a 50-MW wind power station. No second shift or weekend maintenance coverage is assumed in the analyses. The scheduled annual maintenance costs are shown in Table 8-2.

Table 8-3 shows the total projected scheduled and unscheduled annual maintenance costs of $4,513 per wind turbine. This projection may be conservative for a wind turbine with the simplicity of the AWT-26, but until more field experience is accumulated, these numbers will be used for all cost-of-energy calculations. Table 8-3 also shows the estimated annual machine downtime for both the scheduled and unscheduled maintenance. The downtime of approximately 110 hours per year yields a projected machine availability of approximately 99%. This projection is for a mature system (i.e., at least one full year of operation and no generic problems) and assumes that adequate logistics support is available.

Table 8-4 shows the projected number of spares required for wind power stations of various sizes. These numbers are used for the computations of the costs of energy.

AWT-26 Failure Modes and Effects Analysis

Subsystem:	Rotor		
Component:	Tip Brake Hinge Pin		Sht. 1 of 1
Reference Drawing #:	6063200	REV: Ø	FMEA Revision: A

Function: Tip vane pivot point.

Failure Mode: Pin shears or breaks.

Wind Turbine Response and Failure Detection Method:

STBY: None.

START: Vane is flung off, possible excessive vibration shutdown. If excess vibration occures the controller will trip to an excessive vibration failure to fast shutdown to lockout. With only one tip left, an incomplete fast stop sequence fault will also occur.

OPER: Vane is flung off, possible excessive vibration shutdown. If excess vibration occures the controller will trip to an excessive vibration failure to fast shutdown to lockout. With only one tip left, an incomplete fast stop sequence fault will also occur.

SHDN: With one tip flung from turbine, shutdown(with remaining tip) will require more than 15 sec. for most wind speeds, this will cause a lock out condition with an "incomplete normal stop sequence" error message. Excess vibrations may also occur.

LOCK: None.

Consequences of Undetected Failures: Once the pin is broken, the vane may survive some run time before it is flung from the rotor, but the vane will eventually separate.

Corrective Action Required: None

Comments: Semi-annual inspection of the hinge mechanism for excessive slop will reveal any fretting that could lead to failure of the hinge pin.

Reviewed by: Systems Engineer: [signature] Date: 12/13/93

Design Engineer: Richard Scott Date: 12/13/93

Correction Incorporated on Drawing #s:

By:

Date:

Systems Engineer:

Date: File Name/Disk: RB0031.doc

Figure 8-1. Example of failure modes and effects analysis

Table 8-1. AWT-26 Reliability and Maintainability Summary

SYSTEM, SUBSYSTEM, PART	NO. OF FAILURES PER YEAR	DOWN TIME PER FAILURE (HOURS)	DOWN-TIME PER YEAR (HOURS)	REPAIR TIME PER FAILURE (M. HRS.)	HOURS PER YEAR	ANNUAL LABOR COST	REPAIR OR REPLACEMENT COST (INCL. CRANE) ITEM	REPAIR OR REPLACEMENT COST (INCL. CRANE) ANNUAL	TOTAL ANNUAL COST
ROTOR	1.21	—	18.8	—	4.9	$146	—	$1,185	$1,331
BLADES (2)	0.10	31.0	3.1	11.0	1.1	$33	$7,500	$750	$783
TIP BRAKE ASS'Y (2)	0.51	—	14.0	—	1.31	$39	—	$117	$156
BLADE PLATE	0.07	28.0	2.0	4.0	0.3	$8	$360	$25	$34
VANE	0.05	28.0	1.4	3.0	0.2	$5	$400	$20	$25
BRACKETS/FASTENERS	0.10	28.0	2.8	3.0	0.3	$9	$337	$34	$43
PIN	0.02	27.0	0.5	2.0	0.0	$1	$130	$3	$4
SPRINGS	0.02	27.0	0.5	2.0	0.0	$1	$130	$3	$4
DAMPERS	0.25	27.0	6.8	2.0	0.5	$15	$130	$33	$48
TEETERING HUB	0.50	—	1.8	—	2.2	$65	—	$286	$351
ROTOR HUB	0.05	35.0	1.8	9.0	0.5	$14	$2,275	$114	$127
TEETER DAMPERS (2)	0.20	SCHED.	0.0	6.0	1.2	$36	$600	$120	$156
TEETER BEARING ASSEMBLY	0.25	—	0.0	—	0.5	$15	—	$53	$68
BUSHINGS (2)	0.20	SCHED.	0.0	2.0	0.4	$12	$120	$43	$55
HOUSING/FASTENERS	0.05	SCHED.	0.0	2.0	0.1	$3	$200	$10	$13
SLIP RINGS	0.10	SCHED.	0.0	3.0	0.3	$9	$325	$33	$42
DRIVE TRAIN	1.01	—	27.0	—	5.1	$154	—	$1,212	$1,366
GEARBOX & BEARINGS	0.05	33.0	1.7	7.0	0.4	$11	$14,950	$748	$758
GEARBOX OIL SENSOR	0.10	28.0	2.8	5.0	0.5	$15	$50	$5	$20
COUPLING	0.15	29.0	4.4	5.0	0.8	$23	$513	$77	$99
GENERATOR	0.08	28.0	2.1	5.0	0.4	$11	$4,113	$308	$320
BRAKE	0.63	—	16.1	—	3.2	$95	—	$74	$169
BRAKE MECHANISMS	0.16	26.0	4.2	5.0	0.8	$24	$256	$41	$65
POWER UNIT	0.18	26.0	4.7	5.0	0.9	$27	$120	$22	$49
CONTROL VALVE	0.08	25.0	2.0	5.0	0.4	$12	$65	$5	$17
FILTER	0.01	25.0	0.3	5.0	0.1	$2	$15	$0	$2
PRESSURE SWITCHES (2)	0.10	25.0	2.5	5.0	0.5	$15	$40	$4	$19
CHECK VALVE	0.05	25.0	1.3	5.0	0.3	$8	$40	$2	$10
HOSES, CONNECTORS	0.05	25.0	1.3	5.0	0.3	$8	$10	$1	$8
STRUCTURE	0.24	—	6.0	—	2.1	$64	—	$101	$165
MAINFRAME	0.05	29.0	1.5	5.0	0.3	$8	$165	$8	$16
TOWER TOP PLATE	0.05	29.0	1.5	5.0	0.3	$8	$165	$8	$16
YAW BEARING	0.08	34.0	1.4	17.0	1.3	$38	$1,106	$83	$121
TOWER	0.06	—	1.7	—	0.4	$11	—	$2	$13
TOWER SECTION BOLTS	0.03	28.0	0.8	6.0	0.2	$5	$30	$1	$6
BOLTS	0.03	28.0	0.8	6.0	0.2	$5	$30	$1	$6
CONTROLS/ELECTRICAL	1.70	—	39.4	—	11.9	$357	—	$334	$691
SENSORS	0.50	23.0	11.5	4.0	2.0	$60	$200	$60	$120
CABLES, CONNECTORS, ETC	0.50	24.0	12.0	3.0	8.0	$240	$60	$120	$360
ELECTRICAL CONTROLS	0.50	23.0	11.5	3.0	1.5	$45	$200	$100	$145
PROGRAMMABLE CONTROLLER	0.20	22.0	4.4	2.0	0.4	$12	$270	$54	$66
TOTAL WTG	4.15		91.2		24.0	$721		$2,833	$3,553

Notes:
1. Down time includes logistics delays (no second shift, holidays, etc.)
2. Repair times includes items replaced while performing other maintenance.

awtr&m.wq1

Table 8-2. AWT-26 Scheduled Maintenance Costs

ASSEMBLY/COMPONENT	Times per yr.	Manhours per Event	Materials Cost/even	Annual Cost	Maintenance Action
Blades	2	0.5	$20	$70	Inspect, touch up scratches.
Tip Brakes	2	0.5	$5	$40	Inspect, replace hardware.
Hub Structure-Machined	2	0.1	$0	$6	Inspect for cracks.
Damper Assembly	2	0.1	$0	$6	Inspect for leaks.
Teeter Shaft, Bushings	2	0.3	$20	$58	Inspect, replace bushings if required.
Disc and Brake Calipers	2	0.5	$40	$110	Inspect disc wear and check operation.
Bracket Assy, Brake Support	2	0.1	$0	$6	Inspect for cracks.
Brake Pressure System	2	0.3	$25	$68	Inspect for leaks, repair as required.
Gearbox	2	0.3	$40	$95	Inspect, check magnetic plug, run oil sample.
Gearbox Oil	0.25	2.0	$220	$70	Change oil (synthetic).
Gearbox Oil Filter	2	0.3	$5	$28	Inspect, replace annually.
High Speed Coupling	2	0.3	$0	$1	Check for wear and alignment.
Mainframe, Decks	2	0.3	$0	$18	Check for cracks.
Yaw Bearing	2	0.3	$5	$28	Service; check for wear.
Yaw Unwind System	2	0.1	$0	$6	Check for proper operation.
Nacelle Cover	2	0.2	$5	$22	Check operation; replace hardware if required.
Lightening Protection	2	0.2	$8	$28	Check condition of all devices.
Generator	2	0.2	$5	$22	Check for cracks and service bearings.
Power and Control Cables	2	0.2	$0	$12	Checks condition.
Slip Rings	2	0.3	$20	$58	Check brushes; change annually.
Programmable Controller	2	0.5	$0	$30	Check all functions.
Anemometer	1	1.0	$40	$70	Replace and calibrate in shop.
Vibration Switch	2	0.3	$0	$18	Check operation by moving from mounting.
Tower and Tower Top Plate	2	1.0	$0	$60	Check for cracks.
Saftey Cable, Steps, Brackets	2	0.4	$0	$24	Check all fittings and general condition.
Foundation	2	0.1	$0	$6	Check for cracks.
Total				$960	

Table 8-3. Total Annual Maintenance Costs and Downtime

Wind Turbine Subsystem	Number of Failures Per Year	Annual Maintenance Costs/WT ($)	Downtime Per Year (Hours)
Rotor	1.21	1,331	19
Drivetrain	1.01	1,366	27
Structure	0.24	165	6
Controls and Electrical	1.70	691	39
Total WTG	4.15	3,553	91
Scheduled Maintenance and Downtime		960	17
Total Maintenance and Downtime		4,513	108

Table 8-4. Spare Parts Requirements

SYSTEM, SUBSYSTEM, PART	Number Used per Wind Turbine	Cost per Item (1994$)	Number of Initial Spares: Number of Wind Turbines in Wind Power Station				Total Cost of Spares (1994$): Number of Wind Turbines in Wind Power Station			
			20-30	31-60	61-100	101-200	20-30	31-60	61-100	101-200
ROTOR										
BLADES	2	$10,125	2	3	4	6	$20,250	$30,375	$40,500	$60,750
TIP BRAKE ASS'Y	2									
HINGE	2	$115	2	3	4	6	$230	$345	$460	$690
BASEPLATE	2	$165	2	3	4	6	$330	$495	$660	$990
VANE	2	$311	2	3	4	6	$621	$932	$1,242	$1,863
MISC. HARDWARE KIT	2	$150	1	2	3	5	$150	$300	$450	$750
DAMPER	2	$150	4	6	8	10	$600	$900	$1,200	$1,500
TEETERING HUB	1									
ROTOR HUB	1	$2,430	1	2	3	5	$2,430	$4,860	$7,290	$12,150
TEETER DAMPER	2	$1,350	4	6	8	12	$5,400	$8,100	$10,800	$16,200
TEETER BEARING ASSEMBLY	1									
BUSHINGS	2	$110	4	6	8	12	$440	$660	$880	$1,320
THRUST BEARING	2	$20	4	6	8	12	$81	$122	$162	$243
TEETER SHAFT	1	$570	1	2	2	4	$570	$1,140	$1,140	$2,280
HOUSING/FASTENERS	2	$110	1	2	2	4	$110	$220	$220	$440
SLIP RINGS	1	$480	2	3	4	6	$960	$1,440	$1,920	$2,860
DRIVE TRAIN	1									
GEARBOX	1	$31,050	1	2	2	4	$31,050	$62,100	$62,100	$124,200
GEARBOX LUBRICATION SYSTEM	1	$400	2	3	4	6	$800	$1,200	$1,600	$2,400
HIGH & LOW SPEED SEALS	2	$600	3	4	5	7	$1,800	$2,400	$3,000	$4,200
COUPLING	1	$700	2	3	4	6	$1,400	$2,100	$2,800	$4,200
COUPLING REBUILD KIT	1	$50	3	4	5	8	$150	$200	$250	$400
GENERATOR	1	$9,500	1	2	2	4	$9,500	$19,000	$19,000	$38,000
BRAKE	1									
BRAKE CALIPERS	2	$743	4	6	8	12	$2,970	$4,455	$5,940	$8,910
REBUILD KIT AND PADS	1	$300	2	3	4	6	$600	$900	$1,200	$1,800
CONTROL AND CHECK VALVES	1	$150	2	3	4	6	$300	$450	$600	$900
FILTER	1	$5	2	3	4	6	$10	$15	$20	$30
MOTOR AND PUMP	1	$440	2	3	4	6	$880	$1,320	$1,760	$2,641
HOSES, CONNECTORS	1	$150	1	2	3	6	$150	$300	$450	$900
STRUCTURE	1									
MAINFRAME	1	$2,835	0	0	1	2	$0	$0	$2,835	$5,670
NACELLE HARDWARE KIT	1	$250	1	1	2	3	$250	$250	$500	$750
TOWER TOP PLATE	1	$1,200	1	1	2	3	$1,200	$1,200	$2,400	$3,600
YAW BEARING	1	$1,485	1	2	3	5	$1,485	$2,970	$4,455	$7,425
TOWER AND WORK PLATFORM KIT	1	$600	1	1	2	3	$600	$600	$1,200	$1,800
CONTROLS/ELECTRICAL										
SENSORS, KIT OF ALL SENSORS	1	$800	2	3	4	6	$1,600	$2,400	$3,200	$4,800
DROOP CABLE	1	$2,450	1	2	3	4	$2,450	$4,900	$7,350	$9,800
ELECTRICAL CONTROLS KIT	1	$4,000	2	2	2	4	$8,000	$8,000	$8,000	$16,000
POWER ELECTRONICS KIT	1	$2,500	1	2	2	4	$2,500	$5,000	$5,000	$10,000
NACELLE CONTROLLER	1	$3,000	1	2	3	4	$3,000	$6,000	$9,000	$12,000
CONTROL HOUSE CONTROLLER	1	$4,000	1	2	2	3	$4,000	$8,000	$8,000	$12,000
TOTAL WTG	n/a	n/a	n/a	n/a	n/a	n/a	$108,867	$183,648	$217,584	$374,482

Includes handling, shipping, and manufacturer's margin.

9.0 Manufacturing And Commercialization Plans

9.1 Manufacturing Plans

As part of the subcontract, The Pinnacle Consulting Group, Inc., prepared a manufacturing plan for the AWT-26, assuming an annual production rate of 400 wind turbines. This plan is available at the subcontractor's facilities. The floor space required for the blade manufacturing operations, including materials storage and other ancillary space requirements, is approximately 25,000 square feet (2,320 m^2). Four production blade molds are required to produce two sets of blades per working day. The blades are balanced in this facility. Approximately 240 person-hours of labor are required per set of blades. Blade tooling not currently available will cost approximately $300,000.

All of the wind turbine components are purchased ready for assembly (i.e., no machining or painting is required). The wind turbine assembly area will require an additional 20,000 square feet (1,860 m^2). Six stations are used for the assembly (i.e., six machines are being assembled simultaneously), and assembly and testing require approximately 60 person-hours. A "slave" electrical and control panel is used for final checkout and testing. The facility requires a 200-ampere, 480-volt service for generator run-up and balancing tests.

The manufacturing facility will employ approximately 60 direct manufacturing personnel. Quality control, purchasing, engineering liaison, and other support services will add an additional 20 -- 25 people, for a total of 80 -- 85 people.

The tower and the electrical and control panel are both shipped directly to the wind power station site. As noted above, a slave electrical and control panel is used during the checkout and testing of the wind turbine at the manufacturing facility to minimize field reworks.

9.2 Modifications for Production

The configuration of the P2B production prototype closely approximates the final production configuration. Anticipated changes are:

- use of an enlarged nacelle and elimination of the work platform;
- value-engineered tip mechanisms that incorporate the two springs and the damper into an integral unit. This also includes a modified hinge plate to distribute the loads over a wider area;
- value-engineered teeter pin and bearings that substantially reduce the machining of the teeter pin;
- modified mechanical brake brackets to allow mounting the calipers opposite each other for improved load distribution;
- cast gearbox snout in place of the current manufactured snout;
- integral brake disc/coupler casting; and
- cast tower top plate.

Most of these changes have already been factored into the component cost estimates used in the cost of energy analysis.

9.3 Production Costs

The wind turbine component costs have been obtained from suppliers in quantities of 100 units. The individual component costs are confidential and are available for NREL's review at the subcontractor's facilities. The total component cost, less the tower, is approximately $95,000, including the blades. A 140-ft (42.6 m) guyed tubular tower costs approximately $28,000. These figures have been used to compute the cost of energy using NREL's guidelines for general and administrative (G&A) and fee in January 1994 dollars. It should be noted that the actual G&A and fee that is prevalent in the industry for such operations is lower than anticipated by NREL. Therefore, the final production cost for the machines will be lower than that used in the cost-of-energy calculations.

9.4 Cost of Energy

The cost-of-energy calculations have been made using the costs discussed above, and the NREL criteria for the other cost elements. Table 9-2 shows the net energy production at the specified reference site (Rayleigh distribution, mean windspeed = 5.8 m/s at 10 m, vertical wind shear exponent = 0.14). The results and the secondary figures-of-merit-numbers are contained in Table 9-3.

The performance curve used to obtain the annual energy production was not exactly the same as that given in Figure 6-9 which refers to operation in the lower air density of Tehachapi (1.06 kg/m^3). Instead, sea level density (1.225 kg/m^3) has been used with an estimated adjustment for repitching the blades to limit the electrical power to the same maximum of 310 kW. The adjustment was obtained from tuning the PROP code (Reference 15) to duplicate the peak power of the Tehachapi site and observing what changes occurred when the density was increased and when the pitch was altered to return the peak power to 310 kW. This performance curve is defined in Table 9-1.

It should be noted that the performance curve defined in Table 9-1 is not identical to that shown in the available public literature where the maximum power is shown as 275 kW. The value of 275 kW is a nominal one only since the pitch setting can alter the peak power to anywhere in the range of 225 to 320 kW. The current performance curve, with a maximum value of 310 kW, does provide approximately the same energy capture as that shown in the public literature.

Table 9-1. Performance Curve Used for Final Cost-Of-Energy Calculation

Air density = sea level = 1.225 kg/m^3.
Mean windspeed at 10m = 5.8 m/s. Mean windspeed at hub height = 7.20 m/s (16.1 mph).

windspeed bin		hours/year	electrical power	annual energy
mph	m/s		kW	kWh
1	0.45	105.5	0	
3	1.34	309.0	0	0
5	2.24	490.7	0	0
7	3.13	638.9	0	0
9	4.02	745.7	3.4	2560
11	4.92	807.6	5.9	4765
13	5.81	825.5	14.0	11545
15	.6.71	804.1	30.9	24850
17	7.60	750.9	56.1	42117
19	8.49	675.1	85.7	57855
21	9.39	585.8	115.2	67491
23	10.28	491.7	144.6	71098
25	11.18	399.8	175.9	70344
27	12.07	315.3	204.0	64320
29	12.96	241.3	224.5	54185
31	13.86	179.5	241.9	43411
33	14.75	129.7	261.7	33954
35	15.65	91.2	276.4	25213
37	16.54	62.4	286.4	17867
39	17.43	41.5	297.8	12368
41	18.33	26.9	306.7	8254
43	19.22	17.0	307.7	5225
45	20.12	10.4	309.1	3229
47	21.01	6.2	302.7	1892
49	21.90	3.6	295.1	1076
		2.1	0	0
total		**8759.8**		**623,621**

Table 9-2. Summary of Annual Energy Production

Net Annual Energy Production (kWh/yr) -	COE Reference Site		
AEP	**95,425,230 (kWh/yr)**		
Annual Gross energy per turbine		623,621 kWh	
Number of turbines		182	
Total annual site gross production		**113,499,022 kWh**	
Losses			
Annual Availability (%)	98%	8,585 hours	
Hours Downtime		175 hours	
Percent Downtime (%)	2%	2,269,980 kWh	Standard Values
Blade soiling losses(%)	5%	5,561,452 kWh	5%
Array losses (%)	5%	5,283,379 kWh	5%
Electrical line losses (%)	2%	2,007,684 kWh	2%
Control & misc. losses (%)	3%	2,951,296 kWh	3%
Total losses per year		**18,073,792 kWh**	
Net annual energy production		**95,425,230 kWh**	

Table 9-3. Cost-of-Energy Summary

Turbine Type:	AWT-26		
Number of Turbines:	182		
Station capacity (MW):	50		
Site:	COE Reference Site		
Levelized Cost of Energy (COE)		**0.0514**	$/kWh
COE = $\frac{(FCR * ICC) + LCR + O\&M}{AEP_{net}}$			
Where: FCR	= Fixed Charge Rate	0.102	1/yr
ICC	= Initial Capital Cost	37,885,612	$
LRC	= Levelized Replacement Cost	90,485	$/yr
O&M	= Annual Operation and Maintenance Cost	954,252	$/yr
AEP_{net}	= Net Annual Energy Production	95,425,230	kWh/yr
Secondary Figures-of-Merit			
1.	AEP / Rotor Swept Area (Gross energy used)	**1157**	kWh/m^2
2.	AEP / System Weight (Gross energy used)	**37.1**	kWh/kg
3.	AEP /Tower Head Weight (Gross energy used)	**97.9**	kWh/kg
4.	System Cost / Rotor Swept Area	**288**	$/m^2
5.	System Cost / AEP (Gross energy used)	**0.2490**	$/kWh
6.	System Cost / System Weight	**9.2**	$/kg
7.	System Cost / Rated Power Output	**565**	$/kW
8.	Tower Head Cost / Tower Head Weight	**14.41**	$/kg
9.	Tower Cost / Tower Weight	**2.68**	$/kg
Station Configuration			
Station Capacity		50	MW
Number of turbines		182	
Array layout	Distance row-row	573	
	Distance side-side	72	m
	Number of turbines per row	13	
	Number of rows	14	
Turbine Parameters			
Turbine nominal capacity, each		275	kW
Rotor diameter		26.2	m
Swept area		539	m^2
Hub height		43	m

10.0 Conclusions

This project has successfully developed the prototypes of an advanced wind turbine for utility applications. The following general conclusions can be drawn from the program:

1. Cost of energy calculations (see Section 9.4) show that commercial versions of the AWT-26 will be able to meet the goal of producing electrical power at $0.05/kWh (1992 dollars).

2. Conservative design margins are necessary to address the uncertainties which continue to be inherent in wind turbine design.

3. In wind turbine architectures such as the AWT-26, system dynamics are significantly affected by seemingly small changes in system configuration. For example, a 7% change in the rotor speed or addition of strakes to a tubular tower can have significant impacts on the system behavior.

4. The dynamic analysis models currently available are developing into useful tools for system analysis; however, further work is needed before they can be readily used in the design process and relied upon as predictors of system dynamics.

5. The performance analysis tools available are reasonable predictors of actual turbine performance.

6. Reliable measurement of wind turbine performance is a very complex subject. Data from a performance measurement test program must be carefully evaluated prior to its use.

7. The use of load data from a relatively turbulent site with a dynamically active turbine will provide conservative design loads.

8. Development of a new turbine design is an iterative process requiring multiple prototype configurations and extensive testing, data analysis, and redesign. In addition, development of advanced turbine architecture leads to unanticipated problems in areas which are not a concern for other more traditional architectures.

It should also be noted that the program has successfully demonstrated the ability of the NREL staff to make significant contributions to the turbine design process.

11.0 References

1. Malcolm, D.J. and Wright, A.D., "The use of ADAMS to model the AWT-26 prototype," 13th ASME Wind Energy Symposium, Energy Sources Technology Conference, New Orleans, June 1994.

2. Wright, A.D., Osgood, R.O. and Malcolm, D.J., "Analysis of a two-bladed teetering hub turbine using the ADAMS multi-body dynamics code," Windpower '94, American Wind Energy Association annual conference, Minneapolis, May 1994.

3. R. Lynette & Associates, "Advanced wind turbine conceptual study, final report," National Renewable Energy Laboratory, subcontract ZG-0-19090-3, March 1992.

4. R. Lynette & Associates, "ESI-80 rotor performance and reliability enhancement program, final report", Smith Wind Energy Corp., National Renewable Energy Laboratory subcontract HC-2-11101, March 1993.

5. Osgood, R.O., "AWT-26/P1 modal survey," National Renewable Energy Laboratory engineer's summary report, January 1994.

6. Osgood, R.O., "AWT-26/P2 modal survey," National Renewable Energy Laboratory engineer's summary report, January 1994.

7. Osgood, R.O. and Allread, J.S,. "Modal survey test results for R. Lynette & Associates' AWT-26 wind turbine blade," National Renewable Energy Laboratory, May 1993.

8. R. Lynette & Associates, Design Handbooks, AWT-26/P2.

9. R. Lynette & Associates, "Advanced wind turbine near-term product development conceptual study report," National Renewable Energy Laboratory subcontract ZA-2-11295-1, March 1993.

10. International Electrotechnical Commission, "Wind turbine generator system - part 1: Safety requirements", International Standard 1400-1, December 1994

11. Uniform Building Code, 1991

12. Wright, A.D., Buhl, M.I., and Thresher, R.W. "FLAP Code Development and Validation", SERI/TR-217-3125, January 1988.

13. Det Norske Veritas, "Rules for the design construction and inspection of offshore structures. Appendix C, Steel structures", 1977

14. International Electrotechnical Commission, "Wind turbine generator system. Part 12 - Power performance measurement techniques", TC88(WG6), interim 24/1-95

15. Tangler, J.L. "A horizontal axis wind turbine performance prediction code for personal computers. Users' guide", Solar Energy Research Institute, January 1987

16. Wilson, R.E., Walker, S.N., and Freeman, L.N. "User's manual for the Advanced Dynamics Code", Oregon State University, OSU/NREL report 92-01D November 1992, prepared under NREL subcontract no. XF-1-11009 Mod 2

17. "Algor finite element analysis system", Algor Inc., Pittsburgh, 1994.

18. Advanced Wind Turbines Inc. "AWT-26 Operations and Maintenance Manual, version 1.0", August 1994

19. Pinnacle Consulting Group Inc. "New Manufacturing Facility Design", report for R. Lynette & Associates, March 1993

20. Hansen, A.C. and Cui, S., "User's guide to the yaw dynamics computer program YAWDYN version 4", university of Utah, July 1991

21. "ADAMS/solver reference manual version 7.0", Mechanical Dynamics Inc., Ann Arbor, Michigan, October 1993.

22. Downing, S. and Socie, D., "Simple rainflow counting algorithms", International Journal of Fatigue, January 1982.

23. "Guidelines for the development of limit states design", Canadian Standards Association, special publication S408-1981.

24. Sutherland, H.J. and Butterfield, C.P., "A review of the workshop on fatigue life methodologies for wind turbines", Wind Energy 1994, The Energy-Sources Technology Conference, ASME, New Orleans, January 1994.

25. Veers, P.S., "A general method for fatigue analysis of vertical axis wind turbine blades", Sandia National Laboratories, SAND82-2543, October 1983.

26. "Draft acoustic measurement report, R. Lynette type WC-86B and ESI type 80 wind energy conversion systems", Walker, Celano & Associates on behalf of R. Lynette & Associates, October 1992.

27. Lawlor, S.P., "Tower drag and 7P system response", internal memorandum. R Lynette & Associates, 9 September 1993

28. Kelley, N.D., McKenna, H.E, Hemphill, R.R., Etter, C.L., Garrelts, R.L., and Linn, N.C., "Acoustic noise associated with the MOD-1 wind turbine: its source, impact, and control", Solar Energy Research Institute, SERI/TR-635-1166, February 1985.

29. "AWT-26 wind turbine prototype, factory test notebook", Advanced Wind Turbines Inc.

REPORT DOCUMENTATION PAGE

Form Approved
OMB NO. 0704-0188

1.	2. REPORT DATE	3. REPORT TYPE AND DATES COVERED
	December 1995	Subcontract Report

4. TITLE AND SUBTITLE

Advanced Wind Turbine Near-Term Product Development Final Technical Report

5. FUNDING NUMBERS

C:

TA: WE617310

6. AUTHOR(S)

R. Lynette & Associates, Inc.

7. PERFORMING ORGANIZATION NAME(S) AND ADDRESS(ES)

R. Lynette & Associates, Inc.
15042 N.E. 40th Street, Suite 206
Redmond, WA 98052

(206) 885-0206

8. PERFORMING ORGANIZATION REPORT NUMBER

9. SPONSORING/MONITORING AGENCY NAME(S) AND ADDRESS(ES)

National Renewable Energy Laboratory
1617 Cole Blvd.
Golden, CO 80401-3393

10. SPONSORING/MONITORING AGENCY REPORT NUMBER

TP-441-7229

DE96000492

11. SUPPLEMENTARY NOTES

NREL Technical Monitor: Brian Smith

12a. DISTRIBUTION/AVAILABILITY STATEMENT

National Technical Information Service
U.S. Department of Commerce
5285 Port Royal Road
Springfield, VA 22161

12b. DISTRIBUTION CODE

UC-1213

13. ABSTRACT *(Maximum 200 words)*

In 1990 the U.S. Department of Energy initiated the Advanced Wind Turbine (AWT) Program to assist the growth of a viable wind energy industry in the United States. This program, which has been managed through the National Renewable Energy Laboratory (NREL) in Golden, Colorado, has been divided into three phases: 1) conceptual design studies, 2) near-term product development and 3) next-generation product development.

The goals of the second phase were to bring into production wind turbines which would meet the cost goal of $0.05 kWh at a site with a mean (Rayleigh) windspeed of 5.8 m/s (13 mph) and a vertical wind shear exponent of 0.14. These machines were to allow a U.S.-based industry to compete domestically with other sources of energy and to provide internationally competitive products.

In 1992, R. Lynette & Associates (RLA) was awarded a contract under the second phase of the AWT program. This report presents the technical results of that contract. It also includes a summary of RLA's project funded under Phase 1 of the DOE program. It describes the rationale behind the selection of the "baseline" wind turbine, the modifications made to that design, the fabrication and testing of two prototypes, and the plans for machine production.

14. SUBJECT TERMS

horizontal-axis wind turbine

15. NUMBER OF PAGES

16. PRICE CODE

17. SECURITY CLASSIFICATION OF REPORT	18. SECURITY CLASSIFICATION OF THIS PAGE	19. SECURITY CLASSIFICATION OF ABSTRACT	20. LIMITATION OF ABSTRACT
Unclassified	Unclassified	Unclassified	UL